

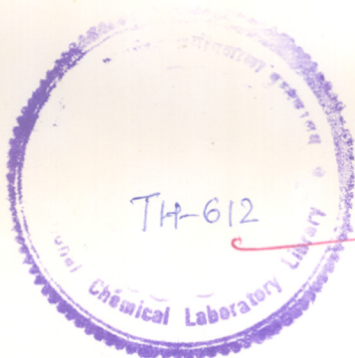
CC
Bali

4/10 - 501

NY

405

COMPUTERISED.



CONFORMATIONAL & HYDROGEN BONDING BEHAVIOUR OF COMPLEX MOLECULES

A THESIS SUBMITTED TO

SHIVAJI UNIVERSITY, KOLHAPUR

FOR THE DEGREE OF

DOCTOR OF PHILOSOPHY

(IN CHEMISTRY)

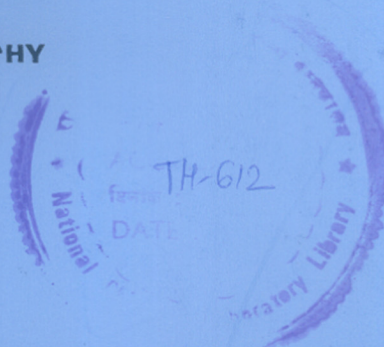
BY

Mrs. A. A. BELHEKAR

M. Sc.



COMPUTERISED



541.57:547.582.4(043)
BEL

PHYSICAL CHEMISTRY DIVISION

NATIONAL CHEMICAL LABORATORY

PUNE-411 008 (INDIA)

AUGUST 1990

COMPUTERISED



CERTIFICATE

Certified that the work incorporated in the thesis
Conformational and Hydrogen Bonding Behaviour of Complex
Molecules submitted by Mrs. Anagha Ashok Belhekar was carried
out by the candidate at the Physical Chemistry Division, National
Chemical Laboratory, Pune 411008, India, under my supervision for
the Degree of Doctor of Philosophy in Chemistry, Shivaji Univer-
sity, Kolhapur. This work was not submitted so far for any
degree.

A handwritten signature in cursive script, appearing to read "C. I. Jose", written over a horizontal line.

(Dr. C. I. Jose)

Research Guide

A C K N O W L E D G E M E N T S



I take this opportunity to express my sincere appreciation and deep sense of gratitude to Dr. C. I. Jose, Scientist, National Chemical Laboratory, Pune, for suggesting this problem and for his invaluable guidance throughout this investigation.

I also wish to acknowledge sincerely the cooperation and timely help given by my colleague, Ms. Mangala Agashe.

Generous help rendered by my colleagues, Dr. S.D. Patil and Dr. S. K. Kamat, during the various stages of this work, is warmly acknowledged.

Finally, I would like to thank Dr. P. Ratnasamy, Head of the Inorganic Chemistry Division, for allowing me to do this work and the Director, National Chemical Laboratory, Pune, India, for kindly permitting me to submit this work in the form of a thesis.

Place: NCL Pune, India.

Date : 13.8.90

A. A. Belhekar

Mrs. A. A. Belhekar

C O N T E N T S

	<u>Page</u>
P R E F A C E	1 – 5
<u>CHAPTER I</u> : INTRODUCTION	6 – 32
1.1 : Conformational behaviour of N – acetyl(amino acid) N' –methyl Amides in solution.	6 – 17
1.2 : Structural changes in amino benzoic acid.	17 – 20
1.3 : Conformation equilibria in	21 – 32
<u>CHAPTER II</u> : THEORETICAL BACKGROUND	33 – 62
2.1 : Fourier transform IR Spectroscopy	33 – 48
2.2 : Integrated Absorption Intensity	48 – 49
2.3 : The shapes of Infrared Absorption bands	49 – 50
2.4 : Band Resolution Techniques	50 – 58
2.5 : Hydrogen Bonding	58 – 62
<u>CHAPTER III</u> : EXPERIMENTAL	63 – 72
3.1 : N-acetyl (amino acid) N' –methyl amides	63 – 67
3.2 : 2-Dimethylamino Benzoic Acid	67 – 70
3.3 : n- Alcohols	70 – 72
<u>CHAPTER IV</u> : RESULTS AND DISCUSSION	
Conformational analysis of N-acetyl (glycine, L-alanine, L-leucine) N'-methyl amide in chloroform solution	73 – 92

<u>CHAPTER V</u>	: RESULTS AND DISCUSSION Characterisation of the various structural species of 2-dimethyl- amino benzoic acid in different solvents	93 – 106
<u>CHAPTER VI</u>	: RESULTS AND DISCUSSION Conformational equilibria in simple primary alcohols	107 – 125
CONCLUSIONS		126 – 130
REFERENCES		131 – 142

LIST OF TABLES

<u>Table No.</u>	<u>Description</u>	<u>Page</u>
I	Melting Point and Microanalyses	64
II	Calculated population of free and intramolecularly hydrogen bonded five-membered ring species in N-acetyl amino acid N'-methyl/dimethyl amides in chloroform	84
III	Predicted and observed proton coupling constants for N-acetyl L-alanine N'-methyl amide	87
IV	Calculated and observed $^{13}\text{C}\dots\text{H}$ vicinal coupling constants for N-acetyl L-alanine N'-methyl amide	90
V	Carboxyl bands of 2-dimethylamino benzoic acid in solution	99
VI	Temperature dependence of rotamer band areas (cm^{-1}) in n-alcohols	114
VII	Hydroxyl band and thermodynamic parameters of n-alcohol rotamers	118
VIII	Dependence of <u>trans</u> species (%) on dihedral angles (ϕ)	122
IX	Temperature dependence of equilibrium constants (K) in n-alcohols	124

LIST OF FIGURES

<u>Fig.No.</u>	<u>Description</u>	<u>Page</u>
1.	Extended (a) and folded (b) forms of N-acetyl amino acid N'-methyl amide	10
2.	(a) : C_5 conformation (b) : Equatorial C_7 conformation (c) : Axial C_7 conformation	12
3.	2-Dimethyl amino benzoic acid	19
4.	(a) : Staggered and (b) : Eclipsed conformations	22
5.	(a) : Staggered, (b) <u>trans</u> and (c) <u>gauche</u> conformers	22
6.	Structures suggested by Krueger	25
7.	Michelson Interferometer	34
8.	Electromagnetic waves from the fixed mirror (solid line) and movable mirror (broken line) at different values of the optical retardation	36
9.	Interferogram from a typical infrared glower.	40
10.	Simple spectra and Interferograms.	41
11.	(a) Spectrum of two lines of equal intensity. (b) Interferogram for each spectral line. (c) Resultant Interferogram.	43
12.	Effect of restriction of the path difference from infinite to finite values.	44
13.	Fourier Deconvolution.	56
14.	Potential Energy Diagram.	60
15.	NH stretching bands of N-acetyl glycine N'-methyl amide.	74

16.	NH stretching bands of N-acetyl L-alanine N'-methyl amide.	75
17.	NH stretching bands of N-acetyl L-leucine N'-methyl amide.	76
18.	NH stretching band of N-methyl acetamide.	81
19.	NH stretching bands of N-acetyl glycine N'-dimethyl amide.	82
20.	NH stretching bands of N-acetyl sarcosine N'-methyl amide.	85
21.	IR spectra of DMA in solvents - cyclohexane and carbon tetrachloride.	94
22.	IR spectra of DMA in solvents - benzene and dioxane.	95
23.	IR spectra of DMA in solvents - acetonitrile and chloroform.	96
24.	IR spectra of DMA in solvents - dimethyl sulphoxide and methanol.	97
25.	2-Dimethyl amino benzoic acid structures.	100
26.	PMR spectrum of 2-dimethyl amino benzoic acid in dimethyl sulphoxide-d ₆ .	103
27.	IR spectrum of 2-dimethyl amino benzoic acid in D ₂ O.	105
28.	Ethanol hydroxyl band (—), Deconvoluted bands (---).	108
29.	n-Propanol, hydroxyl and deconvoluted bands 303 ^o k (—), 328 ^o k (---).	109
30.	n-Butanol, hydroxyl (—) and deconvoluted (---) bands.	110
31.	n-Pentanol, hydroxyl (—) and deconvoluted (---) bands.	111

32. n-Hexanol, hydroxyl (—) and deconvoluted (---) bands. 112
33. Plot of $\log k$ Vs $1/T$. 115

PREFACE

P R E F A C E

Conformations are different arrangements of atoms in a molecule caused by free rotation around bonds. They are interconvertible, but cannot be separated. The terms conformational isomer and rotamer are sometimes used instead of conformer. For any open chain single bond connecting two Sp^3 carbon atoms, there are an infinite number of conformations possible, each of which has a certain energy associated with it. A number of methods have been used to determine conformations. These include X-ray, electron diffraction, IR, Raman, UV, NMR, microwave, photoelectron spectroscopy, optical rotatory dispersion, dipole moment, circular dichroism measurements, etc. Some of these methods are applicable only for solids. However, the conformation of a molecule in the solid state is not necessarily the same as in solution.

Recently, some simple polypeptides (hormones, antibiotics, toxins, etc.) have been found to be biologically active and this activity has been explained on the basis of structural conformation and hydrogen bonding behaviour of these molecules. Hydrogen bonding occurs when the hydrogen atom of a proton donor group A-H is involved in an inter or intramolecular interaction with a proton acceptor group B. While A is an electronegative atom, such as O, N, F, S, Cl, etc., B is a localised site of high electron density such as a lone pair of electrons of an electronegative atom, a π -electron orbital of a multiple bond etc. H-bonding

is a directional and specific interaction which is more localised than weak intermolecular interaction such as repulsion, polarization, dispersion or charge transfer interactions. The strength of H-bond is small ($0.5-60 \text{ kJ mol}^{-1}$) in comparison with ordinary chemical bonds ($200-800 \text{ kJ mol}^{-1}$). In hydrogen bonded gases and liquids, due to frequent collisions of molecules, H-bonds are continually breaking and reforming resulting in a rapid dynamic equilibrium between the non-hydrogen bonded and H-bonded species. Thus at room temperature, only a fraction of molecules may be in the hydrogen bonded form.

Literature survey reveals that even for polypeptides and proteins, meagre data are available regarding their conformations in solutions. Since dipeptide can be considered as a model for polypeptides and proteins, it was thought worthwhile to study the conformation and hydrogen bonding behaviour of simple dipeptides like N-acetyl amino acid N'-methyl amides. From their infrared spectra in the NH stretching region, quantitative estimation of free and intramolecularly hydrogen bonded species in dilute solution can be established.

It has been shown that molecules like 2-dimethyl amino benzoic acid (dimethyl anthranilic acid, DMA) have an intramolecularly hydrogen bonded zwitterionic structure in the solid state, while in CDCl_3 solution predominant species are intramolecularly hydrogen bonded neutral species. Because of the broad profile of the absorption band in the carbonyl/carboxylic

region, it was not possible, so far, to establish the nature of other species in solution. With the advent of Fourier Deconvolution methods, it is now possible to separate closely overlapping bands. In the present work, structural changes in DMA in a large number of solvents like cyclohexane, carbon tetrachloride, benzene, dioxane, etc. have been studied.

While the staggered conformations of ethane due to rotation around C-C bond are well known, conformational behaviour of a C-O bond is less understood and it is not clear whether rotation around single C-O bond in simple alcohols could give rise to different hydroxyl stretching frequencies. Thus, in methanol all the staggered conformations would be equivalent. However, in higher straight chain alcohols, two different staggered conformers, (trans and gauche) are possible. The slightly asymmetric hydroxyl band profile of simple alcohols has been ascribed either solely to the two conformers arising from rotation around C-O bond or rotation around both the C-O and C-C bonds. Due to strong overlapping, it was difficult to separate the band profile with certainty. Such overlapping bands can be separated using recent Fourier Deconvolution method. In the present work, the asymmetric band profiles of free hydroxyl band of straight chain aliphatic alcohols (ethanol to n-hexanol) in dilute solutions have been separated by using Fourier Deconvolution technique. From the ratio of the two rotamers, trans/gauche, (K), at various temperatures, 298-328^oK, ΔH values for this transformation have been calculated for various alcohols.

The work on conformational and hydrogen bonding behaviour of dipeptides, 2-di-methyl amino benzoic acid and n-alcohols has been divided into six chapters in the present work as outlined below.

The vast amount of reported infrared spectral data on dipeptides, N-acetyl amino acid (glycine, L-alanine, L-leucine) N'-methyl amides, in dilute solutions are summarized in Chapter I (1.1). The structural changes in DMA as manifested from dielectric constant measurement as well as electronic and IR spectral analyses and recent structural studies in the solid state and in solution form are discussed in Chapter I (1.2). The present state of understanding of the rotational isomers of n-alcohols and the various techniques by which the broad band profile of the hydroxyl band was separated by earlier workers and their conclusions are reviewed in Chapter I (1.3).

Basic concepts used in interpretation of infrared spectral data to structural problems are elaborated in Chapter II. Thus, Fourier transform infrared spectroscopy, integrated absorption intensity, band shape, band resolution techniques including Fourier Deconvolution, and Hydrogen Bonding, have been detailed here. The experimental details on the preparation and purification of compounds under investigation, spectroscopic measurements and general methods of calculations, are included in Chapter III. The results and discussion on dipeptides, DMA and n-alcohols are elaborated in Chapters IV, V and VI, respectively. This is followed by conclusions and a collective list of references.

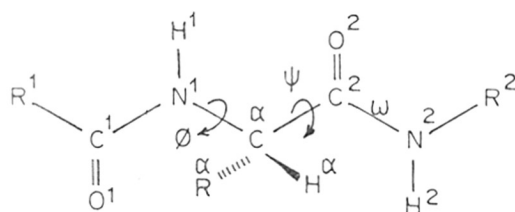
Papers published in connection with the present work are added in Appendix.

CHAPTER I
INTRODUCTION

1.1. CONFORMATIONAL BEHAVIOUR OF N-ACETYL AMINO ACID N'-METHYL AMIDE IN SOLUTION

It is known that the properties of polypeptides are partly determined by their conformational behaviour. Secondary and tertiary structures of polypeptides and proteins play a definite role in determining their biological activity¹⁻⁴. For understanding conformations of polypeptides, model dipeptides such as N-acetyl N'-methyl amides of amino acids have been studied since 1950.

A dipeptide model can be represented as,



the conformations of which depend upon rotations around N¹-C^α (φ) and C^α-C² (ψ). The conventions used regarding torsional angles in the present work are according to the IUPAC-IUB Commission on Biochemical Nomenclature.⁵ The torsional angles for fully extended conformers are φ = ψ = 180°.

The conformations of these molecules are generally identified by using common physicochemical techniques such as infrared, NMR spectroscopy, dipole moment measurements, optical rotatory dispersion, circular dichroism etc. These investigations are performed in solutions using an inactive solvent such as carbontetrachloride at a very low concentration in order to

avoid self association of the solute and to reduce solute-solvent interaction.

One of the experimental techniques for conformational study is the measurement of dipole moments. The relative orientations of the two amide linkages would determine the magnitude of their total dipole moment. However, the necessity to operate in an inactive solvent at a very low concentration of the solute, poses considerable experimental difficulty.

NMR spectroscopy can give very useful information about the conformation, which can be derived from the coupling constants (J) for the $\text{HN}-\alpha\text{HC}$ protons and for the $\alpha\text{HC}-\beta\text{HC}$ protons. The latter can provide information regarding the $\text{H}-\text{C}\alpha-\text{C}\beta-\text{H}$ dihedral angle by using the Karplus relationship,

$$J = A \cos^2 \theta + B \cos \theta + C$$

where A , B and C are constants and θ is the dihedral angle. If an appropriate account of the electronegativity of substituents on a particular $\alpha\text{C}-\text{H}-\beta\text{H}-\text{C}$ fragment is taken and reliable J values are obtained, the method can be used to study rotational isomers.

For the study of peptide conformations, the backbone conformation is of great interest which can be specified by the angles, ϕ and ψ for each residue. It can be seen that the experimental coupling constant $J_{\text{HN}-\alpha\text{C}-\text{H}}$ can be directly related to the dihedral angle by a Karplus like relationship. The equations, derived theoretically, are as follows :



$$J_{\text{HN}} \propto \text{HC} = \frac{11.27 \cos^2 \theta - 4.32 \cos \theta + 0.01 (\text{trans})}{12.06 \cos^2 \theta - 4.48 \cos \theta + 0.01 (\text{cis})}$$

Thus, though the information about the torsional angles, α and ψ can be obtained from NMR studies, this method has limitations because of the high concentration required for recording reliable spectra, which may give rise to associated species. Further, due to fast exchange of labile protons of NH groups, various types of species with free and bonded NH groups can be differentiated with difficulty for the compounds under investigations.

5J long range coupling in saturated systems is usually observed when the protons are separated by four or five bonds and the protons are located in a planar, zig-zag arrangement. This type of coupling has come to be referred to as coupling along a 'W' path and appears to be independent of either the nature or hybridization of the intervening atoms. The magnitude of this type of coupling falls off rapidly as the two protons lose coplanarity and is more commonly observed in unsaturated compounds.

Infrared spectroscopy has been found to be very useful technique to study the conformational behaviour of amide groups in polypeptides. From the position of the infrared NH stretching bands, it is possible to establish whether they are in the free state or involved in an intramolecular hydrogen bonding and from the frequency shift, further information about the strength of

such hydrogen bond and their conformations can be derived. The information about the cis or trans nature of peptide bond can be obtained from infrared spectrum. The amide II (δ NH) and amide III (ν C-N) bands are useful for this type of investigation. In the trans configuration of the peptide linkage, amide II band is found at $\sim 1550 \text{ cm}^{-1}$ and amide III linkage at 1290 cm^{-1} . In the case of cis linkage, the amide II band is found at 1450 cm^{-1} and amide III band at about 1330 cm^{-1} . Thus, infrared spectroscopy is a very useful tool to determine the conformers and estimate their percentage.

Now, let us review briefly the attempts made by earlier workers to determine the conformers in dipeptides and their conclusions.

Infrared spectra of dipeptides were studied by various workers in the NH stretching region in dilute carbon tetrachloride solution (10^{-4} M). Mizushima et. al.⁶ studied acetyl amino acid N'-methyl amides where amino acids were glycine, alanine, valine, norleucine and proline. They observed two bands at 3461 and 3421 cm^{-1} for acetyl glycine N'-methyl amide and three bands at 3460 , 3440 and 3420 cm^{-1} for higher (alanine, valine, etc.) derivatives above 3400 cm^{-1} . Below 3400 cm^{-1} , a broad band at $3360\text{--}3300 \text{ cm}^{-1}$ was found in all the compounds.

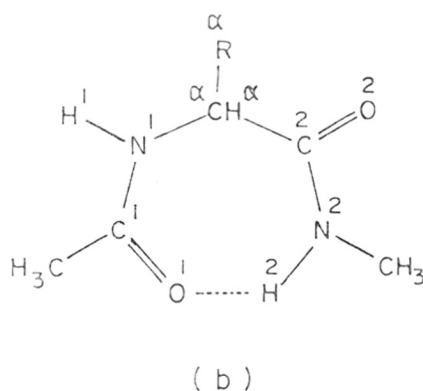
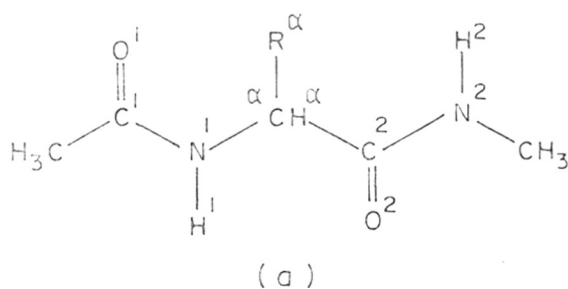


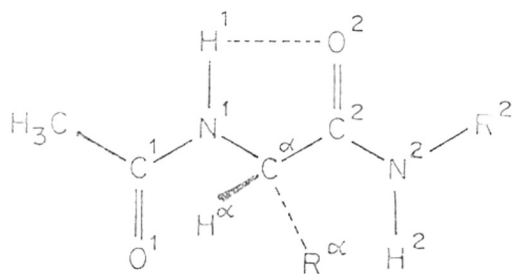
FIG. 1.

They ascribed the bands at 3460 and 3440 cm^{-1} to the free NH vibrations of the extended form (Fig. 1a). They further suggested that the NH bond in the first peptide linkage in these compounds may form a weak hydrogen bond with the C=O group in the second peptide linkage and would exhibit a stretching frequency lower than that of the NH bonds in the second peptide linkage, free from such hydrogen bonding (3440 cm^{-1}). The bands at 3360–3300 and 3420 cm^{-1} were ascribed to the intramolecularly hydrogen bonded and free NH groups of the seven membered ring species, respectively (Fig.1b).

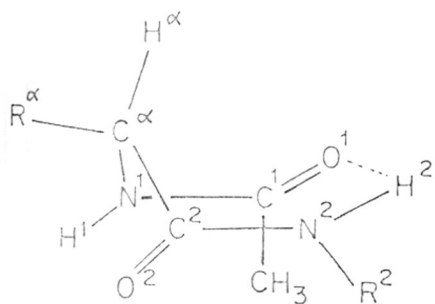
Portnova⁷ et. al. studied alanine dipeptides where $\text{N}^2\text{-CH}_3$

group (Fig. 1b) was replaced by $N^2-CH_2-CH_3$. From area measurement of the two bands at 3440 cm^{-1} due to uncoiled species (Fig. 1a), which may be similar to the extended form of Mizushima et. al.⁶ and at 3370 cm^{-1} due to coiled species (Fig. 1b) similar to the seven membered intramolecularly hydrogen bonded ring species, the concentrations of the two forms were calculated. They reported 74% coiled form in methyl ester of acetyl alanine (DD) and 61% coiled form in methyl ester of acetyl alanine (DL). ΔH and ΔS values for this transformation were calculated from a temperature dependence study of this equilibrium. On the basis of NMR spectra^{8,9}, it was concluded that pseudoaxial rotation of R^α in a seven membered ring was preferred. The angles of rotation α (around $N-C^\alpha$), and γ around $(C^\alpha-C^2)$ were calculated from the $^3J_{HNCH}$ coupling constants by using Karplus equation and were found to be 240° and 120° , respectively. Thus Mizushima⁶ and Portnova⁷ found two conformers, fully extended free and intramolecularly hydrogen bonded seven membered ring species in the compounds under investigation.

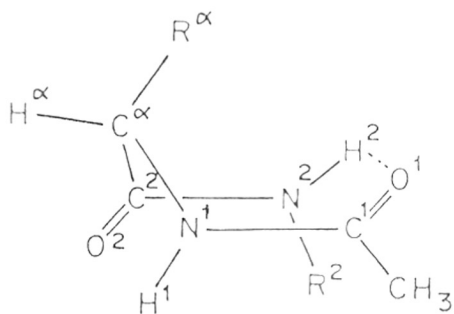
Neel¹⁰ summarized his conformational studies on N-acetyl (glycine, L-alanine, L-leucine etc.) N'-methyl amides and a series of slightly different compounds using IR¹¹⁻¹⁴, NMR and dipolemoment measurements. They observed NH stretching bands in four regions 3460 , 3440 , $3414-25$ and $3325-46\text{ cm}^{-1}$. Bands at 3460 and 3440 cm^{-1} were ascribed to free NH vibration of two possible intramolecularly hydrogen bonded five (C5) (Fig. 2a) and seven



2a



2 b



2 c

FIG. 2a. C₅ CONFORMATION

2b. EQUATORIAL C₇ CONFORMATION

2c. AXIAL C₇ CONFORMATION

(C7) (Fig. 2b) membered ring conformations. Bands at 3414-25 and 3325-46 cm^{-1} were ascribed to bonded NH frequencies of the C_5 and C_7 rings, respectively. The C_7 conformation is a ring structure which is folded by an intramolecular hydrogen bond between H^2 and O^1 (Fig. 2b,c). The amide groups lie in two planes which make an angle of 115° . When R^α is not a hydrogen atom, two different C_7 conformations can exist according to the inclination of the $C^\alpha-R^\alpha$ bond with respect to the intersection line of these two planes. These two forms are called equatorial (Fig. 2b) with $\phi = 105^\circ$ and $\psi = 230^\circ$ and axial (Fig. 2c) with $\phi = 225^\circ$ and $\psi = 130^\circ$. From NMR studies¹⁰⁻¹⁴ of the compounds under investigation, bond angles $\phi = 105^\circ$ and $\psi = 230^\circ$ were obtained due to C_7 (equatorial species).

Avignon and Huang¹⁵ succeeded in measuring the relative amounts of C_5 and C_7 conformers in the case of N-acetyl glycine N-methyl amide, the molar ratio of the C_7 form being equal to 60%.

Thus, the above workers¹⁰⁻¹⁵ found mainly two conformers, C_5 and C_7 , in the present compounds with negligible amount of free non-hydrogen bonded species.

Efremov et.al.¹⁶ studied the same dipeptides of Mizushima et. al.⁶ in non-polar (CCl_4) and weakly polar (CHCl_3) media. The bands in the region 3338-3360 cm^{-1} were ascribed to N^2H^2 bonds in the intramolecularly hydrogen bonded C_7 folded form (Fig. 1b), as assigned by the previous workers^{6,7,10}. In all cases, on

passing from solutions in CCl_4 to those in CHCl_3 , the intensities of these bands decreased with simultaneous increase in the intensity of the band at 3460 cm^{-1} , which was ascribed to the NH stretching band of the extended form (Fig. 1a). They assigned the bands at 3420 cm^{-1} to the free $\text{N}^1\text{-H}^1$ of the intramolecularly hydrogen bonded seven membered (C7) form (Fig. 1b) which is in agreement with those reported by Mizushima et.al.⁶. This assignment was confirmed by measurement of the integral intensities of all the NH bands of the above compounds at various temperatures and concentrations. A rise in temperature of the solutions in CCl_4 and CHCl_3 led to an increase in the intensity of the bands at 3440 and 3460 cm^{-1} and decrease in those at 3350 and 3420 cm^{-1} . Efremov et al.¹⁶ ascribed the large width, high intensity and comparatively low frequency of this band to a direct interaction of the two amide groups in the folded form of the molecule. Neel¹⁰ and coworkers¹¹⁻¹⁵ had ascribed these very features of the 3420 cm^{-1} band to a five membered intramolecularly hydrogen bonded NH species. Thus, Neel¹⁰ and coworkers¹¹⁻¹⁵ were the first to assign the band at 3420 cm^{-1} to C_5 conformer.

Stimson et. al.¹⁷ and Maxfield et.al.¹⁸ studied N-acetyl derivatives of glycine, L-alanine and L-leucine N'-methyl amides in dilute CHCl_3 solution (10^{-4} M). They^{17,18} found it difficult to dissolve blocked glycine (N-acetyl glycine N'-methyl amide) to have concentrations greater than $5 \times 10^{-6} \text{ M}$ in highly purified CCl_4 . They did not observe any band in the region $3300\text{-}3370 \text{ cm}^{-1}$ in dilute CHCl_3 solution, which was assigned by earlier workers⁶⁻¹⁶

to the intramolecularly hydrogen bonded NH in the C_7 equatorial conformation. In order to account for this discrepancy they¹⁷ investigated the solubility of blocked glycine in CCl_4 and found that the solubility was enhanced in impure CCl_4 . The solubility increased also with aging when purified solute and solvents were used. They further observed that the solubility of blocked glycine in CCl_4 was enhanced by adding small amounts ($10^{-3}M$) of phosgene, hydrogen chloride and water. Addition of these impurities also produced a weak broad band in the 3300-3370 cm^{-1} region of the spectrum. But they did not find any absorption in the region 3300-3370 cm^{-1} in $CHCl_3$ solutions of blocked (glycine, L-alanine, or L-leucine) at concentrations below $5 \times 10^{-4}M$. A band at 3370 cm^{-1} found in the spectrum of N-acetyl sarcosine N'methyl amide, however, can only be ascribed to C_7 conformation. The absence of this band in dilute $CHCl_3$ solutions of blocked (glycine, L-alanine, L-leucine) indicated little or no tendency to adopt C_7 equatorial conformation.

Smolikova et.al.¹⁹ studied acetyl L-alanine, L-valine and L-tert-leucine N'methyl amides in dilute CCl_4 and C_2Cl_4 solutions. The bands at 3460 and 3440 cm^{-1} were assigned to the free NH stretching vibrations of all possible conformations of the dipeptide. They found that the extended conformers similar to intramolecularly hydrogen bonded C_5 species (Fig.2a) were the most common constituents in solution. In these conformers, however, the frequency of the N^1H^1 band was modified by the varying proximity of the C^2O^2 group; but the nature of this interaction was

not clear. The intramolecularly hydrogen bonded folded C_7 (axial, equatorial) conformation which has been reported by earlier workers⁶⁻¹⁶ from the presence of a band at $3300-3360\text{ cm}^{-1}$ was not generally prevailing in dilute solutions ($\sim 10^{-5}\text{ M}$) except in specific structural situation with non-bulky side chains (L-alanine and L-leucine derivatives).

Ginzburg²⁰ studied same dipeptides which were studied by earlier workers in dilute CCl_4 solution. The bands at 3420 and 3340 cm^{-1} were assigned to bonded NH groups in the intramolecularly hydrogen bonded five membered ring species $\text{N}^1\text{-H}^1\text{...O}^2$ (C_5) and seven membered ring species $\text{N}^2\text{H}^2\text{...O}^1$ (C_7) respectively. In the glycine derivatives the band at 3465 cm^{-1} was ascribed to free NH group in the intramolecularly hydrogen bonded seven membered ring species. In alanine, leucine, etc. derivatives, the bands at 3445 and 3465 cm^{-1} were assigned to the free NH vibration in the intramolecularly hydrogen bonded seven membered (C_7) and five membered (C_5) ring species, respectively. They argued that the hydrogen atoms of the more highly branched groups strongly repelled the hydrogen atoms of the NH bond, stretching the latter slightly and lowering the NH frequency in derivatives of alanine, leucine, etc.

Thus, it is evident from the reported work of simple dipeptides like N-acetyl amino acid N'-methyl amides in dilute carbon tetrachloride that there is considerable controversy on two accounts. Firstly, whether the band at 3420 cm^{-1} arises from an intramolecularly hydrogen bonded five membered (C_5) ring NH or



free NH group of the folded/coiled intramolecularly hydrogen bonded seven membered (C_7) ring species which were considered the predominant species by Japanese⁶, French¹⁰⁻¹⁵ and Russian^{16,19,20} workers from the $3300-3360\text{ cm}^{-1}$ band. Maxfield et. al.¹⁸ clearly established a band in this region arising from impurities in CCl_4 . They also found that the solubility of some of these compounds in carbon tetrachloride was lower than 10^{-4} M and the preparation of solutions of 10^{-4} M and higher concentration was possible due to the presence of impurities in the solvent. Hruby²¹ on a perusal of the spectroscopic work had suggested the need for additional work in this area.

1.2 STRUCTURAL CHANGES IN AMINO BENZOIC ACIDS

During the investigation of dielectric constants of benzbetaines and N,N-dimethyl anthranilic acid (DMA) in solution, Edsall et. al.²² observed certain unusual properties in the latter. Unlike most of the Zwitterions, DMA was very soluble in alcohol, acetone and benzene and quite soluble even in ether and CCl_4 . It melted at 68°C giving a clear liquid which solidified on cooling and the solid so obtained showed all the properties of the original substance. In contrast, most Zwitterionic acids melt between 200 and 300°C and decompose on melting. Dissociation constants in water²³ and dielectric constant studies²² in benzene, ethanol and water had indicated a Zwitterionic structure of DMA.

N,N dimethyl β -alanine, closely similar to DMA has been reported to be present as a Zwitterion in the solid²⁴ and exists

541.57:547.582.4(043)

BEL

as a mixture of both dipolar and neutral species in chloroform, n-butyl alcohol and benzene, with the former species predominating in n-butyl alcohol and benzene and the latter in chloroform²⁵.

It was found by Uhlig and Doering²⁶ that the electronic spectrum and pK values of DMA in water-methanol mixture (9:1 v/v) differed in a striking manner from those of anthranilic and N-methyl anthranilic acid.

Therefore, in order to understand the abnormal behaviour of the molecule, the present work was undertaken. On the basis of infrared and electronic spectral studies in CCl_4 , benzene, cyclohexane, acetonitrile, dimethyl formamide, ethanol and water, Tramer²⁷ has reported that DMA is present as a mixture of intramolecularly hydrogen bonded neutral and zwitterionic molecules in these solvents. An unambiguous intramolecularly hydrogen bonded structure was reported by Jose et. al.²⁸ for DMA in the solid state from the infrared spectral bands at 1660 and 1370 cm^{-1} which were ascribed to the asymmetric and symmetric stretching modes of COO^- group. The absorption at 1660 cm^{-1} shifting on deuteration was assigned to the NH^+ stretching vibration. The considerable shift of NH^+ from the usual value of 2700 cm^{-1} indicated a very strong hydrogen bond involving charge transfer resulting in Structure I.

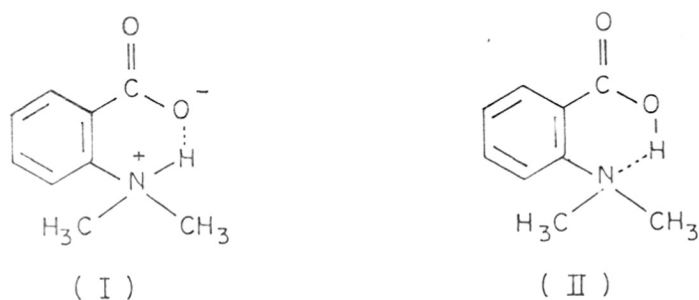


FIG. 3.

The Zwitterionic structure in the crystal of DMA was confirmed by x-ray study²⁹. There was a strong intramolecular $N^+ \cdots H \cdots O^-$ hydrogen bond in which the N-O distance was 2.497 \AA with O-H distance of 1.42 \AA and the angle ONH being 16° . Jose et al.³⁰, however, observed that the infrared spectrum of DMA was different in CCl_4 solution from that in the solid state. They observed prominent bands at 1720, 1445, 1232 and 1115 cm^{-1} in CCl_4 solution, characteristic of carboxylic acid group. PMR studies³⁰ of DMA in CCl_4 solution showed a hydroxyl proton signal at 15.25δ , which was concentration independent, suggesting that the carboxylic proton was involved in an intramolecular hydrogen bonding. Thus, they showed that in CCl_4 there were essentially two types of intramolecularly hydrogen bonded species of DMA, the Zwitterion and the neutral (Fig. 3 I and II). They further investigated the spectra in chloroform, benzene and dimethyl sulphoxide and found a complex band profile in the region 1800-

1600 cm^{-1} suggesting that in solution there was a mixture of more than the above two species. Due to the large breadth of the band, graphical separation was not possible and the nature of these species in solution could not be established at that time.

Recently, Kauppinen et. al.^{31,32} have reported a deconvolution procedure for band separation which was carried out conveniently in Fourier space using a computer programme.

Zundel et. al. have reported similar studies on the proton transfer between neutral and charged forms in a large number of compounds including DMA in various solvents using IR^{33,34} and NMR³⁵ spectroscopic techniques. They concluded that the proton transfer in the equilibrium $\text{O-H}\dots\text{N} \rightleftharpoons \text{O}^-\dots\text{H}^+\text{N}$ was shifted to the right hand side with increasing polarity of the solvent.

Studies in benzoic acid triethyl amine adducts³⁶ have shown that the nature of species in solution depended on the polarity of the solvent. It was observed that in solvents of low dielectric constant like carbon tetrachloride and carbon disulphide, only hydrogen bonded species were present while in solvents of high dielectric constant like dimethyl sulphoxide, charge transfer hydrogen bonded species were found.

From the above studies, it can be seen that compounds resembling DMA are present as both zwitterionic and neutral species and the proportion changes with polarity of the solvent.

1.3 CONFORMATIONAL EQUILIBRIA IN n-ALCOHOLS

Methanol, the simplest of alcohols can have staggered and eclipsed conformation (Fig. 4a,b) due to rotation around C-O bond. The three low energy ^{staggered} conformers are equivalent in methanol³⁷ and also in t-butanol (Fig. 5a). In the case of ethanol, however, two different staggered conformations, trans (Fig.5b) and gauche (Fig. 5c) are possible due to rotation around C-O bond. It should be mentioned that rotation around C-C bond is also possible giving additional rotamers.

In an attempt to investigate the conformers due to rotation around C-O bond, various workers examined their IR spectra in the hydroxyl stretching region. It was found that while methanol and t-butanol gave a single symmetrical band, the other normal alcohols like ethanol, n-propanol etc. gave an unsymmetrical broad band profile, which was ascribed to the presence of more than one species as expected from conformational analysis. Several attempts have been, therefore, made to study the broad band profile and to determine the relative proportions of the rotamers.

Though most of the earlier workers were unable to detect the second (low frequency) band because of the poor resolution of their instruments, it was noticed from the large half^{band} width by Brown et. al.³⁸.

Badger and Bauer³⁹ were the first, who found two OH absorptions for the primary alcohols in the vapour phase and suggested that the additional absorption could be explained on the basis of

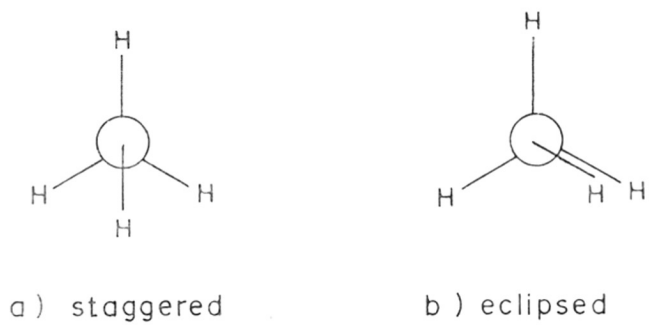


FIG. 4.

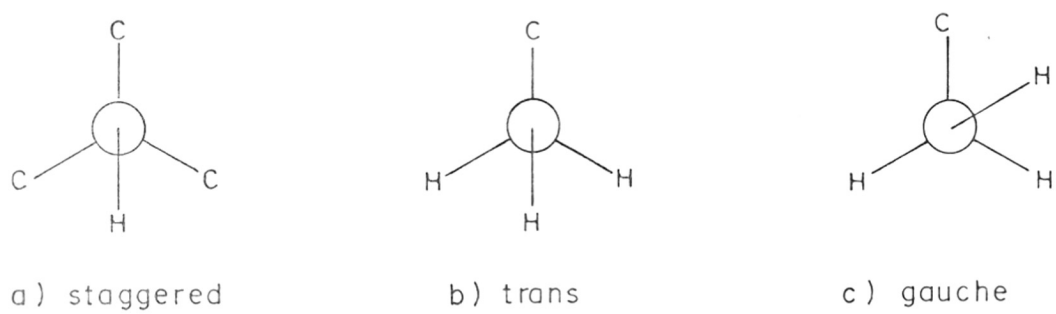


FIG. 5.



rotational isomerism.

Barrow⁴⁰ and Flett,⁴¹ who observed the infrared spectra of primary alcohols in carbon tetrachloride solution, reported that the hydroxyl bands in the fundamental region had a symmetric band shape. However, asymmetric nature was reported by later workers⁴²⁻⁵². The origin of this asymmetric profile of the free hydroxyl band, thus, became a matter of controversy. Intermolecular association was not found to be the cause, as the asymmetric shapes of the hydroxyl bands were found to be concentration independent.

Oki and Iwamura⁴², who studied the hydroxyl band of methanol, ethanol, n-propanol and n-butanol along with other primary, secondary and tertiary alcohols in dilute CCl_4 solution, found the hydroxyl band of methanol to be symmetrical ($\nu = 3743.8 \text{ cm}^{-1}$, $\Delta\nu_{1/2} = 22 \text{ cm}^{-1}$). However, ethanol, n-propanol and n-butanol were found to have a doublet structure. They were ^{the} first to resolve asymmetric band profile assuming Lorentzian band shapes for the hydroxyl absorption bands. They reported the two band positions and half band widths in the above alcohols. The ratios of the separated band areas ($A_{\text{high}}/A_{\text{low}}$) were found to be 1.8, 2.6 and 2.2 for ethanol, n-propanol and n-butanol, respectively.

Flynn et. al.⁴³ studied the hydroxyl bands of alcohols and obtained band area ratios of 7.7, 4.7, 6.9, 5.14 and 4.0 for ethanol, n-propanol, n-butanol, n-pentanol and n-hexanol respectively, using graphical method for resolution. They found

that methanol also gave an asymmetric band with intensity of major band (0.278) and that of minor band (0.007) with the band positions 3644.8 and 3668.1 cm^{-1} , respectively. They suggested Fermi resonance between hydroxyl fundamental band and a combination (overtone) band arising from lower frequency vibration as a possible explanation for the doublet in aliphatic alcohols. Piccolini⁴⁴ showed that the asymmetric band shape of the first overtone of OH stretching vibration of 2-propanol was retained in the first OD overtone region of deuterated 2-propanol and questioned the explanation of Flynn. He⁴⁴ suggested conformational heterogeneity as a possible cause for the asymmetry of the hydroxyl absorption in alcohols. The band area ratio, $A_{\text{high}}/A_{\text{low}}$, for ethyl alcohol found by Piccolini⁴⁴ was 7.92 in the first overtone region. The behaviour of other primary alcohols like 1-propanol, 1-octanol etc. was found to be analogous to ethanol.

Dalton et.al.⁴⁵ studied the hydroxyl bands of normal alcohols like methanol, ethanol and n-pentanol in dilute CCl_4 solution in the fundamental and first overtone region. They found symmetrical bands at 3643 and 7122 cm^{-1} with half band widths of 20 and 37 cm^{-1} respectively for methanol while for ethanol the bands in the fundamental region were doublets at 3636 and 3622 cm^{-1} with half band widths of 20 and 12 cm^{-1} respectively. In the first overtone region, the doublets were at 7105 and 7082 cm^{-1} with half band widths of 45 and 22 cm^{-1} respectively for ethanol. For n-pentanol, the band positions were 3638 and 3623 cm^{-1} with half band widths of 23 and 14 cm^{-1} in the fundamental region and 7110

and 7086 cm^{-1} with half band widths of 45 and 25 cm^{-1} in the first overtone region. They obtained the area ratios of 8 and 5 in the fundamental region; 7.5 and 6 in the first overtone region for ethanol and n-pentanol respectively by using graphical resolution.

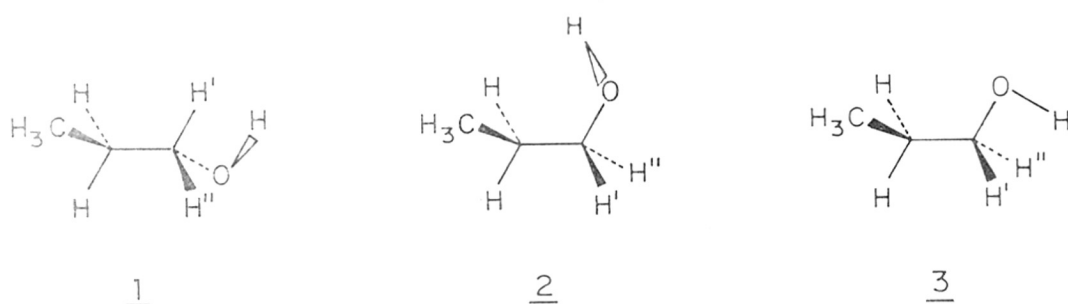


FIG. 6.

Krueger and Mettee⁴⁶ observed the fundamental hydroxyl stretching band of 1-propanol in dilute CCl_4 solution to be composed of three components at 3638 , 3632 and 3626 cm^{-1} and ascribed them to rotational isomers about the C-C and C-O bonds (Fig. 6). Although the conformer with the CH_3 and OH groups trans to each other was most heavily populated at room temperature, one of the two conformers having gauche CH_3 and OH groups, was found to be thermodynamically most stable. A conformational equilibrium scheme was postulated in which the most stable conformer had a methyl CH interacting with one of the lone pairs of electrons on the oxygen atom. They calculated the ΔH values from temperature studies on the basis of apparent peak heights. Based on these results they ascribed the band of the most stable species at 3627 cm^{-1} to $\text{>C}\cdots\text{H}\cdots\text{O}$ intramolecular hydrogen bond between



methyl hydrogen and lone pair of electrons on oxygen atoms.

Saier et.al.⁴⁷ reported the hydroxyl band positions and half band widths for methanol, ethanol, n-propanol, n-butanol, n-heptanol and n-nonanol. The asymmetric bands were resolved into the component major and minor bands by graphical resolution. However, the position and half band width of the individual bands were not reported. They showed that the asymmetry of the hydroxyl band, which was concentration independent, occurred in the deuterated species and in the first overtone vibration as well. The low frequency component bands of certain primary and secondary aliphatic alcohols, (except methanol and ethanol) were attributed to the OH absorptions of hydroxyl groups serving as a proton acceptor in C-H...O hydrogen bonds. They observed a symmetric band for methanol and ethanol and the symmetry was maintained at higher temperatures. They obtained the K (A_{low}/A_{high}) values at various temperatures and calculated ΔH values which were found to be negative. They argued that if minor band was due to conformational isomerism, ΔH should have been positive. Negative ΔH values were characteristic of some type of complexation such as hydrogen bonding, charge transfer, etc. The source of minor band was, thus, ascribed to an intramolecular interaction characterised by $-\Delta H$.

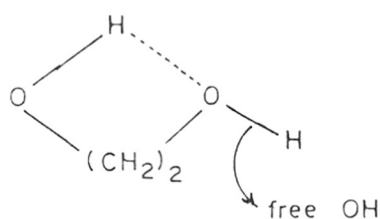
Saier et. al.⁴⁷ have discussed the various possibilities for the source of minor band in the aliphatic primary alcohols like Fermi resonance⁴⁴, the occurrence of a hot band similar to that

observed by Kraihanzel and West⁴⁸ in their study of the acetylenic CH stretching vibration, conformational heterogeneity^{42,44,45,49} of the OH group with respect to the rest of the molecule and the occurrence of an intramolecular interaction. They also considered the observations made by many workers^{48,50-52} regarding the hydrogen bonding interactions of acetylenic groups with several different proton acceptors giving rise to a minor band and short intermolecular C...O distances ($< 3.3 \text{ \AA}$) observed⁵³ in crystals suggesting hydrogen bonding between CH groups and an oxygen atom. They came to the conclusion that the minor band in aliphatic alcohols was due to intramolecular interaction between methyl CH and OH groups.

Fruwert et.al.⁵⁴ studied ethanol, n-propanol, n-butanol, etc. in dilute CCl_4 solution ($1.4 \times 10^{-2} \text{ M}$). They found hydroxyl bands at 3639 and 3624 cm^{-1} for ethanol, (area = 0.399 and $0.036 \text{ cm mole}^{-1}$), 3642 and 3626 cm^{-1} for n-propanol, (area = 0.468 and $0.078 \text{ cm mole}^{-1}$) and 3642 , 3628 cm^{-1} for n-butanol (area = 0.381 and $0.072 \text{ cm mole}^{-1}$). They obtained the area ratios (A high/A low) of 11.1 , 6.2 and 5.3 for ethanol, n-propanol and n-butanol, respectively.

Although the spectra of methanol, ethanol, 2-propanol and t-butanol have been analysed several times previously, Joris et al.⁵⁵ reexamined these spectra in order to compare the band shapes and especially the results of his method of decomposition with those reported in the literature. The band positions, area ratios (AI/AII) and half band widths observed by them were comparable only to those obtained by Oki and Iwamura⁴² mainly because both

of them employed Lorentz functions to describe the component bands. The other investigators separated the experimental spectra graphically into two symmetric bands⁴³⁻⁴⁵. The graphical separation method was found to be less satisfactory because the component bands were assumed merely to be symmetric and not necessarily represent the shapes of actual IR absorption bands. They assumed that the OH frequency was determined primarily by the rotamer type, i.e. immediate environment of the OH group, and not by any other structural features of the molecule. According to Joris⁵⁵, hydrogens of sp^3 hybridized carbon atoms, lacking electronegative substituents, should be incapable of functioning as proton donors in hydrogen bonding^{53,56}. Therefore the suggestion made by Saier et al.⁴⁷ that a very weak C--H...O hydrogen bond lowers the OH stretching force constant appeared dubious. Thus the frequency shift of 12 to 13 cm^{-1}



in primary alcohols (except methanol and ethanol) under investigation cannot be explained on the basis of C--H...O interaction. This will become clear from the IR spectra of diols⁵⁷ where the strong O--H...O hydrogen bond did not significantly alter the

frequency of the free OH bands (see the figure). Further, the area ratios of the resolved bands were determined for all the alcohols by them. The area ratio ($A_{\text{high}}/A_{\text{low}}$) for ethanol was found to be 1.7 close to that obtained by Oki and Iwamura⁴² but different from the values (7.7⁴³, 8⁴⁵, 11.1⁵⁴) obtained by other workers.

Kolbe⁵⁸ studied ethanol, n-propanol, isopropanol, isobutanol etc. in dilute CCl_4 solution. He separated the asymmetric band profile of hydroxyl band into two bands graphically and obtained the area ratios, ($A_{\text{I}}/A_{\text{II}}$), 2.7 and 3.5 for ethanol and n-propanol, respectively. Further, he determined the band area ratios (k) in alcohols at various temperatures and calculated the ΔH values, 6.3 and 7.6 kJ/mol for ethanol and n-propanol, respectively.

In the matrix isolation studies of ethanol, Barnes and Hallam⁵⁹ observed two clear bands. They ascribed the high frequency band (3662 cm^{-1}) to gauche and low frequency band (3657 cm^{-1}) to trans rotameric species, which is according to its statistical distribution.

Van der Maas et al.^{60,61}, who attributed the asymmetric nature of the hydroxyl band in primary alcohols to rotational isomerism, have reported the hydroxyl stretching band of about 70 monohydric saturated alcohols in dilute CCl_4 solution. The concentration, (10^{-1} M), was somewhat higher compared to that used by others. They reported band position, half band width and the asymmetry number, α/β . The rotational barrier energy for OH

group was 0.9 K cal/mol for methanol⁶², < 1.2 K cal/mol for ethanol⁶³ and 0.4 K cal/mol for long chain alcohols⁶⁴. Though rotation about the C-O axis was not free, the barrier was easily overcome at room temperature. Assuming the half band width and integrated intensity for different conformers to be identical, it was possible to get a rough idea about the ratio in which they occurred, if the band was resolved into its individual components. A higher band width was the result of the presence of more than one rotamer. They ascribed values of 21, 17 and 14.5 cm^{-1} to the true half band width of primary, secondary and tertiary alcohols which might be used to distinguish them.

Van der Maas et.al.⁶⁰ have mentioned several causes for the asymmetric band shape, suggested by earlier workers. Thus, Fermi Resonance⁴⁴, interaction of lone pair electrons on oxygen atom with hydrogen on γ -carbon atom^{47,65-68}, and rotational isomerism^{42,44,45,64,69-74}, can be responsible for the asymmetric band shape.

The asymmetric band profile of straight chain aliphatic alcohols was separated into three bands by Salzer et.al.^{75,76}. For methanol, they observed a single band at 3643 cm^{-1} with half band width of 22.9 cm^{-1} and for ethanol, two bands at 3636 and 3624 cm^{-1} with 19.9 and 18.7 cm^{-1} as their half band widths. For n-propanol and higher alcohols, three bands were obtained which were resolved graphically. The positions, half band widths and areas(B) of the individual bands, were found to be 3641, 3632 and 3622 cm^{-1} ;

17.6, 17.12 and 15.3 cm^{-1} , and 1087, 775 and 365 l/mole cm^{-2} respectively, for n-propanol.

Chitale et.al.⁷⁷ studied the conformations of n-propanol in dilute CCl_4 solution. They separated the profile using numerical non-linear least square procedures. They found best agreement with Lorentz functions, though they tried Gaussian as well as Lorentz Gauss sum functions. This resolution showed that the envelope of n-propanol could be decomposed into two Lorentzian components absorbing at 3637 and 3625 cm^{-1} with the half band widths of 18 and 22 cm^{-1} , respectively. The band area ratio was found to be 1.2.

Thus, though it is now well established that the complex band profile has its origin in the rotational isomers, it is not clear whether rotation around C-O bond alone is responsible and/or rotation around the C-C bond is also important.

The main difficulty in resolving this band profile is the strong overlapping, which does not permit the number, position of the component bands and the half band widths to be determined with any certainty to carry out a separation. Commonly employed methods for spectral decomposition are graphical separation^{78,79}, an analog computer (the Du Pont 310 Curve Resolver)^{80,81}, and digital computer⁸²⁻⁸⁴. In the graphical separation (G) the band parameters are arbitrarily assumed. Analog computer method requires the knowledge of band position and width and the sum of the simulated curves should match the spectral band. In the non-

linear least square curve analysis (L), where digital computer is used, the bands are separated assuming Lorentzian band shape and arbitrary band parameters. Graphical separation and non-linear least square curve analysis, as seen earlier, had given widely different component band area ratios, ($K = A_I/A_{II}$), for ethanol (L, 1.7⁵⁵ and G, 11⁵⁴) and for n-propanol (L, 1.2⁷⁷ and G, 4.7⁴³).

Since both these methods assume component band parameters, the results must be termed arbitrary. With the advent of Fourier Transform Spectrometers and availability of software for handling the spectral data directly, band deconvolution methods have been found of increasing applications in band separation. Though Fourier Deconvolution technique has been used in the separation of a variety of complex bands, we found only Bacon and Van der Maas⁸⁵, using a self enhancement procedure similar to Fourier Deconvolution. We have used the above method for the separation of the free hydroxyl band of ethanol, n-propanol, n-butanol, n-pentanol and n-hexanol to determine correct band position, and half band widths of the component bands necessary for unambiguous band separation. From the component band areas thus determined, the rotameric populations were calculated to obtain reliable equilibrium constants and from their measurements at various temperatures, thermodynamic quantity, ΔH , of the rotameric change was extracted.

2.1 FOURIER TRANSFORM IR SPECTROSCOPY^{86,87}

Fourier Transform Infrared spectrometers use some form of Michelson interferometer^{88,89} (Fig.7) where a beam of radiation is divided into two paths and then recombined introducing a path difference. The two beams interfere and the intensity variation of the beam emerging from the interferometer can be measured as a function of path difference by the detector. In the simplest form there are two mutually perpendicular mirrors, one of which moves along an axis perpendicular to its plane. The movable mirror is moved at a constant velocity or placed at equally spaced points for fixed short time periods and rapidly stepped. Between fixed mirror and the movable mirror is a beam splitter, where a beam from an external source can be partially reflected to the fixed mirror (F) and partially transmitted to the movable mirror (M). After the beams return to the beam splitter, they interfere and are partially reflected and partially transmitted. Because of the effect of interference, the intensity of the beams at the detector and returning to the source depends on the difference in path lengths between the two arms of the interferometer. This variation in intensity provides the spectral information of the source in a Fourier Transform Infrared spectrometer. If we have a monochromatic source and a beam splitter having 50% transmission and 50% reflection, we can see how the intensity of the beam at the detector varies with the path difference when the movable mirror is held stationary at different positions. The path difference between the beams $2(\Delta OM-$

CHAPTER II
THEORETICAL BACKGROUND

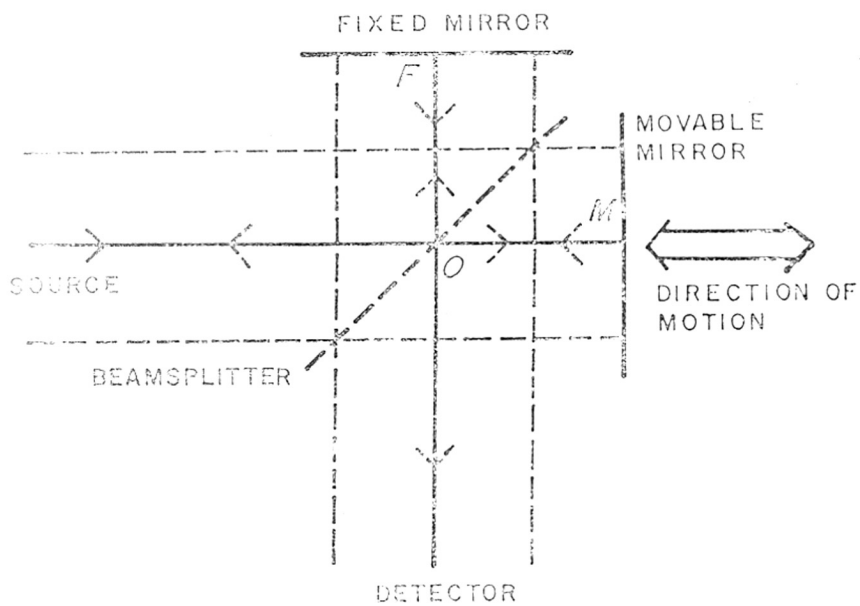
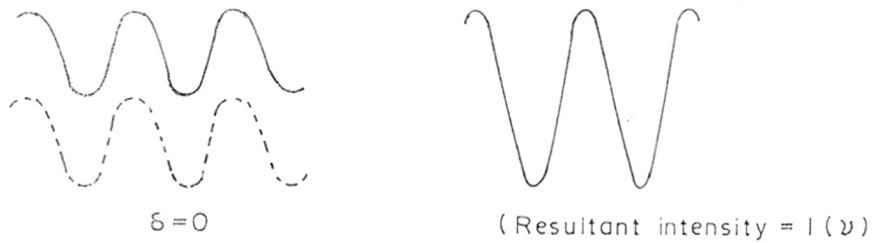


FIG. 7 MICHELSON INTERFEROMETER

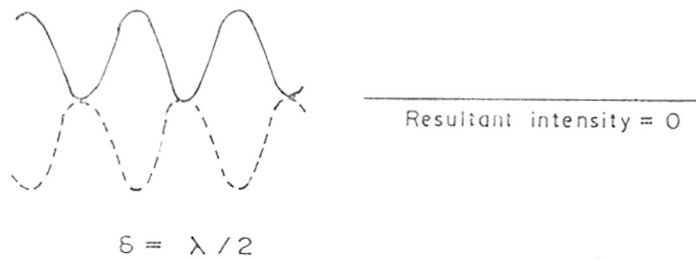


OF) is called retardation (δ). When the mirrors are equidistant from the beam splitter (zero retardation) the two beams are perfectly in phase. At this point the beams interfere constructively (Fig. 8a) and the intensity of the beam passing to the detector is the sum of the intensities of the beams passing to the fixed and movable mirrors. If the movable mirror is displaced by distance $\lambda/4$, the retardation would be $\lambda/2$. The path lengths to and from the fixed and movable mirrors are exactly one half wavelength different. On recombination at the beam splitter, the beams are out of phase and interfere destructively (Fig. 8b). At this point all the light returns to the source and none passes to the detector. A further displacement of the movable mirror by $\lambda/4$ makes the total retardation λ . The two beams are once more in phase on recombination at the beam splitter and a condition of constructive interference again occurs. For monochromatic radiation, there is no way to determine whether the particular point at which a signal maximum is measured, corresponds to zero retardation or a retardation equal to an integral multiple of wavelengths.

If the mirror is moved at constant velocity, then the signal at the detector will be found to vary sinusoidally, a maximum being registered each time when the retardation is an integral multiple of λ . The intensity at any point where $\delta = n\lambda$ is equal to intensity of the source $I(\bar{\nu})$. At other values it is given by



(a)



(b)

FIG. 8 . ELECTROMAGNETIC WAVES FROM THE FIXED MIRROR (SOLID LINE) AND MOVABLE MIRROR (BROKEN LINE) AT DIFFERENT VALUES OF THE OPTICAL RETARDATION

a) ZERO PATH DIFFERENCE

b) PATH DIFFERENCE OF ONE-HALF WAVELENGTH

$$\begin{aligned}
 I'(\delta) &= 0.5 I(\bar{\nu}) (1 + \cos 2\pi \delta / \lambda) \\
 &= 0.5 I(\bar{\nu}) (1 + \cos 2\pi \bar{\nu} \delta)
 \end{aligned}$$

It can be seen that $I'(\delta)$ is composed of a constant (dc) component equal to $0.5 I(\bar{\nu})$ and a modulated (ac) component equal to $0.5 I(\bar{\nu}) \cos 2\pi \bar{\nu} \delta$. Only the ac component is important in spectroscopic measurements and it is this modulated component that is generally referred to as the interferogram $I'(\delta)$.

The interferogram from a monochromatic source measured with an ideal interferometer thus is given by $I(\delta) = 0.5 I(\bar{\nu}) \cos 2\pi \bar{\nu} \delta$. Several factors like beam splitter efficiency, non-uniform response of the detector to various frequencies, non-uniform response of the amplifiers affect the magnitude of the signal measured at the detector.

The simplest equation representing the interferogram is therefore

$$I(\delta) = B(\bar{\nu}) \cos 2\pi \bar{\nu} \delta$$

The parameter $B(\bar{\nu})$ gives the intensity of the source at a wavenumber $\bar{\nu}$ as modified by the instrumental characteristics. The spectrum $B(\bar{\nu})$ is calculated from the interferogram by computing the Fourier transform of $I(\delta)$ which accounts for the name given to this spectrometric technique, Fourier Transform Spectrometry. Mathematically $I(\delta)$ may be said as the Reverse Fourier Transform (F^{-1}) of $B(\bar{\nu})$.

In most commercial Michelson interferometers, usually, the moving mirror is scanned at a constant velocity V (cm/sec.). Therefore, it is necessary to understand the way in which the interferogram varies as a function of time $I(t)$ rather than as a function of retardation $I(\delta)$. The retardation after t seconds from zero retardation is given by $\delta = 2Vt$ cm.

$$\text{so that } I(t) = B(\bar{\nu}) \cos 2\pi \bar{\nu} \cdot 2Vt.$$

For any cosine wave of frequency ' f ' the amplitude of the signal after a time t is given by

$$A(t) = A_0 \cos 2\pi f t$$

where A_0 is the maximum amplitude of the wave. A comparison shows that the frequency of the interferogram $I(t)$ corresponds to radiation of wavenumber $\bar{\nu}$ is given by,

$$f(\bar{\nu}) = 2V\bar{\nu}$$

The spectrum of a source of monochromatic radiation can be easily determined from the amplitude and wavelength (or frequency) which can be measured directly. However, if the source emits several discrete lines, the interferogram is more complex and digital computer is usually required to perform the transform.

When radiation of more than one wave number is emitted by the source, the measured interferogram is the resultant of interferograms corresponding to each wave number. For line sour-

ces, with very simple spectra, interferograms may be found that repeat themselves at regular interval of retardation. It can be seen that at zero path difference (ZPD) all the frequencies interfere constructively and large signal intensity known as centre-burst is observed (Fig. 9). At longer path length, the destructive interference of the various frequencies results in lower intensity signals.

Instead of a single frequency, a band having Lorentzian profile yields sinusoidal interferogram (Fig.10) with an exponential envelope. The narrower the width of the spectral band, the greater is the width of the envelope of the interferogram. Conversely for broad band spectral sources, the decay is very rapid.

When the source is continuous, the interferogram is represented by,

$$I(\delta) = \int_{-\infty}^{+\infty} B(\bar{\nu}) \cos 2\pi \bar{\nu} \delta \cdot d\bar{\nu}.$$

The spectrum is represented by,

$$B(\bar{\nu}) = \int_{-\infty}^{+\infty} I(\delta) \cos 2\pi \bar{\nu} \delta \cdot d\delta$$

These two equations are interconvertible and are known as a Fourier Transform pair. $I(\delta)$ being an even function, we can write

$$I(\delta) = 2 \int_0^{+\infty} B(\bar{\nu}) \cos 2\pi \bar{\nu} \delta \cdot d\bar{\nu}.$$

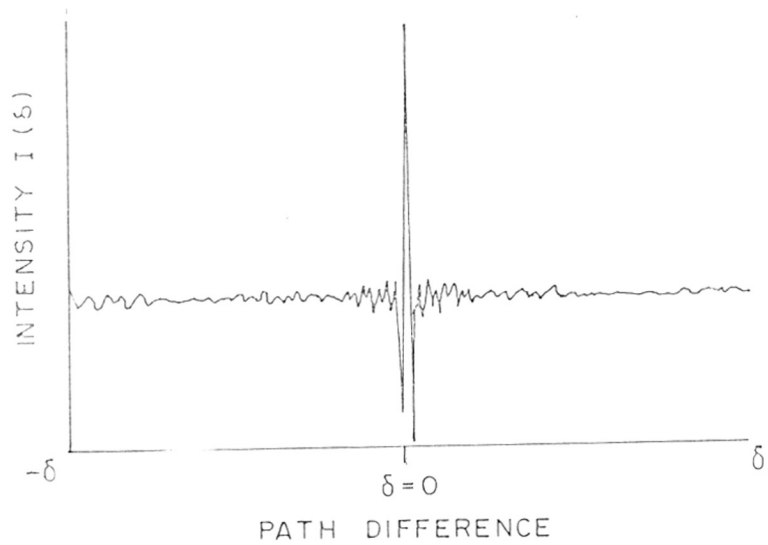
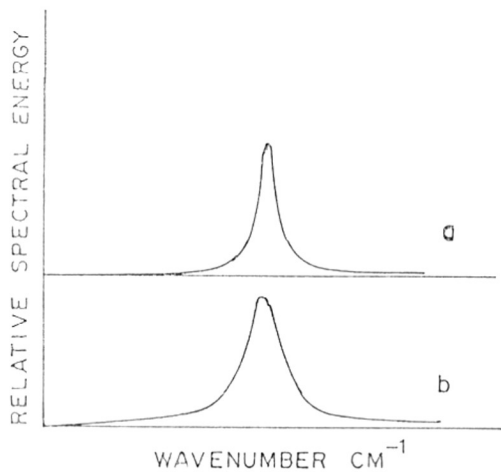
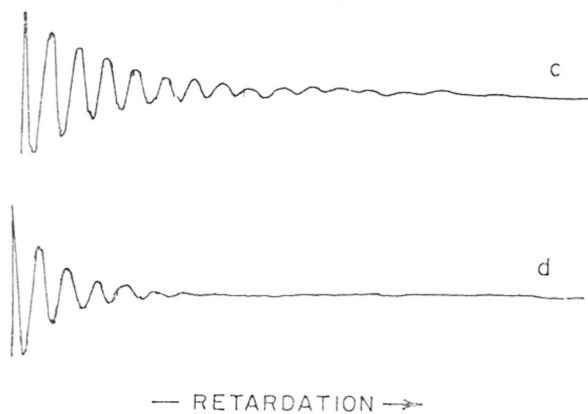


FIG. 9. INTERFEROGRAM FROM A TYPICAL INFRARED GLOWER



a) A LORENTZIAN BAND

b) A LORENTZIAN BAND AT THE SAME WAVENUMBER AS 'a'
BUT OF TWICE THE WIDTH



c AND d THE CORRESPONDING INTERFEROGRAMS

FIG. 10. SIMPLE SPECTRA AND INTERFEROGRAMS

In theory one can obtain a complete spectrum from 0 to $+\infty$ (in cm^{-1}) at infinitely high resolution provided the moving mirror is scanned to infinitely long distance with retardation (δ) varying between 0 to $+\infty$ centimeters. If there are two frequencies (Fig. 11) ν_1 and ν_2 separated by $\Delta\nu$, the two cosine waves come in phase after a retardation of $(\Delta\nu)^{-1}$. To go through one complete period of beat frequency, a retardation of $(\Delta\nu)^{-1}$ is required. The smaller the separation between the frequencies, larger is the retardation of the interferogram, $\Delta_{\text{max}} = \frac{1}{\Delta\nu}$. For resolution of one cm^{-1} , the retardation should be at least one cm.

Since the retardation has to be finite, we would examine how this affects the desired spectrum. By restricting the maximum retardation of the interferogram from infinity to (L) , we are effectively multiplying the complete sine wave interferogram (Fig.12b) (between $+\infty$ to $-\infty$) by a truncation function $D(x) = 1$ $|x| \leq L$, $D(x) = 0$ $|x| > L$ (Box car function). When this truncated interferogram (Fig.12c) is Fourier transformed so that, a single line (Fig. 12a) in the original polychromatic spectrum would generate into a band (Fig. 12d) which would have a half band width given by $\Delta\nu_{1/2} = 1.207/2L$ with a maximum of 21% side lobes at interval of $n/2\Delta$ where $n = 1, 2, 3$. The amplitude of these side lobes can be reduced to a certain degree and the procedure is known as apodization. Various apodization functions like triangular, trapezoidal, Bessel, Gaussian and cosine can be used and each of this would result in its own line shape.

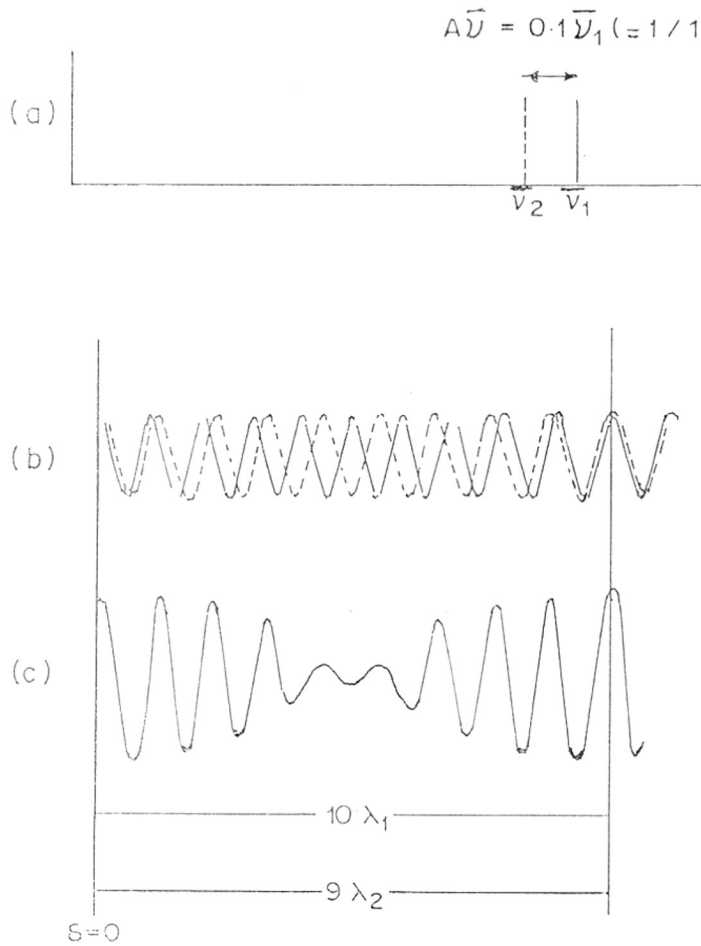


FIG. 11. (a) SPECTRUM OF TWO LINES OF EQUAL INTENSITY AT WAVENUMBERS $\bar{\nu}_1$ (SOLID LINE) AND $\bar{\nu}_2$ (BROKEN LINE) SEPARATED BY $0.1\bar{\nu}_1$

(b) INTERFEROGRAM FOR EACH SPECTRAL LINE SHOWN INDIVIDUALLY AS SOLID AND BROKEN LINES, RESPECTIVELY.

(c) RESULTANT INTERFEROGRAM WITH THE FIRST MAXIMUM OF THE BEAT SIGNAL AT $10/\bar{\nu}_1$

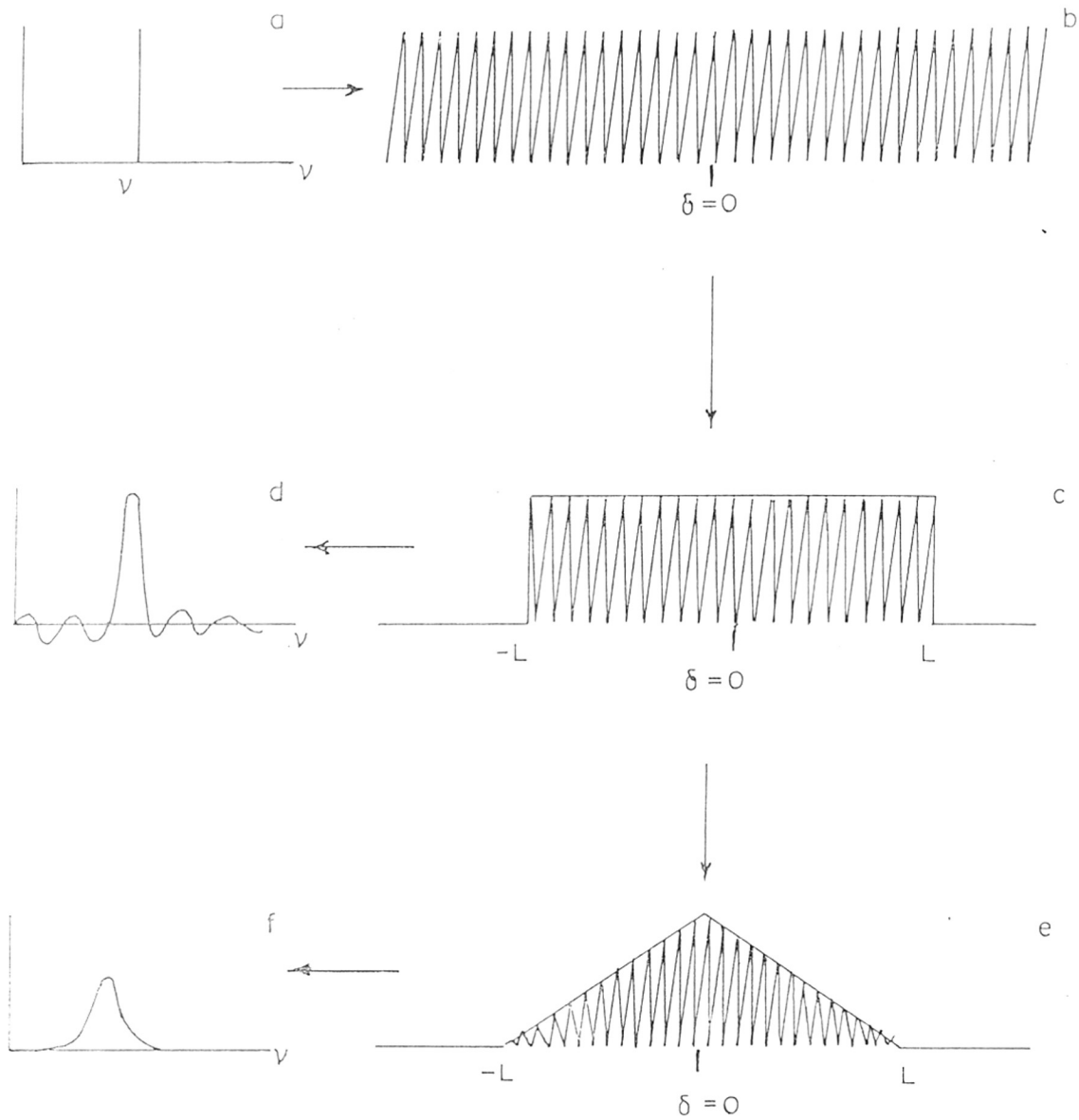


FIG. 12 .

Fig. 12 : Effect of restriction of the path difference
from infinite to finite values

a : Sharp line.

b : Resulting interferogram at infinite path difference.

c : The interferogram when the path difference is finite.

d : The resulting band from the truncated interferogram.

e : The interferogram multiplied by triangular apodization
function.

f : The band resulting from interferogram (e).

The effect of triangular apodization is shown in Fig.12e and the resulting band in Fig.12f. Comparing the bands in Fig. 12d and Fig.12f, it can be seen that the side lobes are reduced from 21% to 4.5% by using triangular apodization and the half band width has increased from $1.207/2L$ to $1.772/2L$.

Happ-Genzel function recommended by the manufacturers of several commercial FTIR spectrometers including Nicolet, are given by $\Delta(\delta) = 0.54 + 0.46 \cos 2\pi\delta/\Delta$, where Δ is maximum retardation in cms and is quite similar to triangular apodization function.

ADVANTAGES OF FTIR

Most of the applications of FTIR spectroscopy are based largely on the increased energy at the detector which may be 10-100 fold compared to the dispersive systems, so that small amounts of materials can be detected. This increased sensitivity is the result of the following advantages, which are inherent in the Michelson interferometer.

(1) : Multiplex (Fellgett) Advantage

All frequencies are measured simultaneously in an interferometer. A complete spectrum can be obtained very rapidly and many scans can be accumulated in the time taken for a single scan of dispersive spectrometer.

(2) : Throughput (Jacquinot) Advantage

The energy throughput in an interferometer is higher than

the dispersive spectrometer, where it is restricted by slits, so that a higher signal to noise ratio is achievable at a shorter time.

(3) : Connes Advantage

The frequency scale of an interferometer is derived from a helium-neon laser, which acts as an internal reference for scans so that the automatic calibration (accurate to 0.1 cm^{-1}) is achieved with much better long term stability.

(4) : Stray Light

Because of the modulation that takes place in an interferometer, there is no stray light.

(5) : Resolution

Resolution is constant in all the regions of the spectrum while it varies in a conventional spectrometer due to change in dispersion.

(6) : Discontinuities

There are no discontinuities in spectral recording which are common in dispersive spectrometers using gratings and filters.

A large variety of samples, whose infrared spectra are difficult to record due to factors like large scattering and therefore poor transmission, ($\sim 5\%$ or less), can be analysed in FTIR.

Many samples which have high absorption (opaque) so that there is hardly any transmitted light, like coal, vulcanised

products containing carbon black, can be analysed using photo-acoustic cell in FTIR.

It is well known that aqueous solutions are difficult to analyse in infrared spectroscopy due to strong absorption of water. But these spectra can be recorded in FTIR using a CIRCLE cell.

Transient species (short lived species) with life time of about 0.02 sec. can be studied using FTIR where fast responding detectors are used.

2.2 INTEGRATED ABSORPTION INTENSITY⁹⁰⁻⁹³

The integrated absorption intensity (B) is a quantity having greater theoretical significance than molar extinction coefficient as given by Lambert-Beer's Law,

$$\epsilon_{\nu} = (1/CL) \log (I_0/I)_{\nu}$$

It is defined as

$$\begin{aligned} B &= \int k d\nu \\ &= 2.303 \int \epsilon d\nu \end{aligned}$$

To determine the area beneath the absorption curve, the integration should be taken over the entire band (which theoretically ranges from $-\infty$ to $+\infty$).

Since integrated absorption intensity is a measure of total energy absorbed by the group over the entire absorption range, it

is a better criterion of band intensity than the molar extinction coefficient. The integrated intensity can be determined by a number of methods such as that of Wilson and Wells⁹⁴ by direct integration, from absorption areas, etc. The knowledge of the shape of an absorption band facilitates the computation.

It has been shown that the peak height and the band width of the spectral band are dependent on the slit function. Thus, an increase in slit width reduces the peak height with simultaneous increase of band width. However, the area of the band remains unchanged. The integrated intensities are therefore used to measure concentrations in the present studies $A = BCL$ where $A =$ Area of the band in cm^{-1} ,

$B =$ Integrated absorption intensity in $\text{mole}^{-1} \text{ dm}^3 \text{ cm}^{-2}$,

$C =$ Concentration in gm mole/litre,

$L =$ Path length in cms.

2.3. THE SHAPES OF INFRARED ABSORPTION BANDS

The infrared absorption bands of liquids are in general much broader ($\Delta\nu_{1/2}$, 10 to 100 cm^{-1}) than those of gases and vapours ($\sim 10^{-1} \text{ cm}^{-1}$). No single mathematical expression can describe an infrared absorption band uniquely as both physical and instrumental factors change the true band shape. Several attempts have been made to derive empirical relation to fit IR absorption bands. The bands are assumed to be symmetrical about the maxima.

The Lorentz shape has been widely assumed to apply to the profiles of infrared absorption bands of liquids. Sheshadri and Jones⁹⁵ have given the general Cauchy function as

$$Y = \frac{a}{x^2 + b^2}$$

where a/b^2 = absorbance and b = half of half band width. Hydrogen bonding and solute solvent interactions have been found to induce a Gaussian component in the band shape which may be represented by,

$$Y_g = \frac{a}{b^2} \exp \left(- (\nu - \nu_0)^2 \ln 2 / b^2 \right)$$

2.4. BAND RESOLUTION TECHNIQUES

Quantitative analysis using infrared band areas requires the separation of the bands closely spaced and overlapped. A complex envelope consisting of two or more overlapping bands can be separated by various methods.

(i) Graphical Separation

The method of the separation of band profile into two or more bands is based on the facts that the absorbances of two or more species at a given frequency are additive and shape of each absorption band is symmetrical about band maximum. However, this requires the knowledge of the band positions and half band widths of individual components. If one half of any band is free from overlap, the reflection around its band maximum is possible and the separation is fairly reliable. In the extreme case of band overlap it is often difficult to decide on the individual band

position and half band width making the graphical separation a very unsatisfactory method.

(ii) Use of Analog Computer

The analog computers have been used for the purpose of curve resolution in the form of an oscilloscope display commonly known as curve resolver⁸¹. The general approach is to simulate the component curves and then add them together for comparison with the observed envelope. The operation is continued until the sum of simulated curves matches the observed spectral curve. This is however a very tedious method requiring again the knowledge of band position and width.

(iii) Use of Digital Computer : LORGAVS Programme

In all 3 parameters are necessary for representing a Gaussian or a Cauchy profile, while a linear combination of these functions such as a sum function needs 4 parameters to be defined. Further, for a system of N different bands would involve optimization of 3N or 4N parameters which certainly is a formidable task.

The various optimization procedures developed so far fall broadly in two categories :

(1) Direct grid search methods, and (2) Gradient methods⁹⁶. The direct search method, though effective, is very time consuming. In the gradient search method which is used in this LORGAVS programme, the first derivative of the function with respect to each variable are computed to guide the search. The

least square procedure seeks to find particular values of parameters $P_j = P_1, P_2, \dots$ which yield an optimum fit of the function $Y(x, P_j)$ to a set of discrete data Y_i versus X_i in the sense of minimizing the unweighted sum of the squares of deviations as

$$S = \sum_i (Y(x_i, P_j) - Y_i)^2 = \text{minimum.}$$

The square of difference is minimized until it reaches or falls below threshold determined by original measurement uncertainty i.e. below a minimum defined by expression

$$\delta \ll Sd^2 \times M$$

where Sd is the standard deviation of measurement and M is the total number of ordinate points. A maximum significant fit is said to be achieved when the quantity S approaches or equals δ .

A commonly used approach to solve a set of non-linear simultaneous equations is to expand the function in Taylor series⁹⁷ which can be truncated at an appropriate stage to yield a polynomial approximation. Such treatment is possible provided the function is continuous and easily differentiable. The method requires approximate estimate of parameters such as peak height, position and band width. If the initially estimated parameters are denoted as P_{j0} , the method seeks to find the corrections ΔP_j such that

$$P_j = P_{j0} + \Delta P_j$$

The least squares procedure then calculates the set of corrections which minimizes the least square criterion given by

$$S = \sum_i (Y(x_i, P_{j0} + \Delta P_j) - Y_i)^2$$

The corrections will be small provided the initial estimates of P_{j0} are good and Y can be proximated by a truncated Taylor series expansion about P_{j0} as

$$Y(x_i, P_{j0} + \Delta P_j) \simeq Y(x_i, P_{j0}) + \sum_j (Y'_{ij}) \Delta P_j$$

where $Y'_{ij} = \partial Y / \partial P_j$ are the partial derivatives of Y with respect to parameters P_j and are evaluated at each X_i and with P_j at P_{j0} . The minimization then becomes

$$S = \sum_i (Y(x_i, P_{j0}) + \sum_j (Y'_{ij}) \Delta P_j - Y_i)^2 = \text{minimum.}$$

If N is the total number of components in the spectrum, a set of $3N$ simultaneous normal equations are obtained for Lorentzian or Gaussian profile by taking each $\partial S / \partial \Delta P_j = 0$

In a matrix notation these equations can be written as $A \cdot \Delta P = B$ where the elements of A and B matrices are given by

$$A_{kl} = \sum_i (Y'_{ik}) (Y'_{il})$$

$$B_k = \sum_i (Y'_{ik}) [Y_i - Y(x_i, P_k^0)]$$

The indices k and l refer to component peaks. The inversion procedure yields the correction vector ΔP which when added to the initial estimate P_j , yield a refined set of estimates of P_j

which are used for the next iteration. The procedure is repeated until the corrections become very small.

The programme LORGAVS uses either Lorentzian or Gaussian distribution equation. The two main features of the programme are (1) Rapid convergence to solution, and (2) A character printer plot output which enables viewer to observe the goodness of fit. The error curve is also plotted. The respective band areas are obtained using the optimized band parameters. It was generally observed that the programme LORGAVS converges to a solution even if the initial estimates of parameters are appreciably deviating from the true values as it involves only three unknown parameters.

(iv) Fourier Deconvolution

We had seen that separation of strongly overlapped closely lying bands is highly uncertain by both graphical and analog computational methods, as the individual band parameters required for an effective separation cannot be made out from the overall band profile. For a long time the need for a reliable method which does not require the pre-knowledge of the band parameters was felt. Fourier Deconvolution technique was first described by Stone⁸² and more recently has been discussed in some detail in a series of three papers by Kauppinen et. al.^{31,32,98}. Fourier Deconvolution was developed for infrared spectroscopy by a group at the National Research Council of Canada, which has much experience in band shape analysis. This method provides a way of computationally resolving overlapped lines that cannot be

resolved instrumentally due to their intrinsic line width and proximity. This does not increase the instrumental resolution but the spectral resolution is improved by an enhancement factor (i.e. the ratio of half band widths before and after deconvolution). The spectra having moderate signal to noise ratio (1000:1) can attain an improvement of 3 in the spectral resolution by this method.

The infrared band contour can be considered as the result of a convolution of a sharp line with a Lorentzian/Gaussian line shape. The removal of this line shape to enhance apparent resolution is called Deconvolution. The deconvolution is carried out more efficiently from the interferograms as the mathematical functions required to be used for the purpose are simple multiplications rather than complex functions required from frequency spectra. However, Friesen et al⁹⁹ have tried deconvolution in frequency domain.

To examine what is deconvolution let us start with a single Lorentzian band (Fig. 13a) with a line shape function

$$E_0(\bar{\nu}) = \frac{6/\pi}{6^2 + \bar{\nu}^2}$$

where 2δ is the width at half height. We had seen earlier that the interferogram of such a band has the shape of decaying sine wave (Fig. 13b). If this interferogram is multiplied by a function $(\exp -2\pi\delta x)$ where x is the path difference which can

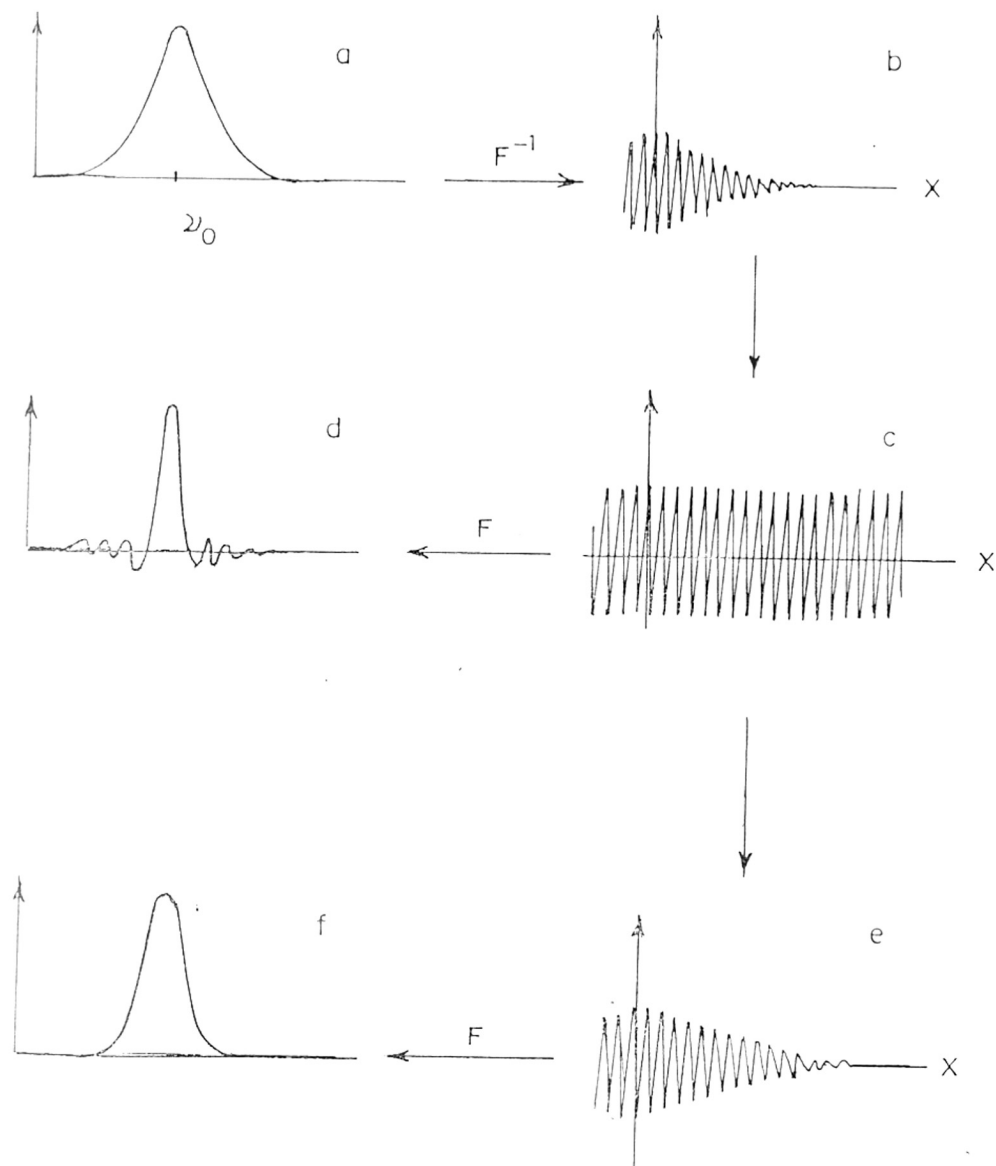


FIG. 13.

Fig. 13 : Fourier Deconvolution

- a : A Lorentzian band.
- b : Decaying sine wave interferogram of (a).
- c : The sine wave interferogram after multiplying
by $\exp 2\pi\epsilon|x|$
- d : The band resulting from interferogram (c).
- e : The interferogram (c) multiplied by Bessel function.
- f : The band resulting from interferogram (e).

have a maximum value of L , it can be shown that we will get a sine wave interferogram (Fig. 13c) which we had seen on Fourier transform would give a spectrum (Fig. 13d) with half band width $1.207/2L$ and side lobes with $\sim 21\%$ maximum intensity. To reduce these side lobes in the spectrum, the interferogram was multiplied by apodization functions. Among the various apodization functions available, we have used the Bessel function $D(x)[1-(X/L)^2]^2$ (Fig. 13e) which gives a band (Fig. 13f) with half band width $1.904/2L$ and side lobes $\approx -4.1\%$. These modified interferograms on Fourier transform would give spectra with half band widths which are much smaller than the original spectra and the ratio of original half band width to final half band width is known as Resolution enhancement factor. In practice this is used as a variable to determine the extent of deconvolution for a given value of initial band width.

One very important feature of Deconvolution is that individual band areas are not altered by the process. Thus quantitative information can be taken from the spectra with enhanced resolution.

2.5 HYDROGEN BONDING^{100,101,102}

In A-H..B type hydrogen bonding a specific covalent A-H group interacts with an acceptor site B. The A-H bond is thereby weakened but not broken. When the covalent A-H bond is broken to form the anion A^- and the protonated base $H-B^+$, we may no longer have hydrogen bonding but an acid-base reaction with proton

transfer.

The formation of a hydrogen bond A-H...B between a proton donor acid and a proton acceptor base is determined by the acidity of the former and the basicity of the latter. In contrast to the complete transfer of a proton in a conventional Bronsted acid-base equilibrium, the formation of the hydrogen bond results only in partial proton transfer, the proton remains in the first potential minimum near A (Fig. 14a). Proton transfer from A to B in a hydrogen bond A-H...B can occur along a potential energy curve similar to one shown in Fig. 14a and b by two mechanisms, quantum mechanical tunneling through the potential barrier separating the two minima and/or direct transfer over the barrier. The latter case can be expected to occur with the resulting formation of a proton transfer complex $A^{\ominus} \dots H-B^{\oplus}$ in a non-polar solvent, whenever the acidity of the proton donor and/or the basicity of the proton acceptor are sufficiently strong. The transition from a hydrogen bonded complex to a proton transfer complex is accompanied by appreciable changes in the IR absorption spectra of the system. The disappearance of the A-H bands and the appearance of the B^{\oplus} -H bands have been observed in the IR spectra of mixtures of some carboxylic acids with pyridine¹⁰³ in $CHCl_3$.

Two other factors, besides the acidity of the proton donor and the basicity of the proton acceptor, can influence proton transfer in a hydrogen bonded complex in solution. One is the

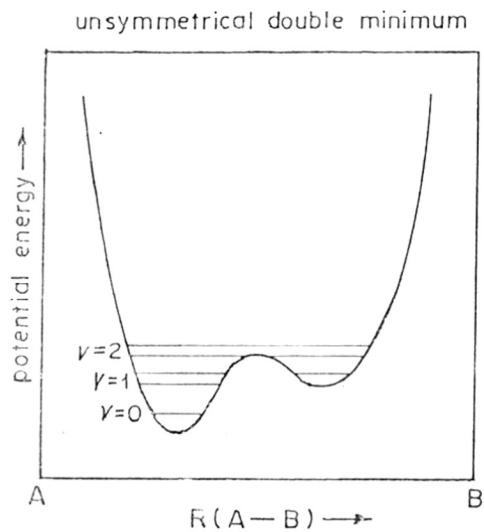


FIG. 14 a.

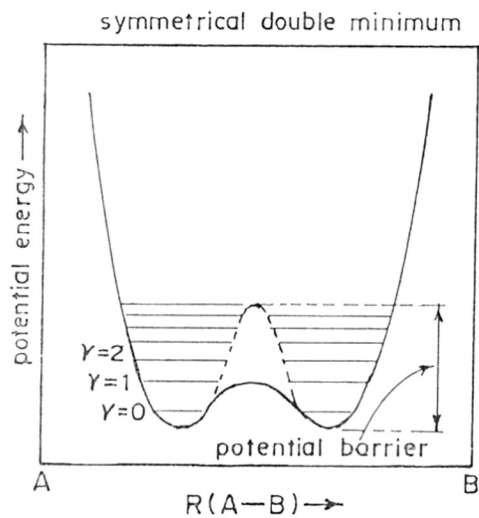


FIG. 14 b.

polarity of the solvent and the other is the specific solvation of the proton transfer complex. The formation of the proton transfer complex results in charge separation and hence should be favoured over the hydrogen bonded complex in solvents with increasing polarity. The formation of proton transfer complexes is accompanied by large increase in dipole moment because of the charge separation. The dipole moments in the range 3-10 D are probably due to the coexistence of hydrogen bonded and proton transfer complexes¹⁰⁴.

Hydrogen bonding between a proton donor group A-H and an acceptor site B (A-H...B) weakens the force constant of the A-H stretching mode and shifts vibrational frequency to a lower value. Stronger the hydrogen bond larger is the shift ($\Delta\nu$) and this is used to detect hydrogen bond formation. The anharmonicity and rate of change of dipole moment ($d\mu/dr$) associated with the A-H stretching vibration increases on hydrogen bonding resulting in an increase in the half band width and the integrated absorption intensity.

H-bond formation increases A-H deformation force constant by constraining the deformation mode and shifts to higher frequency. This shift is appreciably smaller than in A-H stretching mode.

The vibrational modes of the proton acceptor B are also affected by H-bonding. But the frequency shifts are much smaller than those of the donor A-H vibrations. New vibrational modes corresponding to the stretching and bending of H...B bond are found in the far infrared region (below 400 cm^{-1}).

Of all the four changes, the change in the A-H stretching is the most sensitive and therefore has been extensively used in studying H-bond.



CHAPTER III

EXPERIMENTAL



3.1. N-ACETYL(AMINO ACID) N'-METHYL AMIDES

3.1.1. : Preparation and Purification

For preparation of N-acetyl(glycine, L-alanine, L-leucine) N'-methyl amide, the starting materials i.e. glycine, L-alanine and L-leucine were Fluka Puriss/Purum grade chemicals. In each case, amino acid ester hydrochloride was first prepared by passing HCl gas through amino acid dissolved in methanol at 0°C. By using the method of Apple White and Nieman¹⁰⁵, acetyl derivatives and their N'-methyl/dimethyl derivatives were prepared. N-acetyl glycine N'-methyl amide (AGMA) and N-acetyl L-alanine N'-methyl amide (AAMA) were recrystallized at least five times from an ethanol-ethyl acetate mixture (1:9). N-acetyl L-leucine N'-methyl amide (ALMA) was recrystallized from an ethyl acetate-hexane mixture (1:1). N-acetyl glycine N'-dimethyl amide (AGDMA) was purified with difficulty due to its high solubility in organic solvents and low melting point. It was recrystallized from ethyl acetate-hexane mixture (1:1) five times. In the case of N-acetyl sarcosine N'-methyl amide (ASMA), sarcosine was synthesized using chloroacetic acid and methyl amine¹⁰⁶. The purity of all the N-acetyl (amino acid) N'-methylamides was checked by their melting points and microanalyses (Table I).

Pure N-methyl acetamide was obtained from Analytical Fluka grade sample by recrystallization from ethanol.

Merck reagent grade chloroform was washed with water five times with vigorous stirring and dried over calcium chloride (2

days). It was then distilled twice and stored in dark. It was finally dried over molecular sieves (Linde 4A) by keeping over it for an hour before use.

TABLE I : Melting Point and Microanalysis

	m.p.(^o C)	Observed %			Calculated %		
		C	H	N	C	H	N
1. AGMA	158	45.7	7.63	21.1	46.1	7.7	21.5
2. AAMA	182	50.5	8.37	19.0	50.0	8.3	19.4
3. ALMA	165	58.5	10.0	13.9	58.0	9.65	15.0
4. AGDMA	50	48.5	8.51	17.3	50.0	8.3	19.4
5. ASMA	62	48.5	8.62	17.8	50.0	8.3	19.4

3.1.2 : Spectroscopic Measurements

The spectra were recorded on a Perkin-Elmer 221 Infrared Spectrophotometer using an expanded scale ($100 \text{ cm}^{-1} / 8 \text{ cm}$) in the range $3500\text{--}3350 \text{ cm}^{-1}$. Calibration was checked using atmospheric water vapour and carbon dioxide bands. Operating parameters : Slit programme (970 x 2), suppression 4, attenuator speed 1100 and amplifier gain 2.5, were used. Variable path length cells with 4 cm path length (varying from 3.7 to 4.2 cm) made in NCL workshop and similar to Perkin-Elmer standard variable path length cells, were used for all measurements.

The spectrum of N-acetyl glycine N'-methyl amide was resolved into two component bands by using non-linear least

square curve analysis (LORGAUS programme)⁹⁶. For computational work, the spectral envelope was digitized manually at uniformly close intervals (2.5 cm^{-1}) in the frequency range $3500\text{--}3350 \text{ cm}^{-1}$. The best band parameters (position, absorbance and half band width) with minimum standard deviation as well as the areas of the component bands with Lorentzian band shape (LORGAUS programme) were obtained directly from the print outs. Since the LORGAUS programme gave unsatisfactory results in the case of N-acetyl L-alanine and L-leucine N'-methyl amides, the broad NH absorption band was resolved into three components by using graphical method. The areas of the individual bands were then measured by summing up the respective absorbance values and multiplying by the common frequency interval. Appropriate wing corrections were then applied.

In order to determine the concentrations of free and bonded NH groups in these compounds, the integrated absorption intensities of free and bonded NH groups in N-methyl acetamide and N-acetyl glycine N'-dimethyl amide respectively, were determined from the band areas at a few known low concentrations. The mean integrated absorption intensity of NH group of N-methyl acetamide, measured in dilute chloroform solution at three concentrations ($1\text{--}5 \times 10^{-3} \text{ M}$), using procedures reported earlier¹⁰⁷ gave a value of $7.1 \times 10^3 \text{ dm}^3 \text{ mol}^{-1} \text{ cm}^{-2}$. This can only be compared with the values reported for N-methyl acetamide in carbon tetrachloride ($4.3 \times 10^3 \text{ dm}^3 \text{ mol}^{-1} \text{ cm}^{-2}$ ¹⁰⁸ and $5.8 \times 10^3 \text{ dm}^3 \text{ mol}^{-1} \text{ cm}^{-2}$)¹⁰⁹. The free NH integrated absorption intensity (B) has been

reported for a number of N-alkyl acetamides¹⁰⁸ also in carbon tetrachloride which showed a variation of 20% ($18-22 \times 10^{-8} \text{ cm}^2 \text{ mol}^{-1} \text{ S}^{-1}$ i.e. $3.6-4.4 \times 10^3 \text{ dm}^3 \text{ mol}^{-1} \text{ cm}^{-2}$), so that its use as a standard for measuring the free NH group concentration can be justified.

The spectrum of N-acetyl glycine N'-dimethyl amide in chloroform showed a strong band at 3405 cm^{-1} with a weak shoulder at 3445 cm^{-1} ascribable to a small amount of free NH species. Maxfield et. al.¹⁸ found only a single band for this compound in chloroform. In carbon tetrachloride, however, two bands at 3460 and 3412 cm^{-1} for dimethyl¹¹⁰ and 3460 and 3415 cm^{-1} for diethyl¹¹ derivatives, have been reported. N-acetyl amino acid esters¹¹¹ in dilute carbon tetrachloride solution exists as a mixture of the intramolecularly hydrogen bonded five membered ring and free species. Due to the weak nature of intramolecular hydrogen bond, the extent of stabilization offered is small and a certain amount of free species would be expected. The concentration of the free NH band was estimated to be 8% from band area measurements and the integrated absorption intensity of the five membered intramolecularly hydrogen bonded NH group was found to be $14 \times 10^3 \text{ dm}^3 \text{ mol}^{-1} \text{ cm}^{-2}$, which was used for further calculation.

3.1.3. Calculations of concentrations of various species

The concentration of the various free and intramolecularly hydrogen bonded NH species in N-acetyl amino acid N'-methyl

amides were determined from their separated band areas using the integrated absorption intensities of the free and intramolecularly hydrogen bonded NH groups at 3460 cm^{-1} in N-methyl acetamide and at 3405 cm^{-1} in acetyl glycine dimethyl amide, respectively, using the equation $B = A/CL$, where A is the area of the band, C is the concentration in gm mole/litre and L is path length in cms.

Since two free NH groups would contribute twice the intensity of a free NH group (Fig. 1a) and intramolecularly hydrogen bonded five membered ring species (Fig. 2a) would contribute one free NH group intensity, following equations can be written :

$$\begin{aligned} C_I &= C_B \\ C_A &= C_S - C_B \end{aligned}$$

where C_S is the solution concentration, C_I is the concentration of intramolecularly hydrogen bonded species and C_B is the concentration of the bonded species. The C_F (concentration of free species) values can be used as a check on the results since $C_F = 2C_A + C_B$.

3.2. 2-DIMETHYL AMINO BENZOIC ACID

3.2.1. Preparation and Purification

2-Dimethyl amino benzoic acid (dimethyl anthranilic acid, DMA) was obtained by the hydrolysis of the methyl ester of DMA formed by the reaction of anthranilic acid with dimethyl sulphate²². The sample was recrystallized from ether many times to obtain a melting point of 68°C and the percentages of carbon,

hydrogen and nitrogen were found to be 65, 6.9 and 8.4 respectively, from microanalysis. (The calculated values of the percentages of carbon, hydrogen and nitrogen were 65.4, 6.6 and 8.5 respectively). The solvents used in the present work, cyclohexane, carbon tetrachloride, benzene, dioxane, chloroform and acetonitrile were laboratory or analytical reagent grade, while methanol was spectroscopic grade. Reagent grade dimethyl sulphoxide was dried over calcium hydride and vacuum distilled. All the solvents were finally dried over Linde 4A molecular sieves before use. Heavy water (99.9%) was obtained from the Atomic Energy Commission, Trombay, India.

3.2.2. Spectroscopic Measurements

Spectral measurements of DMA were carried out on Nicolet 60SXB Fourier Transform Infrared spectrometer. Since water vapour and carbon dioxide concentrations in the single beam path of FT instrument have to be reduced to give at least 95% transmission in their respective absorption region, the instrument was purged by compressed air supply which was dried over molecular sieves and freed from CO_2 at 80-100 lbs/sq. inch. Before the data collection was initiated, the resolution (2 cm^{-1}) and the number of scans (100) were specified to obtain signal to noise ratio of 1000:1. Once the interferograms had been collected, the apodization (Happ-Genzel function) and phase corrections were applied. Interferograms were then co-added and stored. The next step was transformation of the data to a spectrum. First, the background

spectrum was stored in a file. Then the spectrum of solvent under similar conditions was ratioed against the background spectrum and stored in a reference file. The spectrum of solution was then similarly obtained in the same cell and ratioed against the background spectrum and stored in a sample file. The transmittance spectra were then converted into linear absorbance spectra. The solvent spectrum was then subtracted from the solution spectrum.

The spectra of DMA were recorded in various solvents in the region $1750-1600\text{ cm}^{-1}$, since there are strong water vapour absorptions in this region, the instrument was purged for sufficiently long time to obtain nearly 95% transmission in this region. The solution concentration of 0.06M was maintained in all solvents i.e. carbon tetrachloride, benzene, dioxane, acetonitrile, chloroform, dimethyl sulphoxide, methanol and D_2O except cyclohexane where solubility permitted only $\sim 0.01\text{M}$ solution. The path length was kept constant at 0.01 cm. except D_2O where it was reduced to 0.0025 cm.

Deconvolution was performed for DMA spectra in various solvents using the original NRC programme adopted for use on Nicolet SX systems^{112,113}. The compiled programme IRD-CON·FTN (the macro CON required to call the programme from FTIR) takes a region of the absorbance spectrum stored in OFN file as defined by XSP (starting point on X-axis) and XEP (end point on X-axis) and creates an interferogram of only this region. The Deconvolution is carried out by multiplying this interferogram by a function and then transforming it back to give the Deconvoluted spectrum.

There are two variables in the programme. The first variable νF_0 is the half band width of the Lorentzian line being used for the Deconvolution. The second variable νF_1 , is the resolution enhancement factor. All the points past a point L on the interferogram are set to zero by the programme, where L is proportional to $\nu F_0/\nu F_1$. Concentration of each solution was so adjusted that the maximum absorbance in the spectrum was < 1 . Since the number of calculations were high, the files should not contain more than 512 data points. The variables νF_0 and νF_1 were chosen to be 14-18 cm^{-1} in line with normal carbonyl half band widths^{and} 1.4 to 2.2, respectively. The areas under the original spectra and the deconvoluted spectra (as measured by the computer) were maintained the same. No side lobes were allowed to be shown in the deconvoluted spectra. The separated band positions were then used for determining the various structural species in DMA.

3.3 n-ALCOHOLS

3.3.1. Purification

The n-alcohols used for the present work were Analar E. Merck/B.D.H. samples dried over molecular sieves (Linde 4A) and chromatographically tested. Sample purities were ethanol 99.7%, n-propanol 99.7%, n-butanol 99.8%, n-pentanol 99.0% and n-hexanol 97.9%.

3.3.2. Spectroscopic Measurements

Spectral measurements on n-alcohols were carried out on the same Nicolet 60SXB FTIR spectrophotometer as in the case of DMA,

in carbon tetrachloride solution in the frequency range 3675-3575 cm^{-1} at various temperatures. No detectable change in the spectrum of the solvent was observed by heating to 298-328 $^{\circ}\text{K}$ so that the spectrum of solvent at 298 $^{\circ}\text{K}$ was used at all temperatures for subtraction. Dilute solutions of n-alcohols ($\ll 0.011 \text{ M}$) in carbon tetrachloride were used in a variable path length cell (0.8 cm). The path lengths were periodically checked using interference fringes. The cell was fitted with a nichrome heating coil and the heating was controlled by controlling its voltage¹¹⁴. The emf degenerated in a small silicon diode fitted inside the cell in contact with the solution was amplified and displayed on an electronic temperature indicator. This was pre-calibrated with the help of a calibrated standard thermometer to give reliable temperature read out. The accuracy and reproducibility of this device was found to be $\pm 0.5 \text{ K}$ in the temperature range 298 to 328 $^{\circ}\text{K}$.

Fourier Deconvolution was carried out in the range 3675 to 3575 cm^{-1} using the same Nicolet programme described earlier. The variable VFD was chosen in the range 14-18 cm^{-1} close to half band width of methanol. The variable VFI was chosen 1.7 to 2 so that the total band areas after deconvolution remained the same as original band areas. With these parameters separation of the band was obtained without any side lobes and other artifacts. While the band positions could be easily read out from the deconvoluted spectra, the band areas could not be determined due to inadequate band separation. Therefore, after getting the clear



positions of the component bands by deconvolution, they were resolved graphically. The unoverlapped side of low frequency band was reflected about the band maximum to generate its high frequency side which was then subtracted from the deconvoluted spectrum to obtain the second component band. The areas under the graphically resolved bands were obtained by summing the $\ln (T_0/T)_\nu$ values and multiplying by the common frequency interval $d\nu$ given by:

$$A = \sum_{\nu_1}^{\nu_2} \ln (T_0/T)_\nu d\nu$$
$$= 2.303 d\nu \sum_{\nu_1}^{\nu_2} \log_{10} (T_0/T)_\nu$$

where ν_1 and ν_2 are the graphical limits of integration.

The equilibrium constants (k) were calculated at various temperatures (298-328^oK) assuming the integrated absorption intensities of the two component bands to be the same at every temperature. The thermodynamic quantities were computed using the Arrhenius relation

$$\Delta G = -RT \ln k = \Delta H - T \Delta S$$

ΔH° and ΔS° were obtained from the slope and intercept respectively of the graph $\log k$ vs $1/T \times 10^3$ using the method of least squares.

CHAPTER IV
RESULTS AND DISCUSSION

N-ACETYL-AMINO ACID N'-METHYL AMIDE

CONFORMATIONAL ANALYSIS OF N-ACETYL
(GLYCINE, L-ALANINE, L-LEUCINE) N'-METHYL
AMIDE IN CHLOROFORM SOLUTION

4.1. RESULTS AND DISCUSSION

The infrared spectra of N-acetyl glycine N' methyl amide (AGMA), N-acetyl L-alanine N' methyl amide (AAMA) and N-acetyl-L-leucine N' methyl amide (ALMA) in dilute chloroform solution ($\sim 5 \times 10^{-4}$ M) are shown in Fig. 15, 16 and 17, respectively. While the glycine derivative gave two well defined NH stretching bands at 3450 and 3418 cm^{-1} , the L-alanine and L-leucine derivatives showed mainly three bands at 3450, 3433 and 3415 cm^{-1} . The last band in AAMA and ALMA appeared as a shoulder to the band at 3433 cm^{-1} . There is hardly any absorption below 3400 cm^{-1} . These results are in agreement with those of Maxfield et.al.¹⁸, who studied these compounds in the same solvent and found no band below 3400 cm^{-1} at a concentration of $\sim 10^{-4}$ M. However, they found two bands at 3420 and 3410 cm^{-1} for AAMA and three weak bands at 3425, 3415 and 3405 cm^{-1} in ALMA in place of the 3415 cm^{-1} shoulder observed by us in both the compounds. Efremov et. al.¹⁶, however, reported nearly identical three bands above 3400 cm^{-1} for AAMA in chloroform as found by us. In fact, for most dipeptides only a single band at 3420 cm^{-1} is reported^{6,16,20} in dilute carbon tetrachloride solution, in place of the three weak bands reported by Maxfield¹⁸.

Mizushima et.al.⁶, Neel¹⁰ and Efremov et.al.¹⁶ had observed

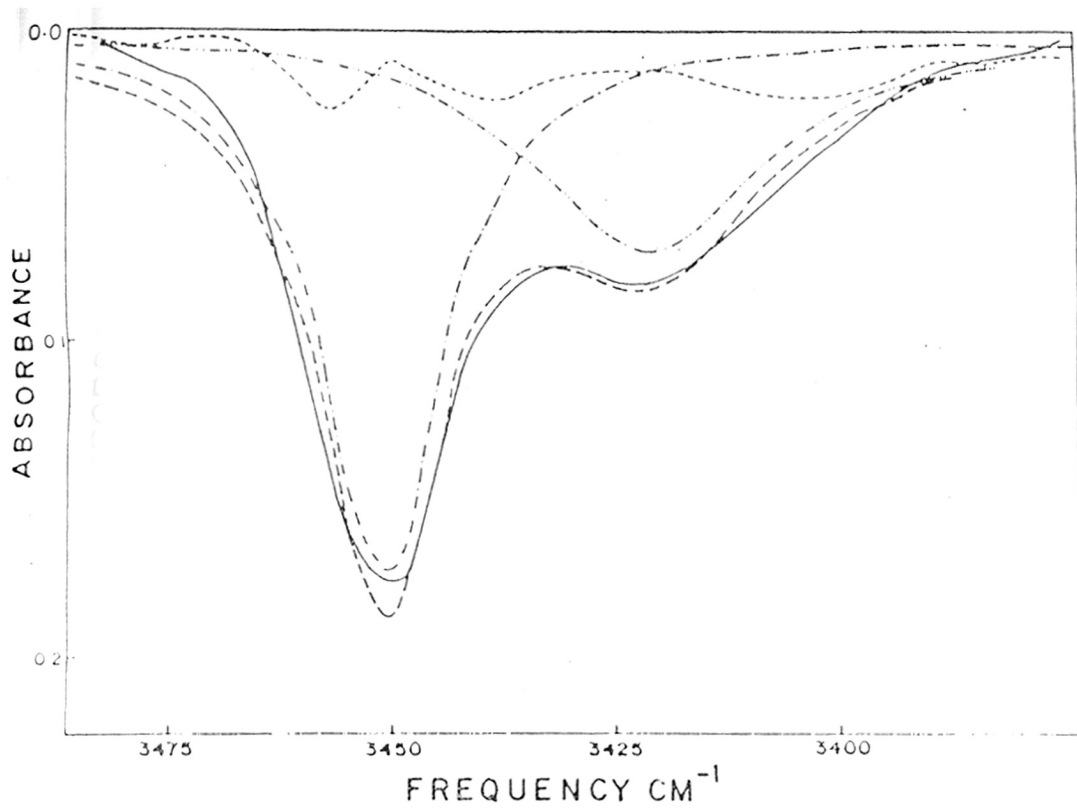


Fig. 15. NH stretching bands of AGMA. (—) Recorded spectrum, (— · — · —) band separation, (---) sum of — · — · —, and (-----) difference.

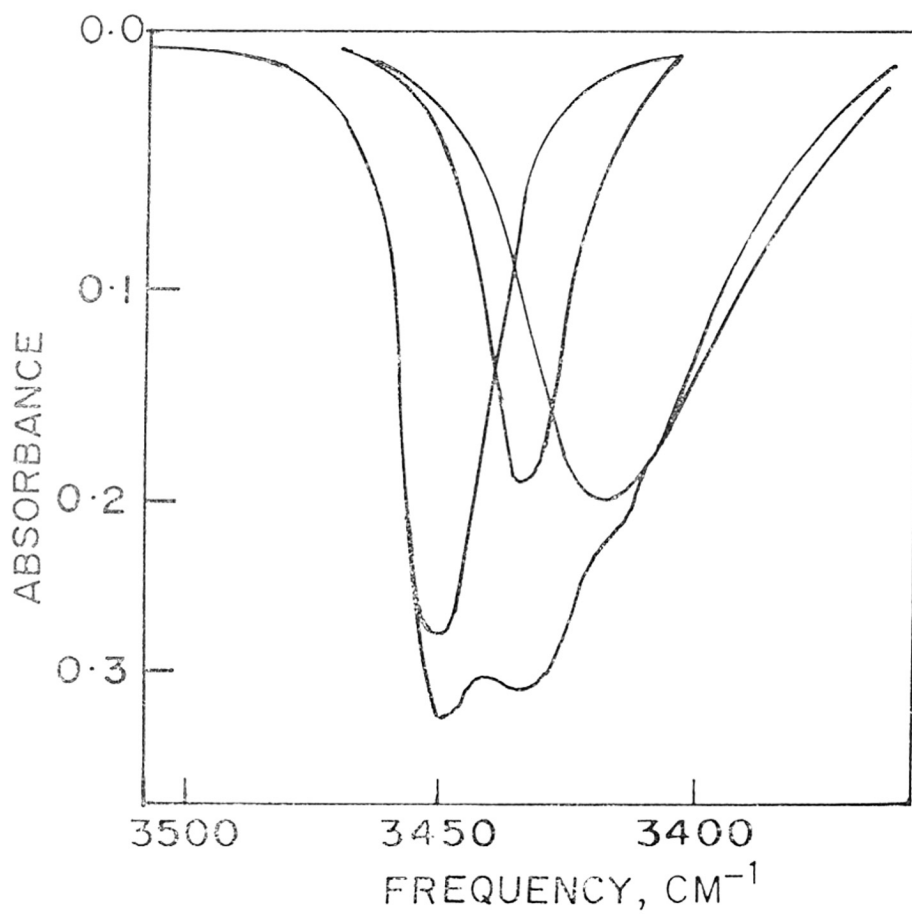


FIG. 16. NH STRETCHING BANDS OF N-ACETYL
L-ALANINE N'-METHYL AMIDE

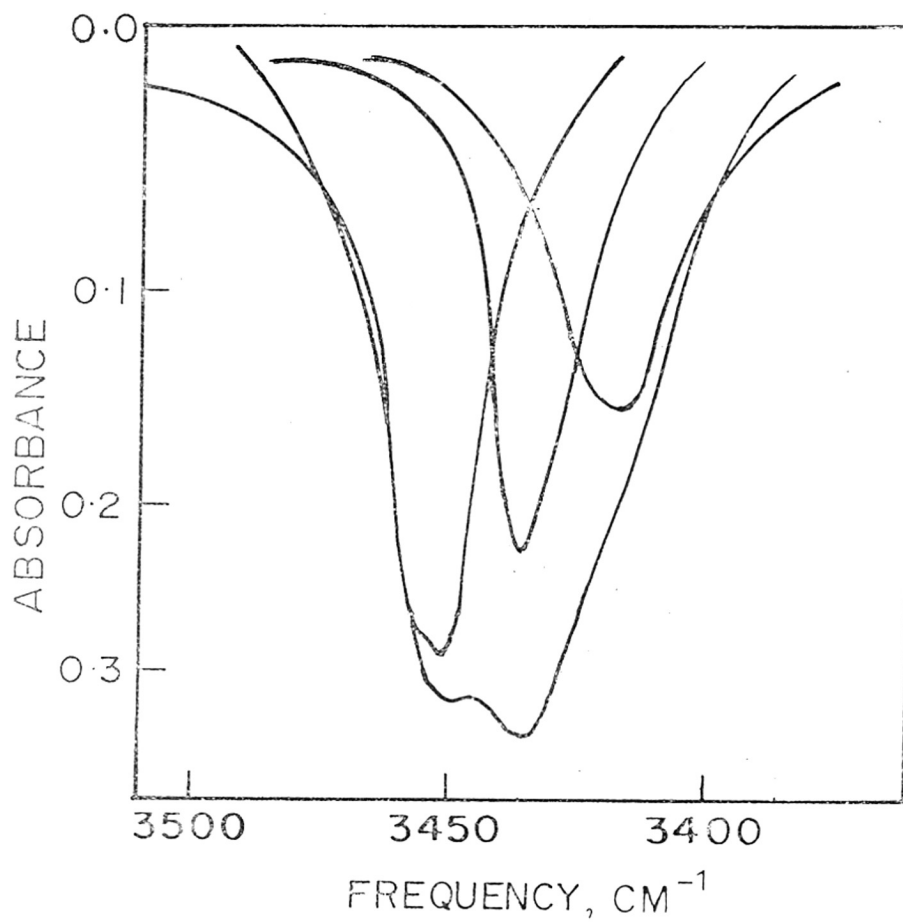


FIG. 17. NH STRETCHING BANDS OF N-ACETYL
L-LEUCINE N¹-METHYL AMIDE

a band at $3300-3360\text{ cm}^{-1}$ in the same dipeptides in dilute carbon tetrachloride solution ($\sim 10^{-4}\text{ M}$) in addition to the bands observed above 3400 cm^{-1} . This band was reported weaker in CHCl_3 relative to that in CCl_4 ¹¹⁵ and was ascribed to the seven-membered intramolecularly hydrogen bonded NH conformers. These species were reported^{8,13} to be as much as 60-75% in glycine, L-alanine and L-leucine derivatives. Efremov et.al.¹⁶ calculated the concentration of the seven-membered ring species to be 30-20% in the various N-acetyl -(amino acid)-N'-methyl amides in dilute chloroform solution. Ginzburg²⁰ has recently reported a band in this region for compounds studied in the present work in dilute CCl_4 solution ($\sim 10^{-4}\text{ M}$). An association band was also located by Maxfield et.al.¹⁸ at higher ($> 10^{-4}\text{ M}$) concentration for the same compounds in this region. Smolikova et.al.¹⁹ found hardly any band in this region for tert-leucine and L-valine derivatives, although a very weak band was observed for L-alanine and L-leucine derivatives in dilute CCl_4 solution ($\sim 2 \times 10^{-5}\text{ M}$).

In order to find out whether the band at $3360-3300\text{ cm}^{-1}$ reported for the title compounds was present in 10^{-4} M CCl_4 solution, we tried to prepare such a solution of AGMA and found that the maximum solubility was close to $5 \times 10^{-6}\text{ M}$. Scheraga et.al.¹⁷ and Maxfield et.al.¹⁸ had also made a similar observation and, further, had shown how the solubility was enhanced in impure CCl_4 containing contaminants like phosgene, HCl, water, etc. A weak broad band at $3370-3300\text{ cm}^{-1}$ was also produced by these impurities as well as by methyl amine from unsublimed AGMA. A

lower solubility ($< 2 \times 10^{-5}$ M) was also found in the case of the L-alanine derivative by us. These results along with those of Smolikova et al.¹⁹, clearly establish that the spectra recorded at 10^{-4} M concentration in carbon tetrachloride by the various workers are suspect and that the band found in the $3360-3300 \text{ cm}^{-1}$ region in both N-acetyl-glycine (and L-alanine)-N'-methyl amides is due to impurities in the solute solvent systems.

The two NH stretching bands in the title compounds at $3460-3440 \text{ cm}^{-1}$ (one NH band in glycine derivatives) are ascribed to the free NH groups, as suggested by nearly all the workers. Burges et al.¹¹⁶ also assigned the band at 3460 cm^{-1} in carbon tetrachloride and at 3450 cm^{-1} in chloroform in glycine derivatives to the free NH stretching vibrations. Though the bands at 3460 and 3440 cm^{-1} were ascribed to free NH groups of extended form (Fig. 1a) by Mizushima et al.⁶, Efremov et al.¹⁶, Maxfield et al.¹⁸ and Smolikova et al.¹⁹ in L-alanine and higher derivatives, Neel¹⁰ and Ginzburg²⁰ assigned these bands to the free NH group of intramolecularly hydrogen bonded five and seven membered ring species, respectively. In the absence of seven-membered intramolecularly hydrogen bonded species the latter assignment will have to be modified. So both the bands are best assigned to free NH of extended form.

With regard to the band at $3420-10 \text{ cm}^{-1}$, Mizushima et al.⁶ and Efremov et al.¹⁶ ascribed it to the free NH group of the seven-membered intramolecularly hydrogen bonded folded form (Fig.

1b). This assignment is untenable now, since it has been shown that the absorption at $3370-3300\text{ cm}^{-1}$ ascribed by them to the seven-membered intramolecularly hydrogen bonded species is actually arising from impurities except in the leucine derivatives. Neel¹⁰ has ascribed the $3420-10\text{ cm}^{-1}$ band to an intramolecularly hydrogen bonded five-membered ring NH in the title compounds in CCl_4 . Marraud et. al.¹¹¹ have found two bands at 3460 and 3440 cm^{-1} in N-acetyl amino acid esters in dilute CCl_4 solution that are ascribed to the free and intramolecularly hydrogen bonded five-membered NH ring species, respectively.

In order to establish the true nature of the absorptions at 3420 cm^{-1} , we recorded the spectrum of N-acetyl glycine N'-dimethyl amide (AGDMA) in dilute chloroform solution which showed two bands at 3445 (weak) and 3405 cm^{-1} (strong). The latter band at 3405 cm^{-1} is very close to 3420 cm^{-1} and can only be ascribed to an intramolecularly hydrogen bonded five-membered ring NH and therefore the band at $\sim 3420\text{ cm}^{-1}$ in the present compounds was assigned to the above species. Further, the absence of $3420-10\text{ cm}^{-1}$ band in the spectrum of N-acetyl sarcosine N'-methyl amide which we have studied and has also been reported¹¹⁷ strongly, supports the above assignment. Thus, the present studies establish that there are only two types of species in dilute CHCl_3 solution of N-acetyl-(amino acid)-N'-methyl amides, the intramolecularly hydrogen bonded five-membered ring species (Fig. 2a) and a form containing only free NH groups (Fig. 1a), also called the non-hydrogen bonded conformation.

In order to determine the concentration of the molecular species in solution, the spectra were resolved using LORGAUS programme discussed in the experimental section. While AGMA spectrum could be separated clearly into two bands, (Fig. 15) we found that the above programme could not resolve AAMA and ALMA spectra in spite of using different values for half band width and position. We believe that the closer proximity of the 3420 cm^{-1} band to the 3440 cm^{-1} band which is present in AAMA and ALMA, is responsible for the difficulty in achieving reasonable separation. So, the graphical method was used for the latter compounds and the spectra were resolved into three bands. The areas of the bands at 3460 and 3440 cm^{-1} assigned to free NH groups were calculated individually and then added to get the area of the non-hydrogen bonded species. The concentrations of the free NH band in the present compounds were determined using the integrated absorption intensity ($7.1 \times 10^3\text{ dm}^3\text{ mole}^{-1}\text{ cm}^{-2}$) of the NH band in N-methyl acetamide in chloroform solution (Fig. 18) determined by us as explained in the experimental section. The area of the band at 3420 cm^{-1} was measured and the appropriate wing correction was applied as explained in the experimental section. From this area, the concentrations of intramolecularly hydrogen bonded five membered ring species (near 3420 cm^{-1}) were determined using the integrated absorption intensity of the bonded NH of AGDMA in chloroform solution (Fig.19) ($14 \times 10^3\text{ dm}^3\text{ mole}^{-1}\text{ cm}^{-2}$), as described in the experimental section. It can be seen that the concentrations of the two species add up to the

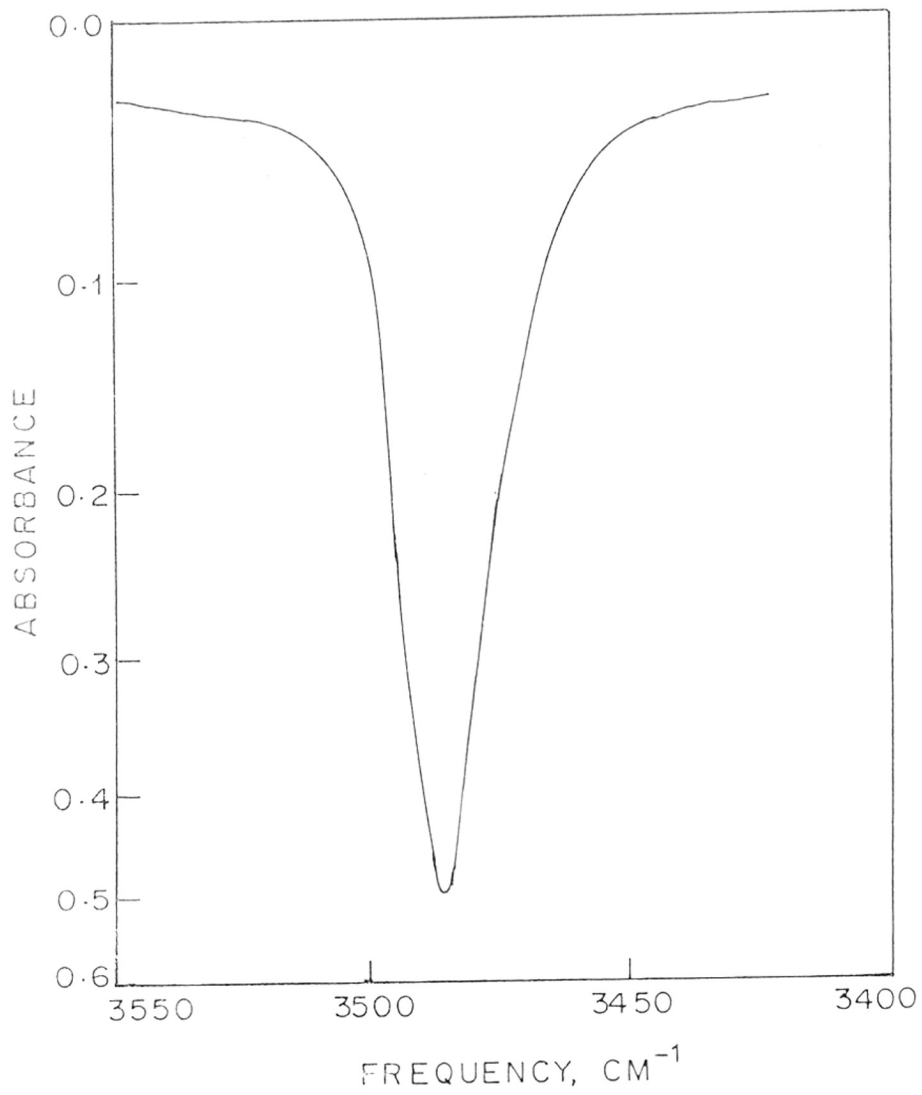


FIG. 18. NH STRETCHING BAND OF
N-METHYL ACETAMIDE

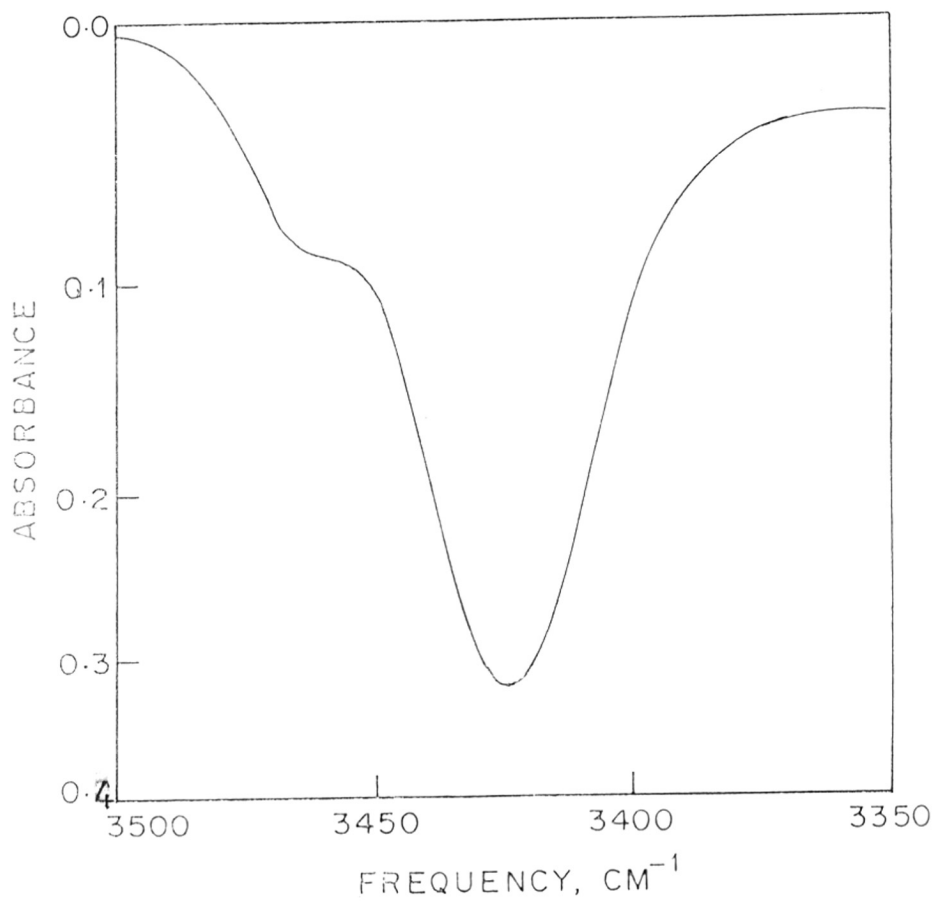


FIG. 19. NH STRETCHING BAND OF
N-ACETYL GLYCINE N'-DIMETHYL AMIDE

total NH group concentrations in all cases within $< 10\%$ which shows the validity of the assumptions regarding the use of integrated absorption intensity.

The relative proportions of the two species in the title compounds (Table II) show that the free form increases with increasing bulkiness of the substituent at the C^α . Such a trend has been reported in the case of a series of N-acetyl-(amino acid)-(glycine, leucine, valine, etc.)N'-dimethylamide by Neel¹⁰. This can be understood since such a group could hinder the rotation around the C-N bond and reduce the possibility of the C=O and NH groups coming closer for intramolecular hydrogen bonding.

We had already seen above, that there is hardly any intramolecularly hydrogen bonded seven-membered ring species formed in the dilute solutions of the present compounds, although such species could be stabilized by their stronger hydrogen bonding interaction over that in the five-membered ring hydrogen bond. In N-acetyl sarcosine N'-methyl amide (ASMA) (Fig.20), where the formation of the intramolecularly hydrogen bonded seven-membered ring species is reported^{6,10}, we have determined the concentration of this species using the integrated absorption intensity of the free NH group (Table II). We have found that these are present to the extent of 30-35%, the remaining species having the non-hydrogen bonded conformation. This raises the question as to why the intramolecularly hydrogen bonded seven-membered ring species are absent in the N-acetyl-(amino acid)-N'-methyl amides

TABLE II

CALCULATED POPULATION OF FREE AND INTRAMOLECULARLY HYDROGEN BONDED FIVE MEMBERED RING SPECIES IN N-ACETYLAMINO ACID N-METHYL/DI-METHYLAMIDES IN CHLOROFORM

	N-Acetyl-glycine N-dimethylamide	N-Acetyl-glycine N-methylamide	N-Acetyl-L-alanine N-methylamide	N-Acetyl-L-leucine N-methylamide	N-Acetyl-sarcosine N-methylamide
Solution concn. ($10^{-4}M$)	7.6	3.5	5.6	5.6	5.7
Area of 3450 band (cm^{-1})	1.51	13.3	23.5	16.9	15.3
Concn. ($10^{-4}M$) of free NH absorbing at 3450 cm^{-1}	0.61	4.7	8.3	5.9	5.4
Area of 3435 band (cm^{-1})			8.2	11.7	11.9
Concn. ($10^{-4}M$) of free NH absorbing at 3435 cm^{-1}			2.9	4.1	4.2
Total free NH concn. ($10^{-4}M$)	0.61	4.7	8.3	10.0	9.6
Area of 3420 band (cm^{-1})	39.0	12.2	21.3	11.6	11.1
Concn. ($10^{-4}M$) of bonded NH group		2.1	3.8	2.1	2.0
Percentage (Mean) of free non hydrogen bonded species	8 %	38 %	47 %	65 %	65 %
Percentage (Mean) of five membered intramolecularly hydrogen bonded species	92 %	62 %	53 %	35 %	35 % *

* Refers to seven membered intramolecularly hydrogen bonded species.

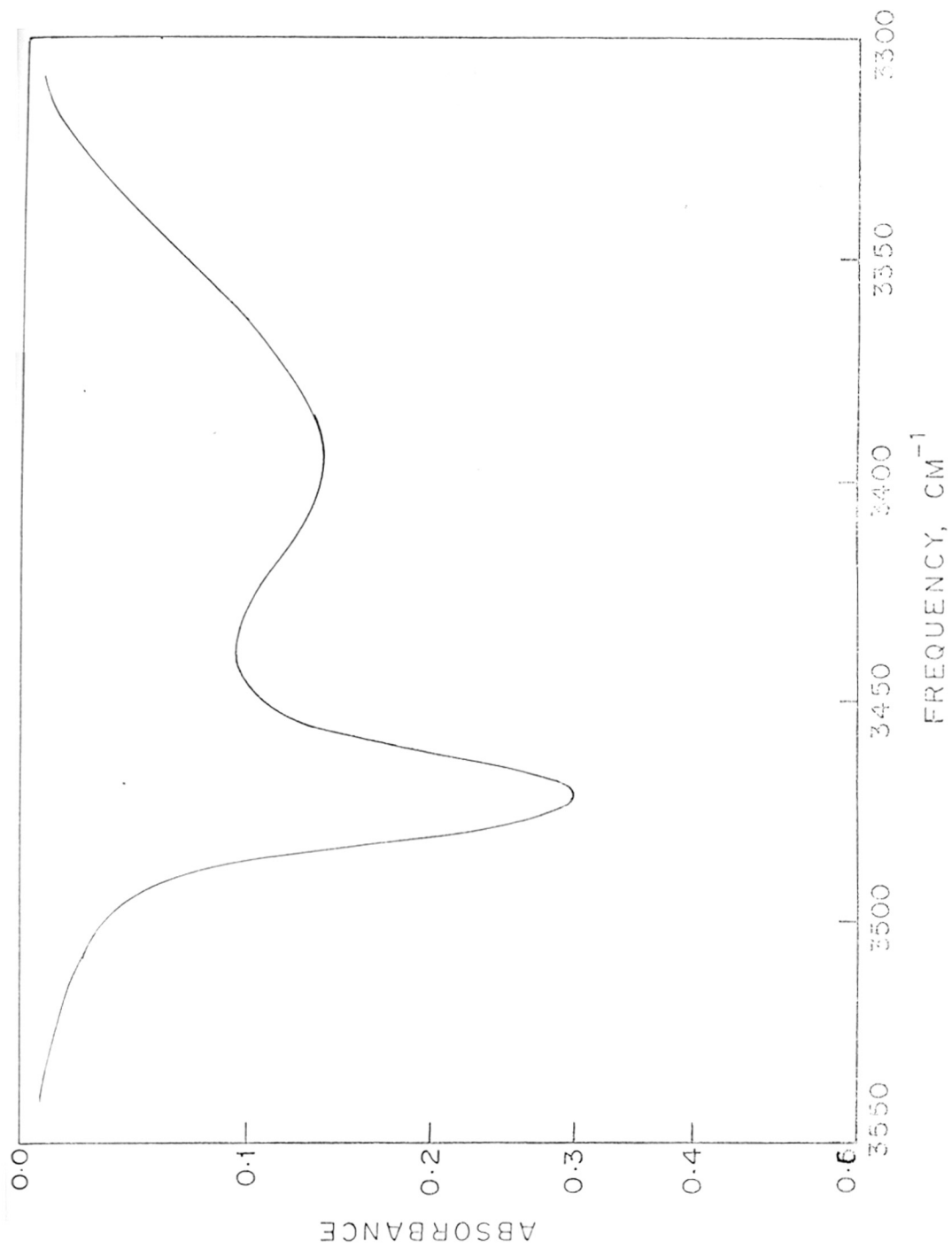


FIG. 20. NH STRETCHING BANDS OF N-ACETYL
SALICYLIC ACID N-METHYL AMIDE

in solution. In a somewhat comparable instance, the diethylene glycol monomethyl ether¹¹⁸ $[\text{CH}_3(\text{OCH}_2\text{CH}_2)_2\text{OH}]$, which could form both five and eight-membered intramolecularly hydrogen bonded species through a single hydroxyl group, the relative proportion of the five and eight membered intramolecularly hydrogen bonded and free species were 62, 31 and 6% respectively. The frequency shifts for the five and eight membered intramolecularly hydrogen bonded hydroxyl group were 40 and 195 cm^{-1} , respectively. It would appear from the above frequency shift that the intramolecular hydrogen bonding interaction in a seven membered ring of the present compounds ($\Delta\nu = 100 \text{ cm}^{-1}$) is far too small to stabilize such species in the presence of the more facile (entropy-wise) five-membered intramolecular hydrogen bond.

4.2. COMPARISON WITH REPORTED NMR RESULTS

In order to see whether the two conformations found by the IR spectroscopic method are supported by NMR results, we compared the reported $^3\text{JHNCH}$ coupling constant¹¹⁹ of 7.5 Hz for N-acetyl-L-alanine-N'-methyl amide in dilute chloroform solution (7×10^{-4} M) with those calculated for possible angles suggested by different authors¹²⁰⁻¹²³ for the above conformations using the Karplus-Bystrov formula¹²⁴ with $A = 9.4$, $B = 1.1$ and $C = 0.4$ (Table III). A perusal of the data revealed that the observed value could arise from a mixture of a five membered conformer with $\vartheta = -180^\circ$ (3.3 Hz) and non-hydrogen bonded conformer with $\vartheta = -120^\circ$ (10.9 Hz), or a five membered conformer with $\vartheta = -155^\circ$ (7.5 Hz) and a non-hydrogen bonded conformer with $\vartheta = -84^\circ$ (7.5 Hz).

Table III
Predicted and observed proton coupling constants
for N-acetyl L-alanine N'-methylamide(Hz)

<u>Five membered conformer</u>	ϕ	3J	γ	5J	
				I	II
Pullman and Maignret ¹²²	-180	3.3	180	0.34	0.34
Cung et. al. ¹²⁰	-160	6.8	170	0.19	0.26
Smolikova et.al. ¹²¹	-150	8.4	150	0.11	0.11
<u>Non-hydrogen bonded</u>					
Bystrov et.al. ⁸	-60	3.3	-60	0.34	0
Renugopal Krishnan et.al. ¹²³	-120	10.9	-60	0	0
Maxfield et.al. ¹⁸	-84	7.5	60	0.15	0.34
			150	0.15	0.11
Observed ¹²⁴		7.5	-150	0.11	0.26
				0.11	<0.03



It was found from conformational energy calculations (see later) that $\phi = -180^\circ$ is not allowed with β carbon atom on the side chain, so that the mean value of 7.5 Hz arises from conformers having $\phi = -155$ and -84° .

Davies et. al.¹²⁴ have shown that five bond long range proton-proton coupling existing between the C-H group of the amino acid in peptide bond, and the methyl groups (acetyl and N-methyl) could be used to predict the torsional angles. Although the observed 5J coupling constant for peptide bond 1 (0.1) Hz is close to 0.15 Hz for $\phi = -155^\circ$ (C5 conformation) and 0.15 Hz for $\phi = -84^\circ$ (non-hydrogen bonded conformation), the observed 5J coupling constant for peptide bond 2 (< 0.03) is very different from the calculated values, 0.2 Hz (for C5 conformation) and 0.11-0.34 Hz (for non-hydrogen bonded conformation).

Solkan and Bystrov¹²⁵ have theoretically calculated the vicinal spin-spin interaction constants between 1H and ^{13}C nuclei in a peptide fragment for various angles and have shown how these, together with the $^3J_{HNC}$ coupling constant, permit a determination of the torsional angle unambiguously. Gavrillov, Solkan and Bystrov¹²⁶ have subsequently measured the vicinal coupling constants $^1HNC \propto ^{13}C'$, $^1HNC \propto ^{13}C^\beta$ and $^1HC \propto N^{13}C'$ of AAMA in methanol (concentration = 1M). Using the observed $^3J_{HNC}$ coupling constant of 7.5 Hz in dilute chloroform, we have read out from their graphs the three coupling constants for the

four angles (Table IV) and compared them with their experimental results¹²⁶. The agreement between the observed values and those calculated for the φ angles -160° and -80° are better than those for $+40^\circ$ and $+90^\circ$, although a much better agreement should be expected. This can be due to the higher concentration and the relatively polar solvent used for the ^{13}C studies.

Thus, in the case of N-acetyl L-alanine N'-methyl amide, by comparing the various NMR $^3J_{\text{HN-CH}}$ coupling constants, torsional angles, φ , of -155° and -84° can be derived for intramolecularly hydrogen bonded five-membered ring species and free non-hydrogen bonded species, respectively. From $^1\text{H}-^{13}\text{C}$ spin-spin interaction constant these angles are deduced to be -160° and -80° almost matching with the above results. Now, we will compare these results with those obtained by conformational energy calculations to get additional support.

4.3. COMPARISON WITH CONFORMATIONAL ENERGY CALCULATIONS

Several theoretical analyses of the conformations of blocked single residues have been carried out¹²⁷⁻¹³⁰. Recently, Zimmerman et. al.¹³¹ have concluded from their conformational energy calculations that there are several low energy conformations for N-acetyl (amino acid)-N'-methyl amide. The C_7 equatorial conformation (Fig. 2b) (φ, ψ : $-84^\circ, 79^\circ$) was calculated to have the lowest energy. The intramolecularly hydrogen bonded C_7 conformation, however, has been shown to be absent in the present compounds, but conformations with $\varphi = -84^\circ$ and

TABLE IV.

CALCULATED AND OBSERVED $^{13}\text{C} \dots ^1\text{H}$ VICINAL COUPLING
CONSTANTS FOR N-ACETYL L-ALANINE N'-METHYLAMIDE (Hz)

Calculated for ϕ ¹²⁵	$1_{\text{HNC}^{\alpha}13\text{C}'}$	$1_{\text{HNC}^{\alpha}13\text{C}^{\beta}}$	$1_{\text{HC}^{\alpha}\text{N}13\text{C}'}$
-160	2.6	0.5	1.0
-80	0.8	2.8	0.6
+40	7.0	0<	4.0
+90	0	4.0	4.0
Observed ¹²⁶	<1	1.9	2.5

ψ angle different from 79° such that an intramolecular hydrogen bond is not formed, are possible. A look at the conformational energy map¹³¹ shows that variations in the ψ angle within 60° - 150° would bring about only marginal change from the lowest energy (1 Kcal). Thus, a distorted C_7 conformation without any intramolecular hydrogen bond estimated to be 50% in the L-alanine derivative is satisfactorily explained by the energy calculations. For the other significant conformer, ($\phi, \psi : -150^\circ, 70^\circ$) the 3J coupling constant calculated as before gave a value of 8.4 Hz, which is higher but with a value of $\phi = -155^\circ$, an agreement with the reported value is possible. Thus, both the above non-hydrogen bonded conformers could represent 50% of the total conformational species in chloroform solution.

The other probable conformer based on conformational energy calculation is the hydrogen bonded C5 species ($\phi, \psi : -180^\circ, \pm 180^\circ$). However, for β carbon on the side chain this conformation is not allowed. Cung et. al.¹²⁰ and Smolikova et. al.¹²¹ have suggested C5 conformation with $(-160^\circ, 170^\circ)$ and with $(-150^\circ, 150^\circ)$ for ϕ and ψ angles which would give calculated $^3J_{HNCH}$ coupling constants of 6.8 and 8.4 Hz, respectively. These are much closer to the expected value of 7.5 Hz, so that contribution from this species to the extent of 50% as obtained in the present studies would meet the conformational energy calculations.

From the results obtained by NMR studies, it can be concluded that the ϕ angles of -155° and -84° can be possible in intra-

molecularly hydrogen bonded five-membered ring species and non-hydrogen bonded species respectively, in the case of N-acetyl L-alanine N'-methyl amide. The results obtained from conformational energy calculations support the above observations and the probable ϕ and ψ angles for free non-hydrogen bonded species are $(-84^\circ, 60-150^\circ)$ and for five-membered intramolecularly hydrogen bonded species $(-155^\circ, 160^\circ)$.

CHARACTERIZATION OF THE CATIONIC POLYMERIZATION
OF 2-DIMETHYL AMINO BENZOIC ACID IN DIMENSIONAL ANALYSIS

RESULTS AND DISCUSSION

CHAPTER V
RESULTS AND DISCUSSION
2-DIMETHYL AMINO BENZOIC ACID

CHARACTERISATION OF THE VARIOUS STRUCTURAL SPECIES
OF 2-DIMETHYL AMINO BENZOIC ACID IN DIFFERENT SOLVENTS

RESULTS AND DISCUSSION

Infrared spectra of 2-dimethyl amino benzoic acid (dimethyl anthranilic acid, DMA) in various solvents in the region 1800-1625 cm^{-1} at identical concentration (0.06 M) are shown in Fig. 21-24(—). It can be seen that the band structure is the simplest in cyclohexane (saturated solution $\sim 0.01\text{M}$) with the carbonyl absorption at the highest ($\sim 1738 \text{ cm}^{-1}$) frequency. However, as the solvent was varied to carbon tetrachloride, benzene, dioxane, acetonitrile, chloroform, dimethyl sulphoxide and methanol, peak absorbances continuously decreased with the band profile simultaneously broadening out, indicating additional absorptions. A clear separation of the bands could not be achieved even after taking considerably lower concentrations (0.01 M).

Tramer²⁷ had recorded the IR spectra of DMA in carbon tetrachloride and benzene solution. From the high value of C=O stretching frequency along with broad bands at 2650 and 2250 cm^{-1} , he concluded that DMA exists as an intramolecularly hydrogen bonded neutral species. Jose et. al.³⁰ have also studied the spectra of DMA in carbon tetrachloride, cyclohexane, benzene, chloroform and dimethyl sulphoxide. They had observed bands similar to those obtained by Tramer²⁷ in carbon tetrachloride and from the PMR

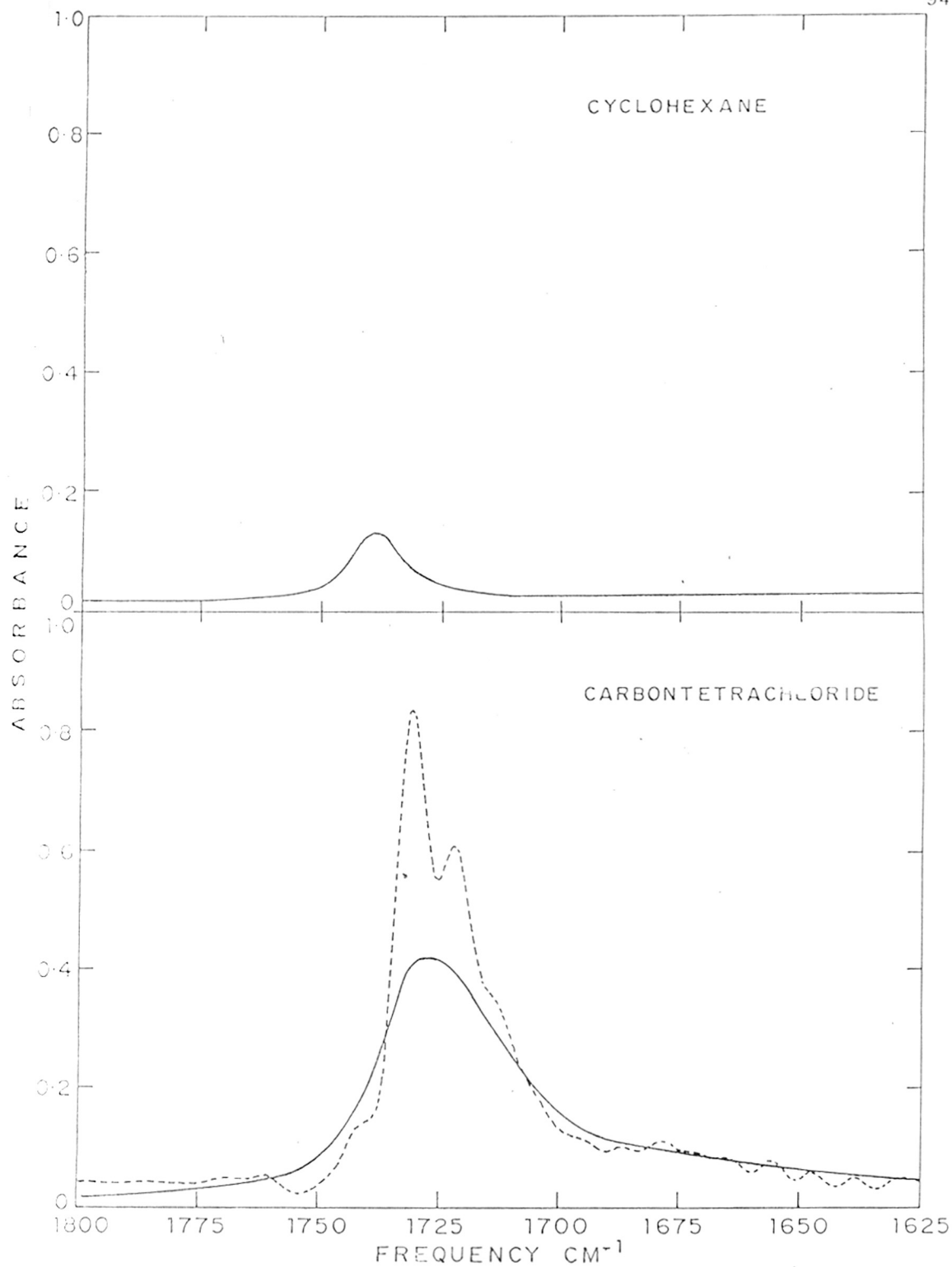


FIG. 21. I.R. SPECTRA OF DMA IN SOLVENTS

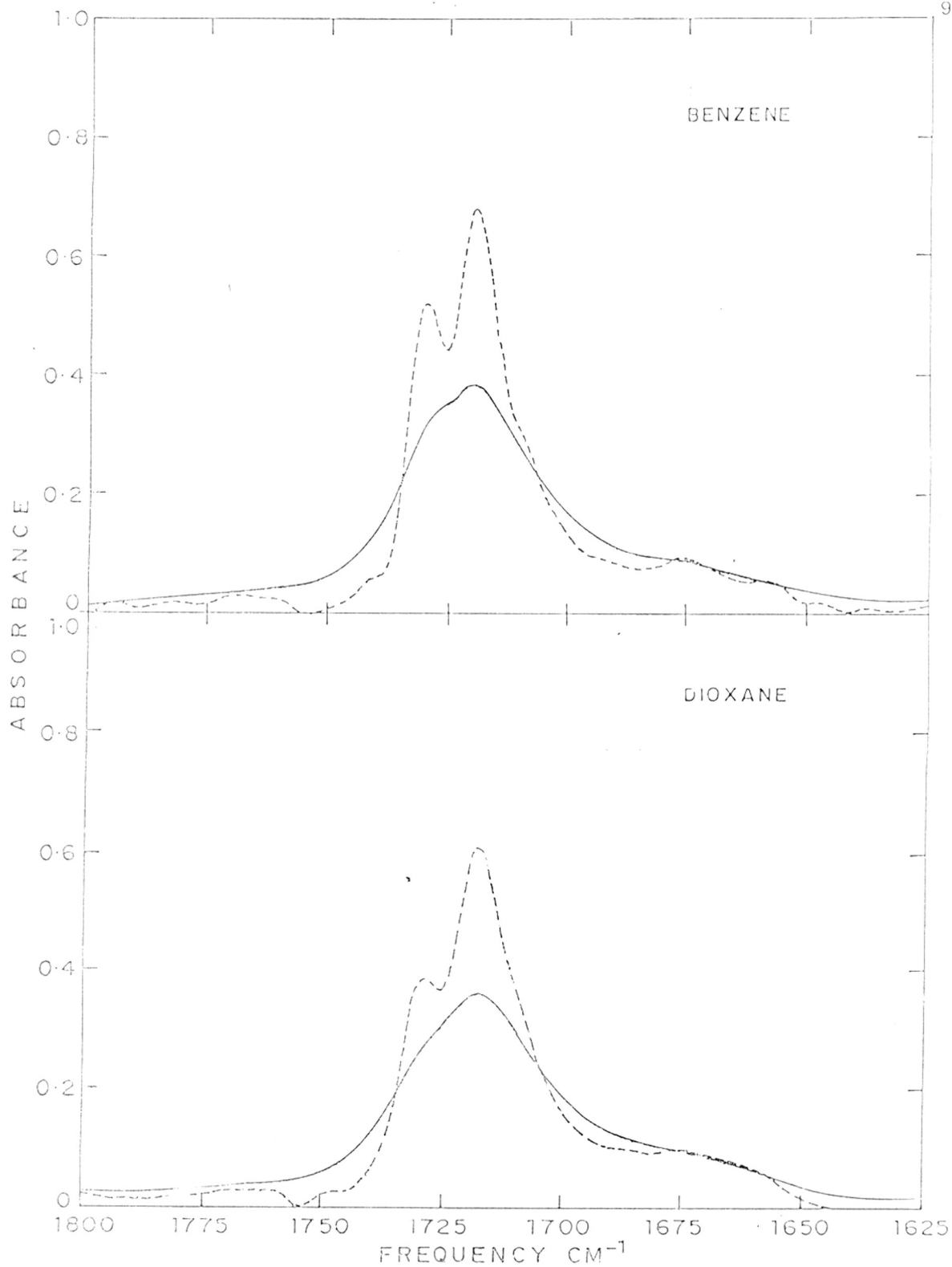


FIG. 22. I.R. SPECTRA OF DMA IN SOLVENTS

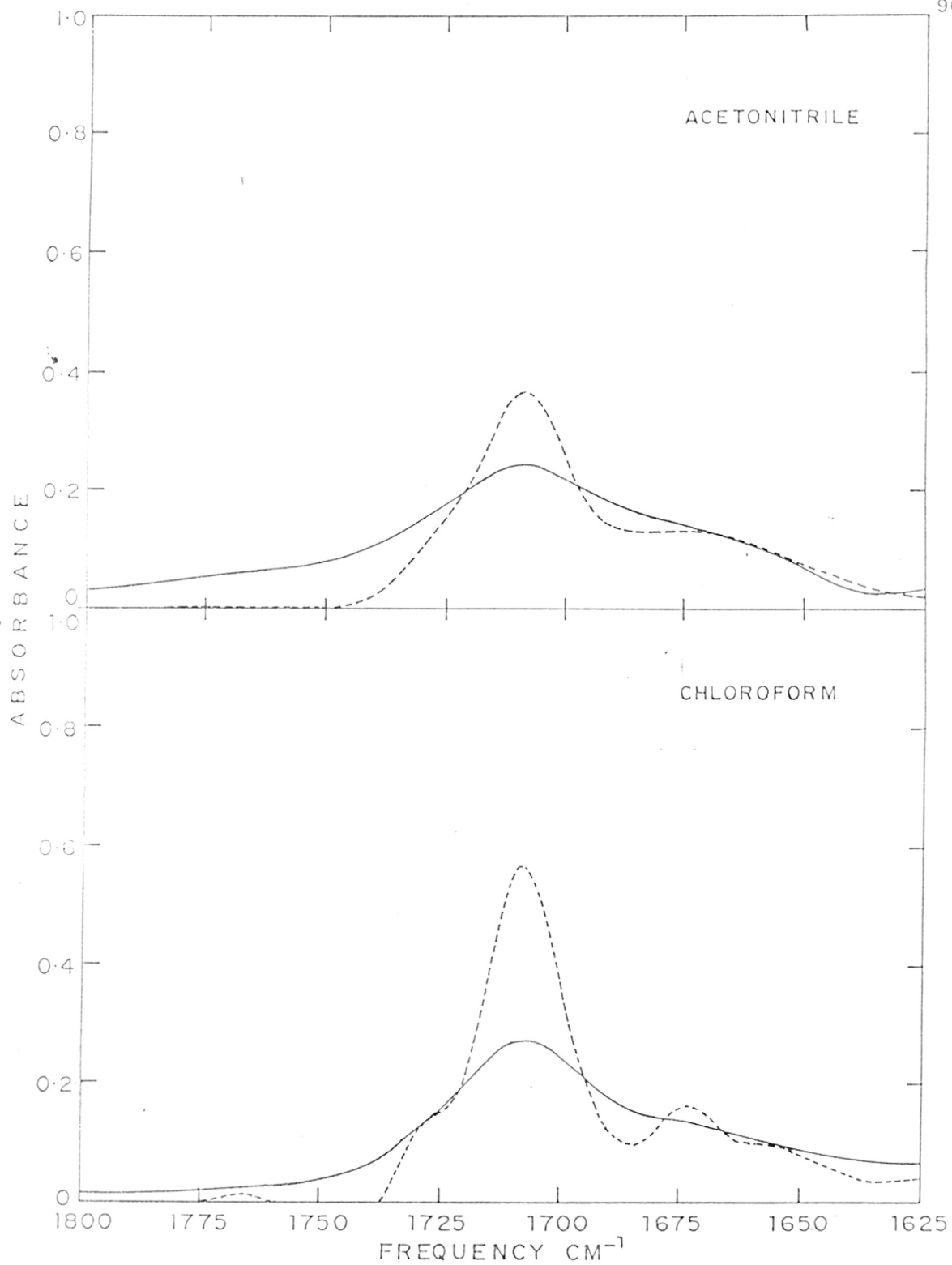


FIG. 23. I. R. SPECTRA OF DMA IN SOLVENTS

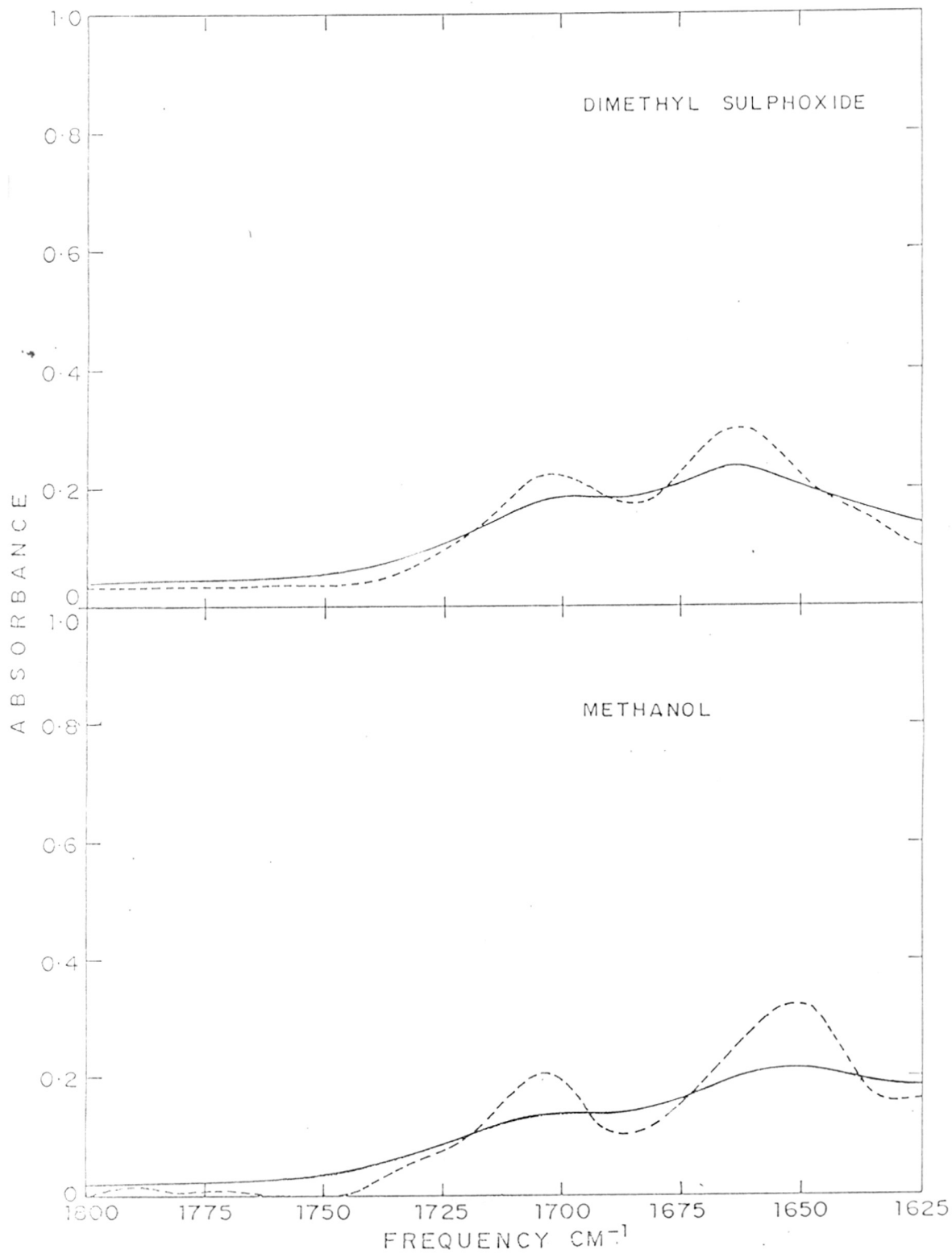


FIG. 24 . I.R. SPECTRA OF DMA IN SOLVENTS

chemical shift of 15.25δ for the hydroxyl proton, they concluded that the predominant species in carbon tetrachloride were the intramolecularly hydrogen bonded neutral species. In the other solvents the carbonyl bands had become broader indicating the presence of additional species. With a view to investigate the broadening of the carbonyl band, Fourier deconvolution was performed.

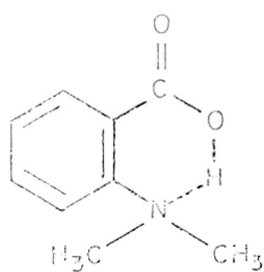
The spectra after Fourier deconvolution are shown in Fig. 21-24 (←→). It is evident that the deconvolution has resulted in a fairly good separation of the bands so that their positions could be located (Table V). It is worth pointing out that no indication of additional bands was observed in the case of DMA in cyclohexane on deconvolution. In carbon tetrachloride, benzene and dioxane, there are two sharp bands at 1730 and 1718 cm^{-1} with an unresolved band at 1709 and a broad weak band at $\sim 1675 \text{ cm}^{-1}$. In acetonitrile, chloroform, dimethyl sulphoxide and methanol, two broad bands at 1709 and 1670-1650 cm^{-1} with weak unresolved bands at higher frequencies were observed.

From the unusually high value of 1738-1730 cm^{-1} for the carboxylic carbonyl in non-polar solvents like cyclohexane, carbon tetrachloride etc. it is evident that the carboxylic group is in the unfavourable trans form stabilized by an intramolecular hydrogen bond between the carboxylic hydroxyl and the lone pair of electrons on the nitrogen of the orthodimethyl amino group (Fig. 25a). The high value of C=O stretching frequency (1731 cm^{-1}) in carbon tetrachloride, compared to 1680-1700 cm^{-1} expected

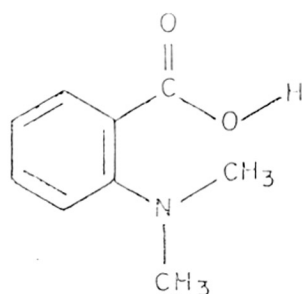
TABLE - V

CARBOXYL BANDS OF 2, DIMETHYLAMINO-BENZOIC ACID IN SOLUTION

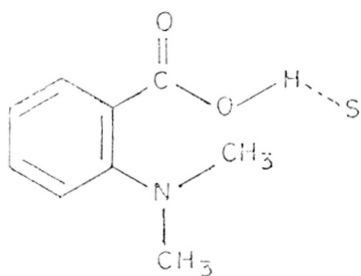
Solvents	Frequency in cm^{-1}			
1. Cyclo hexane	1738 m			
2. Carbon-tetrachloride	1731 s	1722 s	1710 m	1677 mb
3. Benzene	1730 m	1720 s	1708 w	1675 wb
4. Dioxane	1729 m	1719 s	1709 sh	1680 mb
5. Chloroform	1727 m		1709 vs	1672 mb
6. Acetonitrile	1729 w		1708 vs	1675 mb
7. Dimethyl-sulphoxide	1729 w		1703 m	1663 s
8. Methanol	1728 w		1705 m	1685 sb
9. Water (Heavy)				1565 m



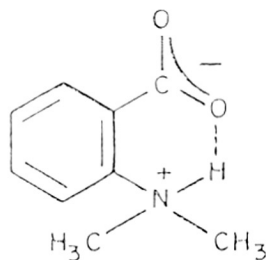
A



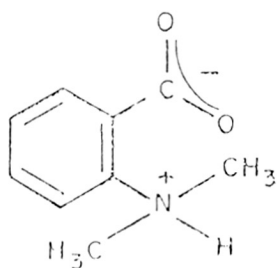
B



C



D



E

FIG. 25. 2-DIMETHYL AMINO BENZOIC ACID STRUCTURES

for dimeric aromatic acids, was suggestive¹³² of trans structure of the carboxylic group. The multiple band structure for the hydroxyl stretching vibration at 2540, 2230, 2090, and 1950 cm^{-1} reported³⁰ earlier in carbon tetrachloride, supported the involvement of the hydroxyl group in strong intramolecular hydrogen bonding characteristic of double minimum potential type^{133,134}. The chemical shift of 15.25 δ in CCl_4 for this hydroxyl proton in the PMR spectrum also confirmed the presence of such species. Thus, the predominant species in carbon tetrachloride are intramolecularly hydrogen bonded neutral species (Fig. 25a). The low frequency bands at 1720 and 1709 cm^{-1} in carbon tetrachloride solution can be ascribed to the cis carboxylic acid group which has a strong tendency to dimerise (Fig. 25b) and to the cis carboxylic acid solvated monomer (Fig. 25c). As the solvent was made more polar, these species were found to increase. The weak band at 1675 cm^{-1} in carbon tetrachloride is very close to the value of 1650 cm^{-1} ascribed to intramolecularly hydrogen bonded zwitterionic species. These species were also found to increase on going to solvents like dimethyl sulphoxide and methanol.

In benzene and dioxane, a strong band is observed at 1719 cm^{-1} which can be ascribed to dimeric species. Medium or weak bands at 1730, 1709 and 1670 cm^{-1} show the presence of other species discussed above.

In chloroform and acetonitrile, there is a strong band at 1709 cm^{-1} showing the presence of solvated monomeric species with

weak bands at 1728 and 1675 cm^{-1} due to other species. The chemical shift of the hydroxyl proton obtained from PMR spectrum of DMA in chloroform is nearly ^{the} same as that obtained in carbon tetrachloride (15.25 δ) which shows strong intramolecular hydrogen bonding between the hydroxyl and the dimethyl amino group (Fig. 25a). The infrared spectrum of DMA in chloroform also showed medium broad bands at 2500 and 1900 cm^{-1} , characteristic of strong unsymmetrical hydrogen bonding of a double minimum potential type¹³³. Thus, intramolecularly hydrogen bonded neutral species are present in chloroform and acetonitrile. The lowering of C=O stretching frequency may be ascribed to the slightly larger delocalization in the carboxylic group in these solvents. From the deconvoluted infrared spectra, it can be seen that the width of the band at 1709 cm^{-1} in chloroform and acetonitrile was larger compared to the bands in carbon tetrachloride, benzene and dioxane.

In more polar solvents like dimethyl sulphoxide and methanol, charge transfer takes place resulting in Zwitterions which would form charge transfer intramolecular hydrogen bond (Fig.25d). The asymmetric stretching mode of such a carboxylate group could absorb at 1670 cm^{-1} , close to what has been observed in the Zwitterionic intramolecularly hydrogen bonded solid DMA²⁸ at 1650 cm^{-1} . In order to confirm the nature of these species, the PMR spectrum of DMA was recorded in dimethyl sulphoxide -d₆ (Fig.26) which showed a hydroxyl proton chemical shift of 17.3 δ (with respect to TMS), much higher than that found for the hydroxyl

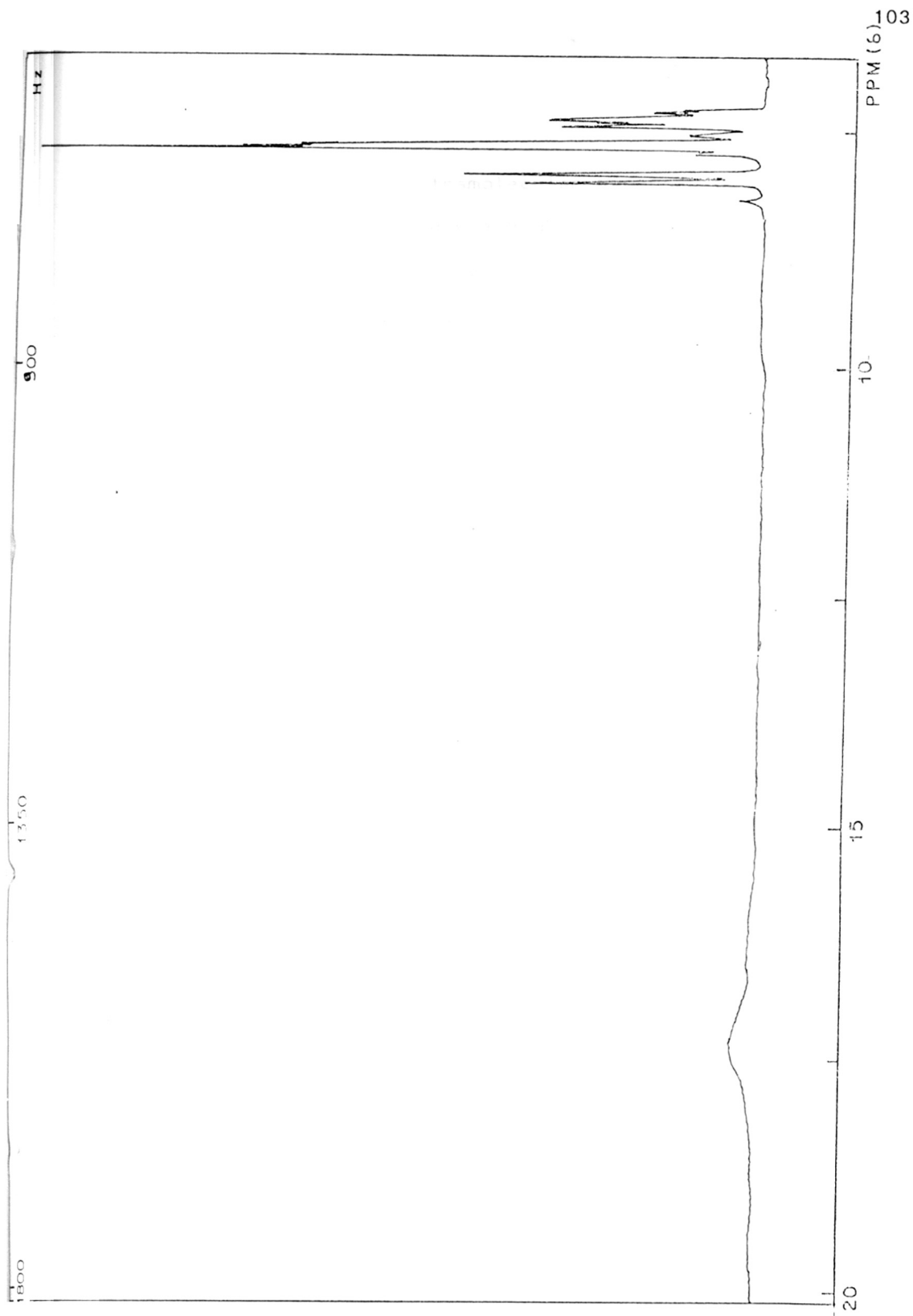
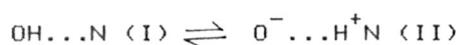


FIG. 26. PMR SPECTRUM OF 2-DIMETHYL AMINO BENZOIC ACID IN DIMETHYL SULPHOXIDE - d_6

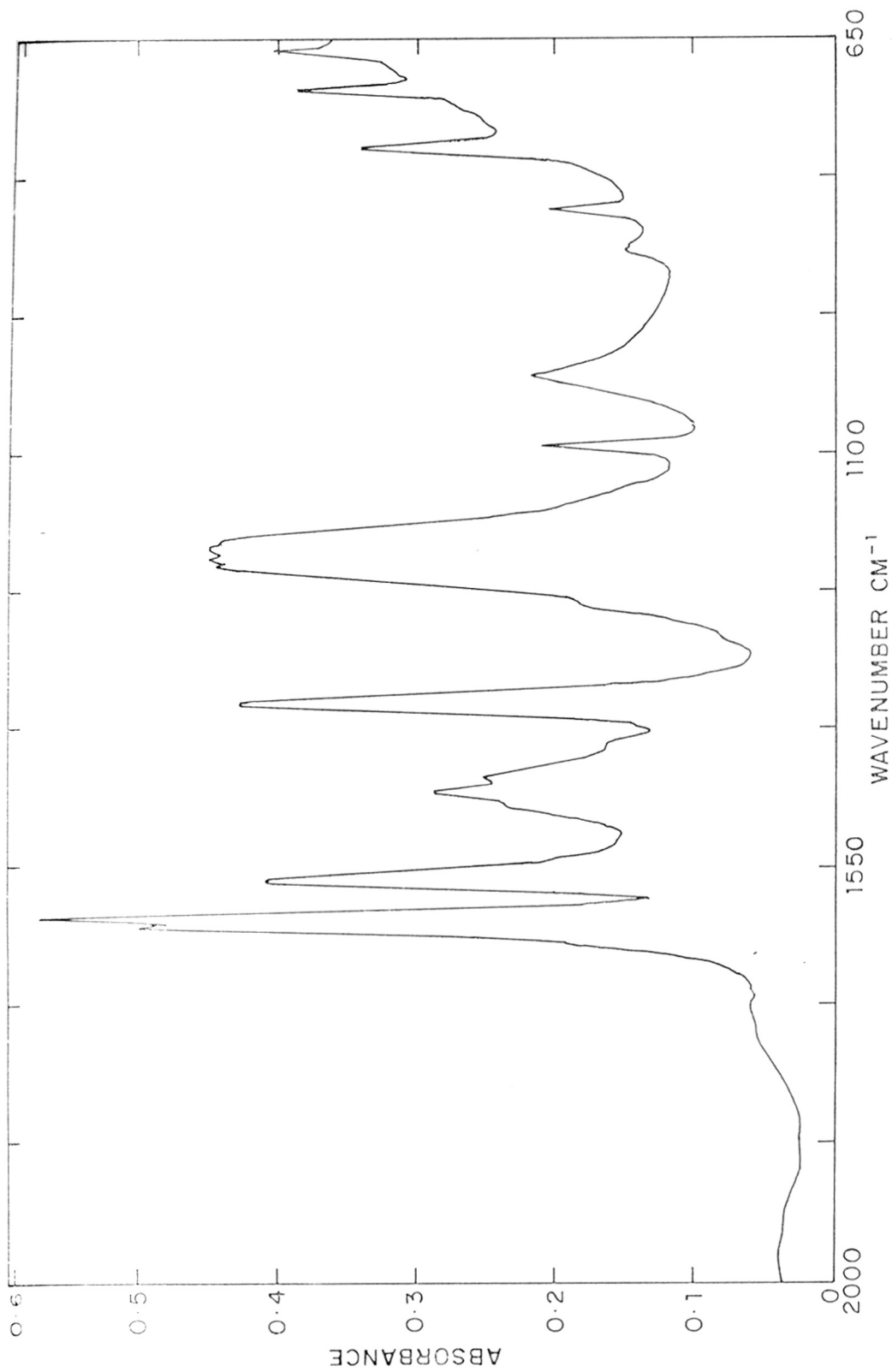
group in the neutral intramolecular hydrogen bond of DMA in carbon tetrachloride. Such a high value could only be ascribed to charge transfer hydrogen bond i.e. $N^+ \cdots H \cdots O^-$.

Zundel et. al.³⁵ have studied the PMR spectra of DMA to see the effect of various solvents on the proton polarizability. They investigated the proton transfer between the two structures



from the PMR chemical shifts in various solvents. They obtained the values of 17.85, 17.72 and 17.06 δ in DMSO, CH_3CN and CH_2Cl_2 , respectively. In structure II, the hydrogen bonded proton was less screened by the electrons than in structure I and hence the chemical shift of the hydroxyl proton was found at lower field with increase in the polarity of the solvent. Brzezinski and Zundel³⁴ have observed similar behaviour in a closely related compound, N,N dimethyl 5-R anthranilic acid-N oxide, in similar solvents.

The IR spectrum of DMA showed a single band near 1600 cm^{-1} in the aromatic region in organic solvents. However, in D_2O a doublet at 1606 and 1613 cm^{-1} has been observed (Fig. 27). The medium broad band at 1565 cm^{-1} is very similar to the band in the spectrum of the sodium salt of DMA in the solid state¹³⁵ with absorption bands at 1605 , 1585 and 1560 cm^{-1} . As doubling could arise from conjugative effects, the band near 1565 cm^{-1} has been ascribed to the carboxylate groups of the zwitterionic species of DMA which is solvated and not involved in intramolecular hydrogen

FIG. 27. IR SPECTRUM OF 2 DIMETHYL AMINO BENZOIC ACID IN D₂O

bonding (Fig. 25e). It is worth noting that the strong solvating power of water in relation to dimethyl sulphoxide and methanol, is capable of breaking the strong intramolecular charge transfer hydrogen bond between the COO^- and $\text{N}^+(\text{CH}_3)_2\text{H}$ groups. This is largely due to the ability of water to solvate both the above groups while the other two solvents could solvate only one of them.

From the above studies, it can be concluded that predominant species in cyclohexane and carbon tetrachloride are intramolecularly hydrogen bonded neutral species. As we change the solvent to benzene, dioxane, chloroform and acetonitrile, these species go on decreasing with simultaneous increase in the intramolecularly hydrogen bonded charge transfer species. In dimethyl sulphoxide and methanol, intramolecularly hydrogen bonded charge transfer species are predominant. In D_2O , the zwitterionic species without any intramolecular hydrogen bonding are found to be predominant.

CONFORMATIONAL EQUILIBRIA IN SIMPLE PRIMARY ALCOHOLSRESULTS AND DISCUSSION

The infrared spectra of ethanol, n-propanol, n-butanol, n-pentanol and n-hexanol in dilute carbon tetrachloride solution ($\ll 0.011$ M) in the range 3675 to 3575 cm^{-1} are given in Fig. 28-32. The free hydroxyl band of ethanol (0.0066 M), n-butanol (0.011 M), n-pentanol (0.0098 M) and n-hexanol (0.0082 M) and their deconvoluted and separated band spectra at 303°K are shown in Fig. 28, 30, 31 and 32, respectively. The hydroxyl band of n-propanol (0.0092 M) and the deconvoluted spectra with band separation at two temperatures 303 and 328°K are given in Fig. 29. It is clear that except in the case of ethanol, the band positions (ν high frequency and ν low frequency) and to a great extent half band widths are clearly established by the spectral deconvolution, for carrying out unambiguous band separation. In the case of ethanol, even with variations in the half band width parameter between 15 and 20 cm^{-1} and enhancement factor of 1.5 - 2 , no clear separation could be effected. However, the two bands obtained after deconvolution are considerably sharper than the original spectrum to effect a satisfactory separation. It was found during deconvolution that the unsymmetrical band profile of the above alcohols could be separated into two bands only and no more, for all reasonable values of half band width and enhancement factors, without developing side lobes and other artifacts. In the case of methanol, Fourier deconvolution with similar

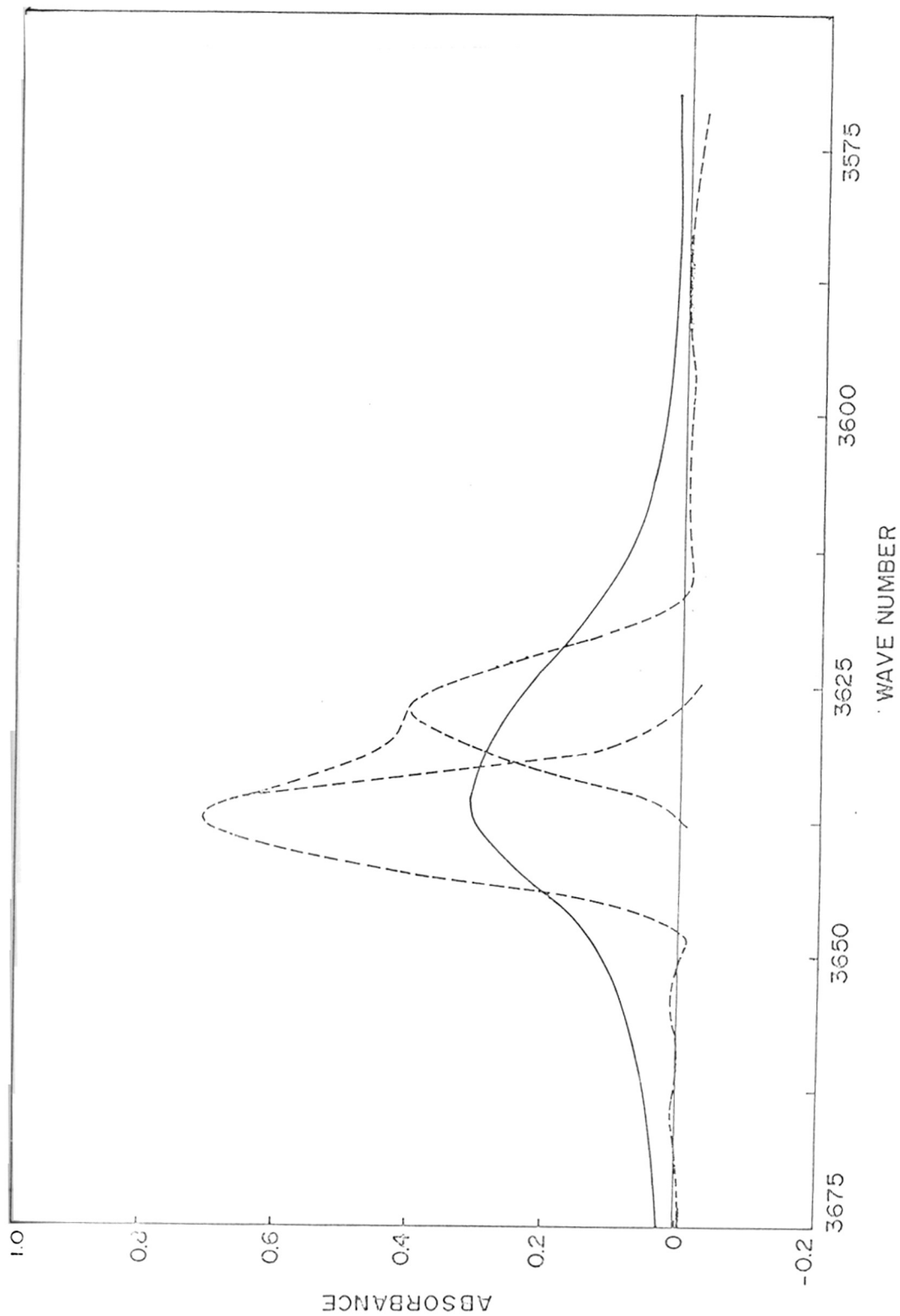


FIG. 28. ETHANOL HYDROXYL BAND (—) DECONVOLUTED (-----) BANDS

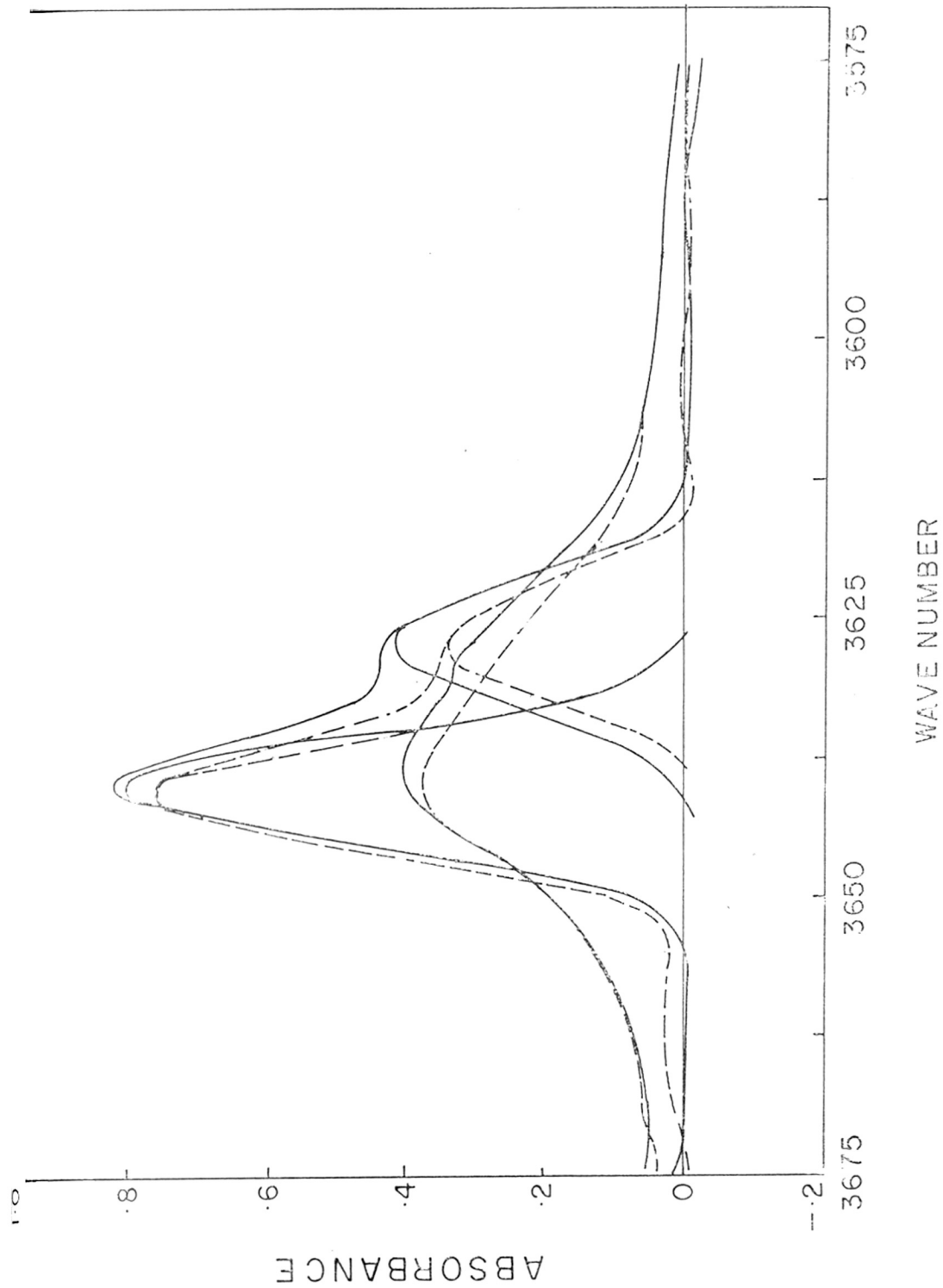


FIG. 29. - n-PROPANOL HYDROXYL AND DECONVOLUTED BANDS
305°K (-----) 328°K (-·-·-·-)

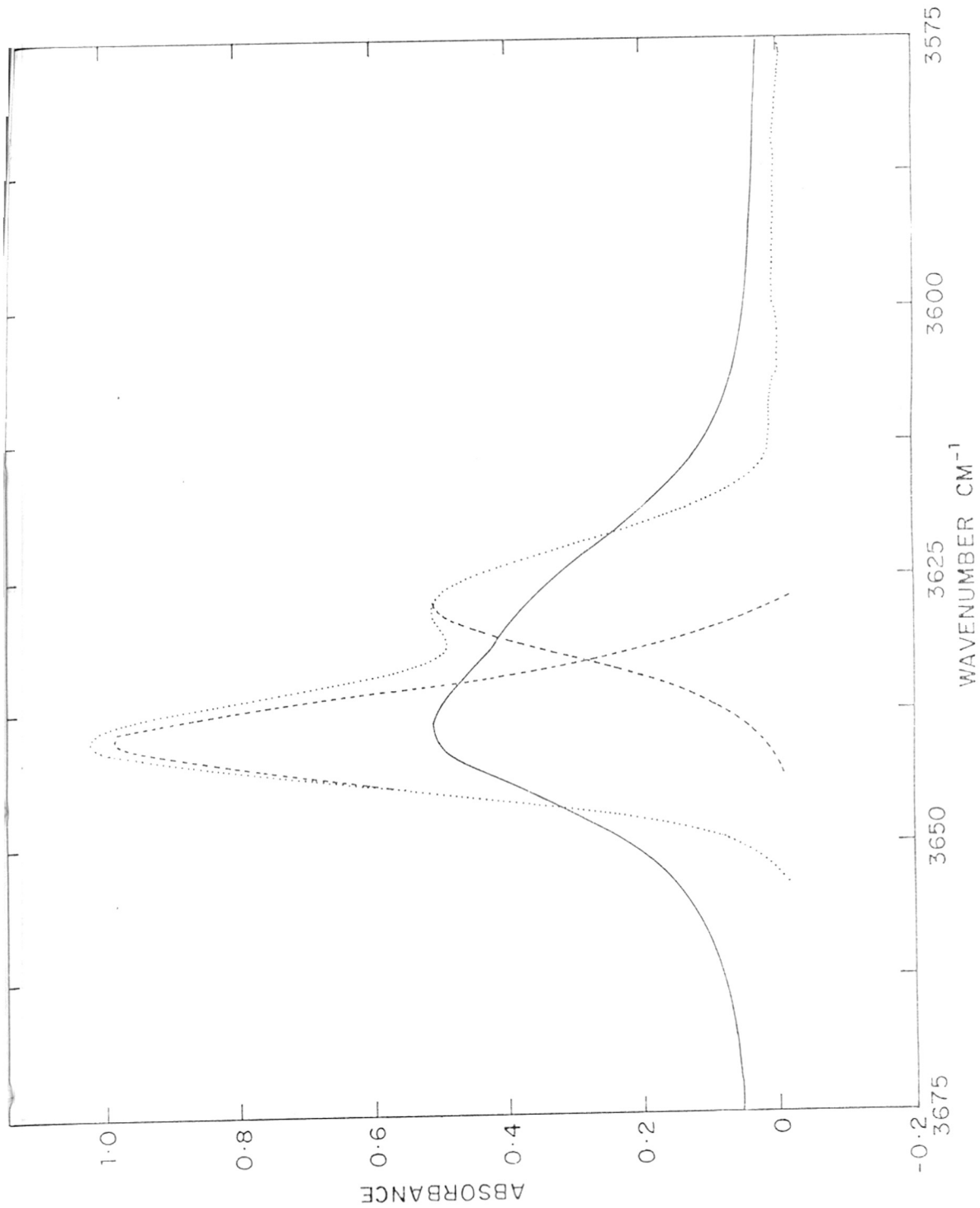


FIG. 30. n-BUTANOL, HYDROXYL (—) AND DECONVOLUTED (· · · · ·) BANDS.

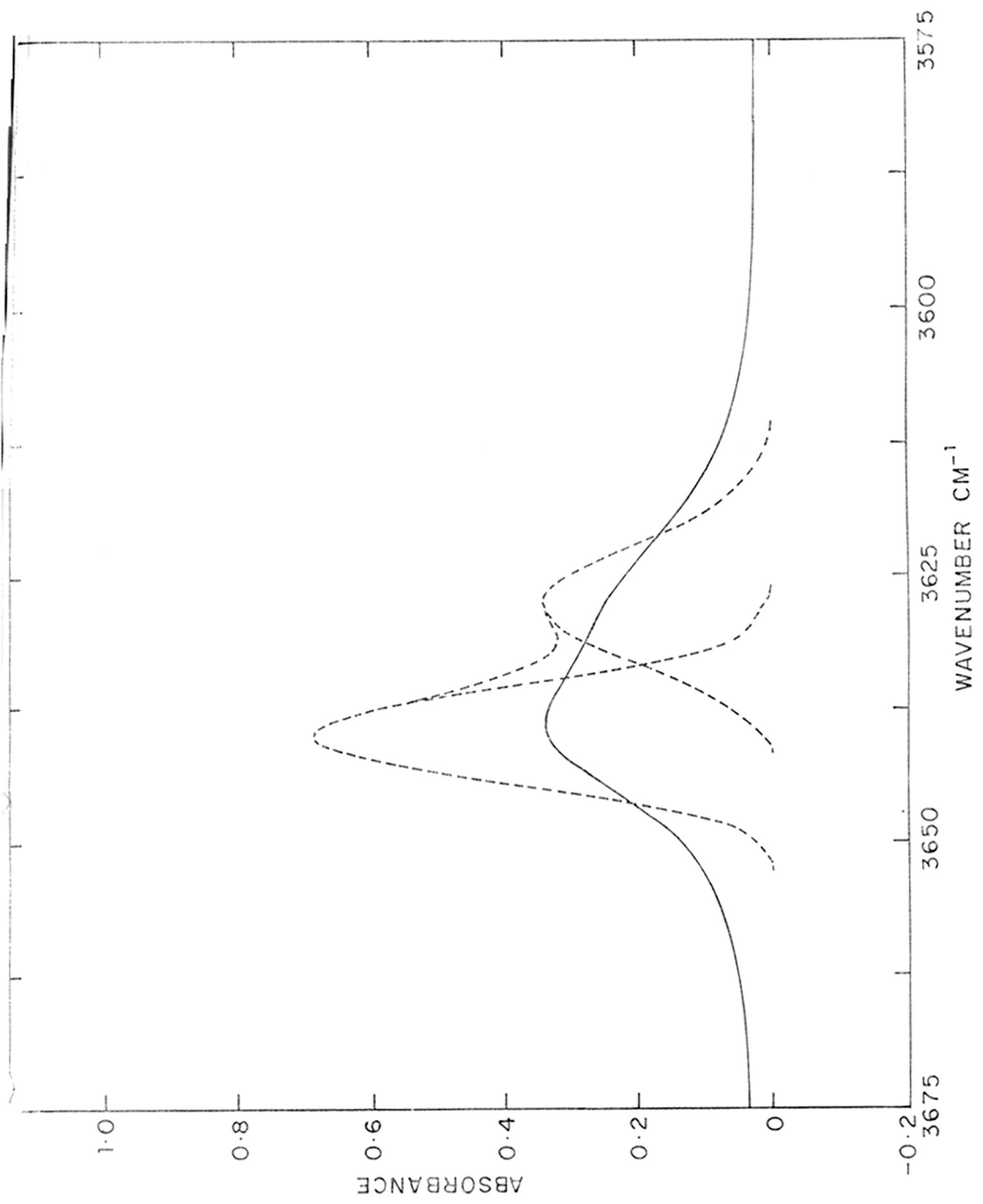


FIG. 31. n-PENTANOL, HYDROXYL (——) AND DECONVOLUTED (-----) BANDS.

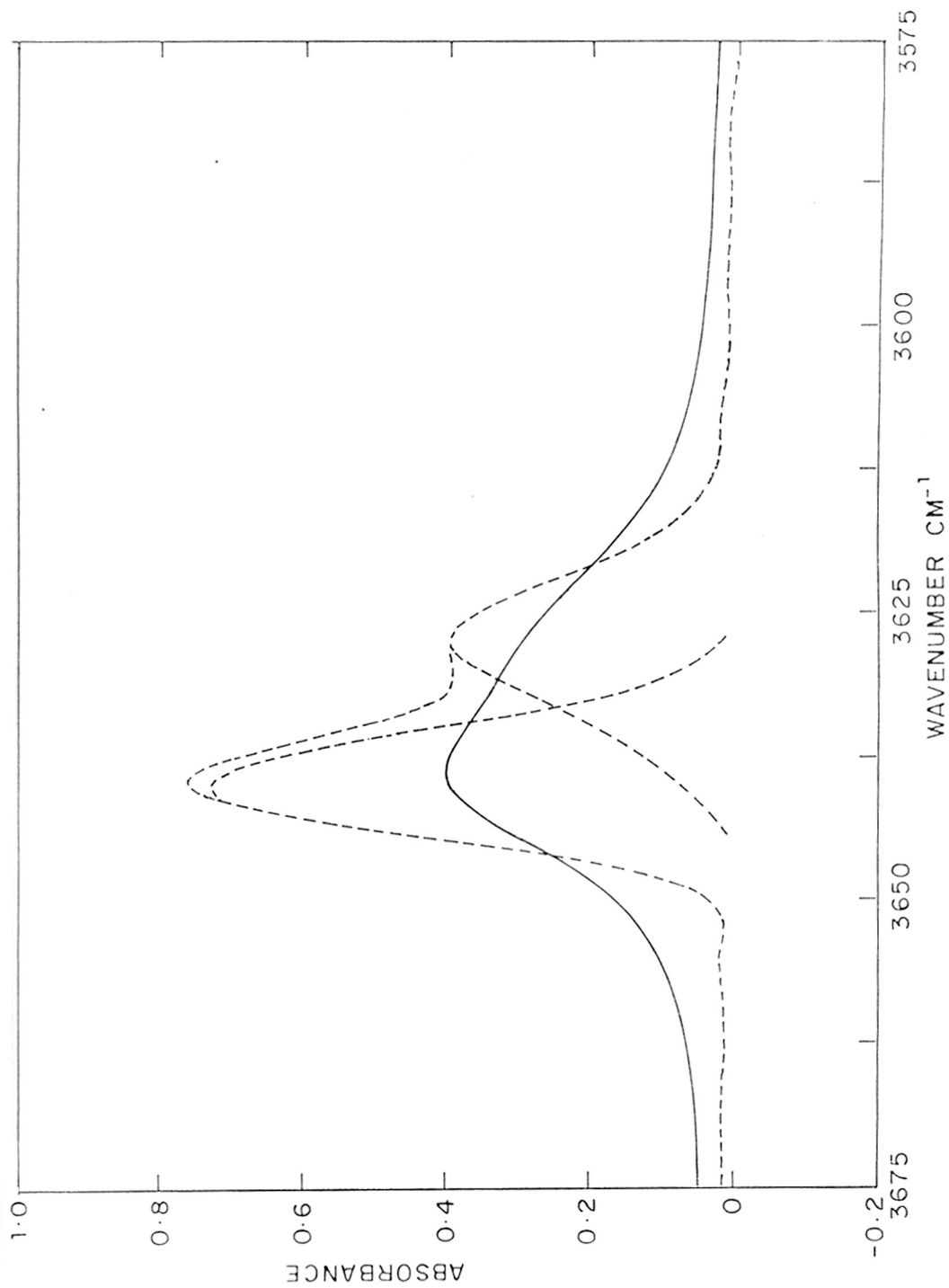


FIG. 32. n-HEXANOL, HYDROXYL (—) AND DECONVOLUTED (---) BANDS

parameters did not produce any splitting of the band. Thus, the present results clearly establish that unsymmetrical band profile of n-alcohols consists of two bands, ascribable to two rotational isomers resulting from rotation around the C-O bond. Many earlier workers have separated the hydroxyl band of primary alcohols into two bands using graphical/non-linear⁷⁸⁻⁸⁴ least square curve analysis, but due to the assumption of arbitrary band parameters their results were unreliable. Some workers^{46,75} have separated the band profile into three components and postulated rotation around $C^{\alpha}-C^{\beta}$ bond to explain their results. In view of the uncertainties involved in the resolution of the unsymmetrical profile of the parent spectra, it is difficult to attribute much significance to these separations and possibility of additional rotamers from rotation around $C^{\alpha}-C^{\beta}$ bond.

In Table VI, the typical band areas for the two rotamers of ethanol, n-propanol, n-butanol, n-pentanol and n-hexanol at various temperatures, 303-328^oK, are given. Two/three concentrations were taken for each alcohol and mean values of areas are reported. The positions, half band widths of the component bands and mean equilibrium constants at 303^oK are given in Table VII with reported parameters for comparison. The ΔH values obtained from a plot of $\log K$ vs $1/T \times 10^3$ (Fig. 33) are also given in this table along with reported values. An examination of the various band parameters shows that the high frequency band of n-propanol to n-hexanol (3639-40 cm^{-1}) is decidedly higher than 3637 cm^{-1} of ethanol, though the low frequency band is nearly the

TABLE VI

TEMPERATURE DEPENDENCE OF ROTAMER BAND AREAS (CM^{-1}) IN N-ALCOHOLS

Temp. (K)		303	308	313	318	323	328
Ethanol	BH	16.8	16.8	16.1	15.2	14.0	14.2
0.0066 M	BL	10.2	9.5	8.6	8.2	7.3	6.9
n-Propanol	BH	23.8	23.5	22.9	22.6	22.5	22.4
0.0092 M	BL	13.4	12.6	10.6	10.4	9.6	9.2
n-Butanol	BH	25.1	25.0	24.7	24.4	24.2	24.2
0.011 M	BL	15.2	14.0	13.6	13.2	12.8	11.6
n-Pentanol	BH	24.4	24.3	23.9	23.8	23.5	23.2
0.0098 M	BL	15.9	15.3	14.6	13.9	13.4	12.6
n-Hexanol	BH	17.9	17.9	17.1	17.3	17.3	16.9
0.0082 M	BL	12.1	10.9	10.4	10.1	9.8	9.2

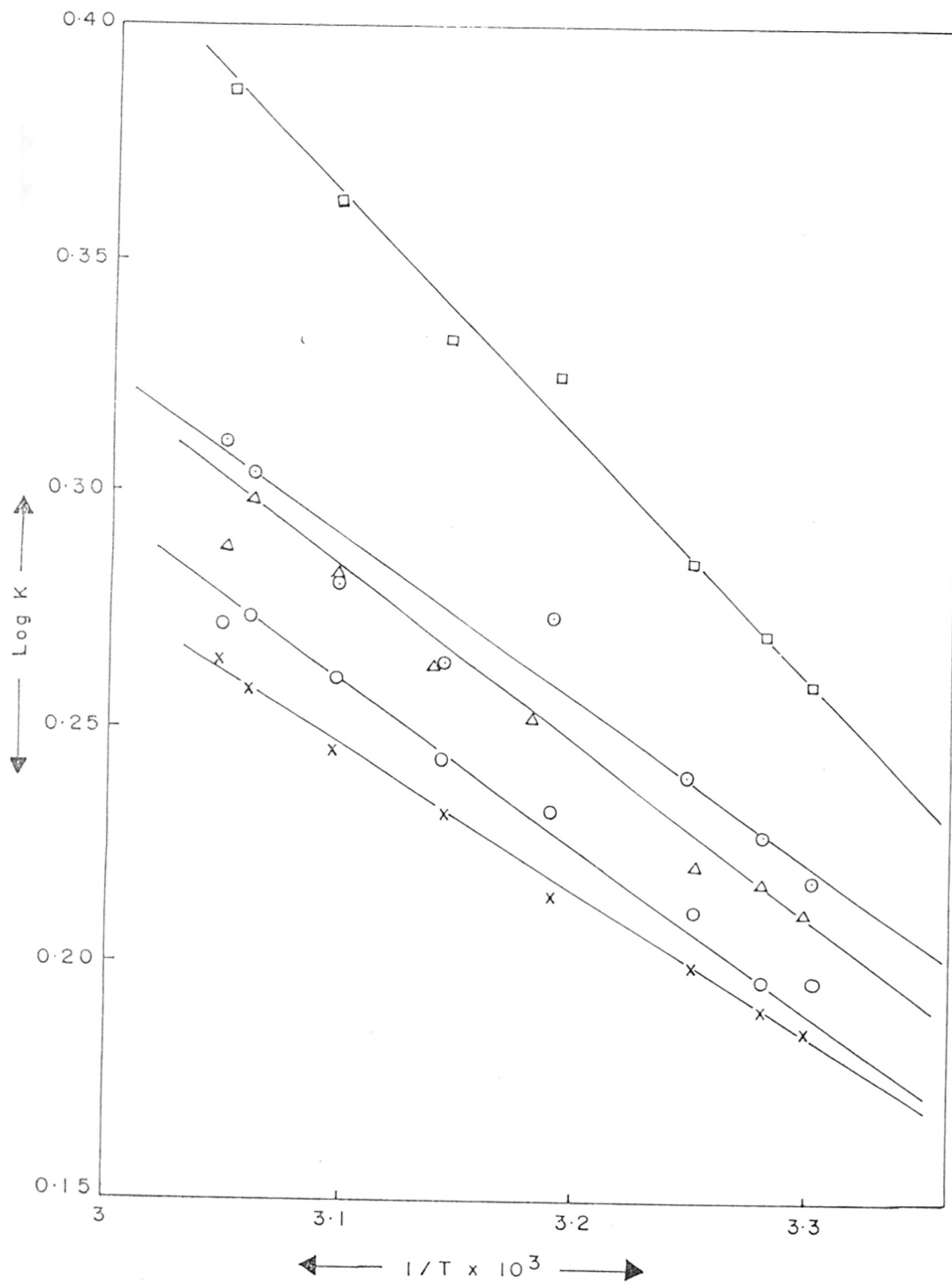


FIG.33 PLOT OF $\log K - 1/T \times 10^3$ FOR ETHANOL O, n-PROPANOL \square , n-BUTANOL Δ , n-PENTANOL x, n-HEXANOL O

same in all ($3627-28 \text{ cm}^{-1}$). The low frequency band had a higher half band width ($22-24 \text{ cm}^{-1}$) compared to the high frequency band (20 cm^{-1}). The present band positions and half band widths are quite close to those of Oki and Iwamura⁴², but generally different from those of others. Since these parameters are crucial for the curve resolution, even small changes in them can alter the band area results. Thus, using non-linear least square analysis⁷⁷ band position and half band widths of $3637, 18 \text{ cm}^{-1}$ and $3625, 22 \text{ cm}^{-1}$ ^{determined} for n-propanol were considerably different from those obtained in the present case. This also resulted in a K value of 1.2 ⁷⁷ as against 1.76 found from Fourier Deconvolution method used in the present work.

The assignments of the bands to specific rotamers were based on the early work of Oki and Iwamura⁴², who argued that the hydroxyl frequency in alcohols depended on the disposition of the O-H bond with respect to the α C-H and α C-alkyl bonds (Fig.5). Thus, the $3637-40 \text{ cm}^{-1}$ band in the present alcohols was ascribed to the trans conformer in which the O-H bond is gauche to the two methylene C-H bonds and the band at 3627 cm^{-1} to the two gauche conformers in which the O-H bond is gauche to the α C-H and α C-alkyl bonds. Since trans conformer frequency is somewhat lower than the frequency in methanol (3643 cm^{-1}), it is quite likely that the O-H group makes an angle different from 60° with respect to the α -methylene C-H bonds. These assignments of Oki and Iwamura⁴² are generally accepted by others though

Kolbe⁵⁸ prefers the assignment of the high frequency band to the gauche conformer to agree with their statistical distribution. Some support to the present assignment comes from the spectra of secondary alcohols, like 2-propanol, which have band profiles separable into components at 3627 and 3617 cm^{-1} , corresponding to the expected conformers in which the O-H bond is gauche to \propto C-H and \propto C-alkyl and two C-alkyl bonds, respectively.

The above assignments are in line with the observations of Krueger et. al.¹³⁶ and Bellamy et. al.¹³⁷ who found that NH/OH stretching frequencies in amines/alcohols were higher when \propto -CH bonds were lying trans to the lone pair electrons. The CH bonds in turn had also shown lower frequencies. McKean¹³⁸ had found support to the lower CH stretching frequencies when they lie trans to oxygen/nitrogen lone pair in the form of bond lengthening. Bond length calculations of a few selected nitrogen compounds like CH_3NH_2 , $(\text{CH}_3)_2\text{NH}$ etc. using dissociation energies had shown their lengthening. In the context of the present alcohols, methanol would have two CH bonds lying trans to the oxygen lone pairs in both its conformers giving rise to high frequency for OH bond. In the primary alcohols, the trans form would have two CH bonds trans to the oxygen lone pairs while the gauche form would have one CH bond only trans to the oxygen lone pair. Thus, the higher frequency of the trans form relative to the gauche form can be understood.

From Table VII, it can be seen that the trans species in these alcohols predominate to the extent of 1.6:1 over the gauche

Table VII

Hydroxyl band and thermodynamic parameters of N-alcohol rotamers

Alcohol	ν_H/cm^{-1}	ν_L/cm^{-1}	$\Delta\nu_{1/2}/\text{cm}^{-1}$			K		$\Delta H/\text{KJ mol}^{-1}$	
			H	L	Found	Reported	Found	Reported	
Ethanol	3637.0	3627.0	21.0	10.0	1.65	1.7 ⁵⁵ , 1.8 ⁴² , 8.0 ⁴⁵	6.8	6.3 ⁵⁸	
						7.7 ⁴³ , 11.0 ⁵⁴ , 2.7 ⁵⁸			
n-Propanol	3639.5	3627.5	20.0	23.0	1.76	2.6 ⁴² , 4.7 ⁴³ , 6.2 ⁵⁴	9.8	7.6 ⁵⁸	
						3.5 ⁵⁸ , 1.2 ⁷⁷ , 3.8 ⁴⁷			
n-Butanol	3640.0	3628.0	19.0	22.0	1.59	2.2 ⁴² , 6.9 ⁴³ , 5.3 ⁵⁴ , 3.6 ⁴⁷	5.9	-	
n-Pentanol	3639.0	3627.0	17.0	22.0	1.49	5.0 ⁴⁵ , 5.1 ⁴³	6.0	-	
n-Hexanol	3639.5	3627.0	18.0	23.5	1.47	4.0 ⁴³	6.8	-	

as against statistical distribution of 1:2. The reversal in the rotameric population can be ascribed to the larger separation between the O-H and C-alkyl substituent in the trans species than in the gauche form where they are much closer and could cause steric repulsion. Further, microwave spectrum of ethanol¹³⁹ showed predominance of trans conformer over the gauche species.

Bakke¹⁴⁰ has recently determined $^3\text{JHC.OH}$ coupling constants from PMR studies of a series of alcohols including ethanol in dilute $\text{CCl}_4/\text{CFCl}_3$ solution (0.01 M) and arrived at rotameric population. In the case of ethanol, he found the predominant conformer to be gauche with 65% population (statistical value) as against the infrared results which showed the trans species to be predominant to the extent of 62%. Bakke¹⁴⁰ in fact, suggested the reversal of the present infrared assignments of bands of 3637 and 3627 cm^{-1} to trans and gauche species, respectively to agree with the PMR results. He felt that reliable values of rotameric concentrations could not be obtained from band separation of the unsymmetrical broad hydroxyl band profile. He had, however, found that the rotameric population calculated from $^3\text{JHC.OH}$ coupling constants in 2-propanol (gauche 75 %) was in reasonable agreement with infrared results (gauche 63%) based on the assignment of 3627 cm^{-1} band to gauche species in which the O-H bond lies between the C-alkyl and C-H bonds as in ethanol.

The rotameric populations in the secondary alcohols obtained from NMR and IR studies do not differ but in the primary alcohols

the conclusions are not in agreement. In the case of ethanol, the rotameric population of trans species is found to be 62% from the present IR studies as against 65% gauche species calculated by Bakke¹⁴⁰ from NMR results. To understand this discrepancy in the rotameric populations derived from NMR $^3J_{\text{HCOH}}$ coupling constants, one will have to look into the assumptions made by Bakke¹⁴⁰ with regard to the possible conformations of ethanol and other alcohols.

It is assumed that the rotation around the C-O bond results in staggering of the O-H bond with respect to the C-H/C-C bond in a dihedral angle of 60° (Fig. 5). We feel that in the gauche species of ethanol and other n-alcohols, O-H may be making dihedral angles much smaller than 60° and 180° , with the methylene C-H bonds to avoid steric interaction with the CH_3 /alkyl group. This can be checked by assuming various dihedral angles in the gauche species and using Karplus¹⁴¹ equation,

$$^3J_{\text{HCOH}} = A + B \cos \theta + C \cos 2\theta$$

where $^3J_{\text{HO.CH}}$ is the vicinal proton-proton coupling constant for H-C-O-H fragment and θ is the dihedral angle between the planes H-C-O and C-O-H. The values of A, B and C were calculated from the $^3J_{\text{HC.OH}}$ coupling constants reported by Hammakar¹⁴², (11.6, 1.95 and 12.3 Hz for dihedral angles of 0, 60° and 180° , respectively) for di-t-butyl carbinol. These A, B and C values calculated as described above were 5.4, -0.35 and 6.55, respectively. Using these values the coupling constants for θ

angles of 30° , 60° and 150° were calculated as follows

$$J^{30} = 5.4 - 0.35 \times \cos 30 + 6.55 \times \cos 60 = 8.372 \text{ Hz}$$

$$J_{60} = 5.4 - 0.35 \times \cos 60 + 6.55 \times \cos 120 = 1.95 \text{ Hz}$$

$$J^{150} = 5.4 - 0.35 \times \cos 150 + 6.55 \times \cos 300 = 8.978 \text{ Hz}$$

From these values the coupling constant for the two gauche conformations with θ angles of 30° and 150° can be calculated as

$$\begin{aligned} J_g &= \frac{J^{30} + J^{150}}{2} \\ &= \frac{8.372 + 8.978}{2} \\ &= 8.675 \text{ Hz} \end{aligned}$$

The coupling constant for trans conformation can be deduced from

$$J_t = \frac{2 J_{60}}{2} = 1.95 \text{ Hz}$$

Bakke¹⁴⁰ had recorded the PMR spectra of ethanol in dilute CCl_4 solution ($< 10^{-2}$ M) and obtained $^3\text{J}_{\text{HCOH}}$ coupling constant of 5.1 Hz. This is the average value for the trans and the two gauche conformers of ethanol. If T and G represent their concentrations, then $5.1 = T \times 1.95 + G \times 8.675$ and $1 = T + G$.

From the above two equations, we get 53% trans and 47% gauche form which are in general agreement with IR results. The above

calculations show that by suitable choice of angles in the gauche species and using Karplus equation the observed $^3\text{J}_{\text{HCOH}}$ coupling constant of 5.1 Hz can be matched.

We have attempted an exercise to calculate the population of trans species by assuming various dihedral angles in the gauche species in the case of ethanol as shown in Table VIII.

<u>Dihedral angles</u> in degrees		<u>Population of</u> <u>trans species %</u>
60	180	39
45	165	50
35	155	53
30	150	53
25	145	53
15	135	47

Thus, for dihedral angles less than 60° , the population of the trans species increases and the trend looks such that IR and NMR results come closer. Therefore assignments made on the basis of infrared spectra need not be reversed as suggested by Bakke¹⁴⁰. Some refinements and improvements can be made in the dihedral angles, so as to match the NMR results with IR assignments, as in secondary alcohols.

Similar calculations were made by Rader¹⁴⁴ and Fraser et. al.¹⁴⁵ assuming dihedral angles of 60° and 180° for the gauche conformation of ethanol. They obtained 33% and 39% trans species respectively, which are comparable to those found by Bakke¹⁴⁰.

The rotamer equilibrium constants obtained for the various alcohols as can be seen from Table VII, are closer to those reported from non-linear least square curve analysis using arbitrary band parameters and Lorentzian band shape (1.2-2.6) and is much smaller than those determined graphically using arbitrary band parameters (2.7-11.0). It is interesting to note that general agreement was obtained with the results of Oki and Iwamura⁴², whose assumed band parameters of ethanol, n-propanol, and n-butanol were closer to those determined by the deconvolution method. The rotameric equilibrium constants of the various normal alcohols from ethanol to n-hexanol in the present study varied only marginally from one another (Table VII), thus confirming that sterically unhindered straight chain substituents do not affect the conformational equilibria arising from rotation around the C-O bond to any appreciable extent.

The variation of k with temperature in the range 303-328^oK are given in Table IX. It can be seen that the k values increase with temperature. Same type of trend has been observed by Fruwert et. al.⁶⁸ in the temperature study of n-alcohols. The variation of band areas with temperature is shown in Table VI. The band areas are found to decrease with temperature.

The observed ΔH values can only be compared with the results obtained on ethanol and n-propanol by Kolbe⁵⁸ who ascribed the higher frequency band to gauche (opposite to our assignment) and obtained values of 6.3 and 7.6 kJ/mol respectively. Micro-wave spectral investigations report a difference of 1.3 and 1.2

Table IX
 Temperature dependence of equilibrium
 constant (k) in n-alcohols

Temp. (k)	303	308	313	318	323	328
Ethanol (0.0066M)	1.65	1.77	1.87	1.85	1.92	2.06
n-Propanol (0.0092 M)	1.72	1.86	2.16	2.17	2.34	2.43
n-Butanol (0.011 M)	1.65	1.78	1.82	1.85	1.89	1.9
n-Pentanol (0.0098 M)	1.53	1.59	1.64	1.71	1.75	1.84
n-Hexanol (0.0082 M)	1.48	1.64	1.64	1.71	1.76	1.84

kJ/mol between the gauche and trans isomers in ethanol¹³⁹ and n-propanol¹⁴³, respectively. We are not aware of any ΔH value reported for other alcohols studied by us. ΔH value of 8.9 kJ/mol has been reported⁶⁸ for n-octanol in carbon tetrachloride. While intramolecular hydrogen bonding between C-H and the lone pair electrons on oxygen has been suggested for the formation of the gauche form, the possible difference in the hydrogen bonding interaction between the solvent CCl_4 and the rotamers ($\text{Cl}\dots\text{H}-\text{O}$) has also been suggested⁵⁸ for the stability of the trans conformers. However, only a detailed ΔH study of rotameric equilibria in other types of alcohols can offer a satisfactory explanation.

Thus, the present study has confirmed that the broad hydroxyl band profiles in primary alcohols are the results of rotational isomerism of the C-O bond. In straight chain alcohols, the high frequency trans conformer predominates over the gauche conformer approximately to the extent of 1.6:1 with an enthalpy difference of ~ 7 kJ/mol, suggesting little hindrance to rotation around C-O bond from a CH_2 chain.

CONCLUSIONS

C O N C L U S I O N S

In the present work, we have studied the conformational behaviour of three types of molecules i.e. dipeptides, 2-dimethyl amino benzoic acid and n-alcohols in dilute solutions. The dipeptides, N-acetyl (glycine, L-alanine, L-leucine) N'-methyl amides are present as fully extended free form and intramolecularly hydrogen bonded five membered ring species in dilute chloroform solution (10^{-4} M). The populations of free non-hydrogen bonded species were found to be 38, 47 and 65 per cent for N-acetyl glycine N'-methyl amide, N-acetyl L-alanine N'-methyl amide and N-acetyl L-leucine N'-methyl amide, respectively. It can be seen that the percentage of free fully extended form increases as the bulkiness of the substituent on C^α is increased.

The controversy regarding the solubility in carbon tetrachloride and the existence of the seven membered ring species in N-acetyl glycine, L-alanine, L-leucine N'-methyl amide could be settled by the present work. We found that solutions of concentrations greater than 10^{-5} M could not be prepared in carbon tetrachloride, though in most of the earlier work solutions of the order of 10^{-4} M have been claimed. In agreement with the latest results of Maxfield et. al., such solubilities were possible due to impurities in carbon tetrachloride. The band ascribed to the seven membered intramolecularly hydrogen bonded species, probably, has its origin in impurities in the solvent as shown by Maxfield

et al. In chloroform, we could not find any band in the region 3370-3300 cm^{-1} ascribable to the seven membered intramolecularly hydrogen bonded ring species.

The present results on the conformational population in N-acetyl L-alanine N'-methyl amide were compared with PMR results and conformational energy calculations to give the probable ϕ and ψ angles of $(-155^\circ, 160^\circ)$ and $(-84^\circ, 60-150^\circ)$ in intramolecular five-membered and non-hydrogen bonded free species, respectively.

Earlier studies of 2-dimethyl amino benzoic acid (dimethyl anthranilic acid, DMA) in various solvents had shown that the predominant species in CCl_4 were intramolecularly hydrogen bonded neutral species. The various other species in solution could not be recognised as the band in the carbonyl region was broad and could not be separated. In the present work, using Fourier Deconvolution method, this broad band was resolved into component bands and the possible additional species ascribable to these bands were determined.

In cyclohexane and carbon tetrachloride predominant species were intramolecularly hydrogen bonded neutral species giving rise to a strong band at 1731 cm^{-1} suggesting trans structure of the carboxylic group. The low frequency bands in carbon tetrachloride showed the presence of other species like dimeric species, solvated monomeric species and intramolecularly hydrogen bonded Zwitterionic species. In benzene and dioxane dimeric species were predominant (strong band at 1720 cm^{-1}) along with other

species mentioned above. In chloroform and acetonitrile, solvated monomeric species were predominant which can be seen from a strong band at 1709 cm^{-1} . The medium or weak bands showed the presence of other species in these solvents. In dimethyl sulphoxide and methanol, a strong band at 1670 cm^{-1} was assigned to intramolecularly hydrogen bonded Zwitterionic species. Other species were also found in small amounts. In D_2O , there were exclusively non-intramolecularly hydrogen bonded solvated Zwitterionic species.

The intramolecular hydrogen bonding in the neutral DMA molecule was unsymmetrical in nature, as indicated by the absorption in the IR spectrum at 2540, 2230, 2090 and 1950 cm^{-1} in carbon tetrachloride solution, characteristic of double minimum potential type (Hadzi type I). This was confirmed from the PMR spectrum where the hydroxyl proton chemical shift was found at $15.25\ \delta$ (with respect to TMS) in the same solvent.

The asymmetric broad band profile in the hydroxyl stretching region of n-alcohols in dilute carbon tetrachloride solution was ascribed to several causes like Fermi resonance, intramolecular hydrogen bonding between methyl C-H bond and lone pair of electrons on oxygen atom, conformational heterogeneity etc. The last factor has been subsequently found as the most probable explanation for this asymmetry. The broad band was therefore resolved by many workers using graphical or non-linear least square curve analysis method. The band parameters like band position and half band width used for this separation were arbitrarily chosen by

different workers giving rise to divergent results. We have used Fourier Deconvolution method where no band parameters were assumed to resolve the broad band unambiguously in the case of a few n-alcohols. The band positions could be established by deconvolution method and the separation therefore did not involve any uncertainty.

The high frequency band in all the alcohols was assigned to trans species by comparing with the single symmetrical band of methanol and low frequency band to the gauche species. Assuming the same integrated absorption intensity for these trans and gauche bands, the equilibrium constant was determined at various temperatures and ΔH values (~ 7 kJ/mole) for gauche-trans conversion in solution were calculated. The observed ΔH values were compared with those obtained by Kolbe for ethanol and n-propanol.

The present results give trans:gauche ratio of 1.6:1 in all alcohols. These results did not agree with those reported from NMR studies for ethanol according to which there were 65% gauche and 35% trans species. We have explained this discrepancy in the NMR results in terms of the possible changes in dihedral angles in the gauche conformer. We found that these angles could be smaller than 60° and 180° in contrast to what are normally assumed to avoid steric interaction with the CH_3/alkyl group of the substituent on C^α . Assuming the dihedral angles of 30° and 150° and using Karplus equation, we arrived at 47% gauche and 53%

trans species in general agreement with IR results.

Thus, usefulness of Fourier Deconvolution for separating strongly overlapping bands has been established in the present work and its applications in other areas are likely to be much larger.

REFERENCES

1. H. H. GILBERT, *Journal of Polymer Science*, **10**, 175 (1953).
2. H. H. GILBERT, *Journal of Polymer Science*, **10**, 185 (1953).
3. H. H. GILBERT, *Journal of Polymer Science*, **10**, 195 (1953).
4. H. H. GILBERT, *Journal of Polymer Science*, **10**, 205 (1953).

REFERENCES

1. H. H. GILBERT, *Journal of Polymer Science*, **10**, 175 (1953).
2. H. H. GILBERT, *Journal of Polymer Science*, **10**, 185 (1953).
3. H. H. GILBERT, *Journal of Polymer Science*, **10**, 195 (1953).
4. H. H. GILBERT, *Journal of Polymer Science*, **10**, 205 (1953).
5. H. H. GILBERT, *Journal of Polymer Science*, **10**, 215 (1953).
6. H. H. GILBERT, *Journal of Polymer Science*, **10**, 225 (1953).
7. H. H. GILBERT, *Journal of Polymer Science*, **10**, 235 (1953).
8. H. H. GILBERT, *Journal of Polymer Science*, **10**, 245 (1953).
9. H. H. GILBERT, *Journal of Polymer Science*, **10**, 255 (1953).
10. H. H. GILBERT, *Journal of Polymer Science*, **10**, 265 (1953).

REFERENCES

1. S. Mizushima, "Structure of Molecules and Internal Rotation," Academic Press, New York, 1954.
2. G. Pimentel and O. McClellan, "The Hydrogen Bond," W. H. Freeman and Company, London, 1960.
3. S. Mizushima and T. Shimanouchi, "Advances in Enzymology," 23, 1, 1961.
4. G. N. Ramachandran, C. Ramakrishnan and V. Sasisekharan, J. Mol. Biol., 7, 95, 1963.
5. IUPAC-IUB Commission on Biochemical Nomenclature, J. Mol. Biol., 52, 1, 1970.
6. M. Tsuboi, T. Shimanouchi and S. Mizushima, J. Am. Chem. Soc., 81, 1406, 1959.
7. S. L. Portnova, V.F. Bystrov, V. I. Tsetlin, V. T. Ivanov and Yu. A. Ovchinnikov, J. Gen. Chem., 38, 424, 1968.
8. V. F. Bystrov, S.L. Portnova, V.I. Tsetlin, V. T. Ivanov and Yu. A. Ovchinnikov, Tetrahedron, 25, 493, 1969.
9. V. F. Bystrov, S.L. Portnova, T.A. Balashova, V.I. Tsetlin, V.T. Ivanov, P.V. Kostetzky and Yu.A. Ovchinnikov, Tetrahedron Lett., (No.60), 5283, 1969.
10. J. Neel, Pure and Appl. Chem., 31, 201, 1972.

11. M. Marraud, J. Neel and M. Avignon, *J. Chim. Phys.*, 67, 959, 1970.
12. C. Cung, M. Marraud, J. Neel and A. Aubry, *J. Chim. Phys.*, 73, 213, 1976.
13. M. Avignon, P.V. Huong, J. Lascombe, M. Marraud and J. Neel, *Biopolymers*, 8, 69, 1969.
14. M. T. Cung, D. Caret, P. Granger, M. Marraud and J. Neel, *Compt. Rend.*, C269, 580, 1969.
15. M. Avignon and P.V. Huong, *Biopolymers*, 9, 427, 1970.
16. E. S. Efremov, L.B. Sanyavina, V. N. Zheltova, A. G. Ivanova, P. V. Kostetskii, V.T. Ivanov, E.M. Popov and Yu. A. Ovchinnikov, *Chem. Nat. Compd.*, 9, 308, 1973.
17. E. R. Stimson, S.S. Zimmerman and H. A. Scheraga, *Macromolecules*, 10, 1049, 1977.
18. F. R. Maxfield, S. J. Leach, E. R. Stimson, S. P. Powers and H. A. Scheraga, *Biopolymers*, 18, 2507, 1979.
19. J. Smolikova, J. Pospisek and K. Blaha, *Coll. Czech. Chem. Commun.*, 46, 772, 1981.
20. I. M. Ginzburg, *J. Gen. Chem.*, 52, 1445, 1982.
21. V. J. Hruby, "Chemistry and Biochemistry of Aminoacids, Peptides and Proteins," Vol. 3, Weinstein B. Ed., Marcel Dekker, New York, pp. 1-188, 1974.
22. J. T. Edsall and J. Wyman Jr., *J. Am. Chem. Soc.*, 57, 1964, 1935.

23. H. C. Brown, D. H. McDaniel and O. Hafflinger, "Dissociation Constants in Determination of Organic Structures by Physical Methods," Vol. I, Acad. Press, New York, 1955.
24. C. P. Nash, E. L. Pye and D. B. Cook, J. Phys. Chem., 67, 1642, 1963.
25. G. M. Barrow, J. Am. Chem. Soc., 80, 86, 1958.
26. E. Uhlig and K. Doering, Ber., 97, 1127, 1964.
27. A. Tramer, J. Mol. Struct., 4, 313, 1969.
28. K.R.K.Rao and C.I. Jose, Spectrochim. Acta, 30A, 859, 1974.
29. N.N. Dhaneshwar and L.M. Pant, Acta Crystallogr., 29B, 2980, 1973.
30. K.R.K. Rao and C.I. Jose, J. Mol. Struct., 18, 447, 1973.
31. J.K. Kauppinen, D.J. Moffat, H.H. Mantsch and D. G. Cameron, Appl. Spectrosc., 35, 271, 1981.
32. J. K. Kauppinen, D. J. Moffat, H. H. Mantsch and D. G. Cameron, Anal. Chem., 53, 1454, 1981.
33. M. Rospenk, J. Fritsch and G. Zundel, J. Phys. Chem., 88, 321, 1984.
34. B. Brzezinski and G. Zundel, J. Phys. Chem., 87, 5461, 1983.



35. B. Brzezinski and G. Zundel, *J. Magn. Reson.*, 48, 361, 1982.
36. D. F. DeTar and R.W. Novak, *J. Am.Chem. Soc.*, 92, 1361, 1970.
37. E. V. Ivash and D. M. Dennison, *J. Chem. Phys.*, 21, 1804, 1953.
38. T. L. Brown and M. T. Rogers, *J. Am. Chem. Soc.*, 79, 577, 1957.
39. R. M. Badger and S. H. Bauer, *J. Chem. Phys.*, 4, 711, 1936.
40. G. M. Barrow, *J. Phys. Chem.*, 59, 1129, 1955.
41. M. St. C. Flett, *Spectrochim. Acta*, 10, 21, 1957.
42. M. Oki and H. Iwamura, *Bull.Chem. Soc., Japan*, 32, 950, 1959.
43. T.D. Flynn, R.L. Werner and B. M. Graham, *Aust. J. Chem.*, 12, 575, 1959.
44. R. Piccolini and S. Winstein, *Tetrahedron Lett.* 13, 4, 1959.
45. F. Dalton, G.D. Meakins, J. H. Robinson and W. Zaharia, *J. Chem. Soc.*, 1566, 1962.
46. P.J. Krueger and H. D.Mettee, *Can. J.Chem.*, 42, 347, 1964.
47. E. L.Saier, L.R. Cousins and M.R. Basila, *J.Chem.Phys.*, 41, 40, 1964.

48. C.S. Kraihanzel and R. West, *J.Am.Chem.Soc.*, 84, 3670, 1962.
49. P. Arnaud and Y. Armand, *Compt.Rend.*, 253, 1426, 1547, 1961.
50. S. C. Stanford and W. Gordy, *J. Am.Chem.Soc.*, 63, 1094, 1941.
51. L.L.Ferstandig, *J. Am.Chem.Soc.*, 84, 1323, 3553, 1962.
52. A. Allerhand and P. Von R. Schleyer, *J.Am.Chem.Soc.*, 85, 1715, 1963.
53. D. J. Sutor, *J.Chem.Soc.*, 1105, 1963.
54. J. Fruwert, G.Hanschmann and G. Geiseler, *Z. Phys. Chem.*, 228, 277, 1965.
55. L. Joris, P. Von R. Schleyer and E. Osawa, *Tetrahedron*, 24, 4759, 1968.
56. G. A. Sim, *Ann.Rev. Phys. Chem.*, 18, 67, 1967.
57. A.B. Foster, A. H. Haines and M. Stacey, *Tetrahedron*, 16, 177, 1961.
58. A. Kolbe, *Z. Phys. Chem. (Leipzig)*, 250, 183, 1972.
59. A. J. Barnes, H.E. Hallam and D. Jones, *Proc. Roy. Soc. London, Section A*, 335, 97, 1973.
60. J.H. Van der Maas and E.T.G. Lutz, *Spectrochim, Acta*, 30A, 2005, 1974.
61. J.H. Van der Maas and E.T.G. Lutz, *Spectrochim, Acta*, 34A, 915, 1978.

62. W. Weltner Jr. and K.S. Pitzer, J. Am. Chem.Soc., 73, 2606, 1951.
63. G.M. Barrow, J. Chem.Phys., 20, 1739, 1952.
64. W.A.P. Luck and W. Ditter, Ber. Bunsenges, Phys. Chem., 75, 163, 1971.
65. J. Weinman, Bull. Soc. Chim., France, 4259, 1967.
66. J. Weinman and S. Weinman, Compt. Rend., 264, 1248, 1967.
67. J. Weinman and S. Weinman, Bull. Soc. Chim., France, 925, 1969.
68. J. Fruwert, G. Geiseler, W. Geyer and S. Sieber, Z. Phys. Chem., 241, 74, 1969.
69. P. Arnaud and Y. Armand, Compt. Rend., 255, 1718, 1962.
70. Y. Armand and P. Arnaud, Ann. Chim., 9, 433, 1964.
71. C. R. Eddy, J.S. Showell and T.E. Zell, J. Am. Oil Chemist's Soc., 40, 92, 1963.
72. H.S. Aaron and C.P. Rader, J. Am. Chem. Soc., 85, 3046, 1963.
73. H.S. Aaron, C.P. Ferguson and C.P. Rader, *ibid*, 89, 1431, 1967.
74. W. Ditter and W.A.P. Luck, Ber.Bunsenges Phys. Chem., 73, 526, 1969.
75. R. Salzer, J. Fruwert and G. Franz, Z. Phys. Chem. (Leipzig), 259, 154, 1978.
76. R. Salzer, Z. Phys. Chem.(Leipzig), 260, 43, 1979.

77. S. M. Chitale and C. S. I. Jose, *J. Chem. Soc. Faraday Trans. 1*, 82, 663, 1986.
78. N. Mori, S. Omura, N. Kobayashi and Y. Tsuzuki, *Bull. Chem. Soc., Japan*, 38, 2149, 1965.
79. S. Wada, *ibid*, 35, 707, 1962.
80. R. H. Muller, *Anal. Chem.*, 38, No. 12, 121A, 1966.
81. *Chem. Eng. News*, 43, 50 (Nov.15), 1965.
82. H. Stone, *J. Opt. Soc.*, 52, 998, 1962.
83. D. Papousek and J. Pliva, *Collection Chem. Commun.*, 30, 3007, 1965.
84. J. Pitha and R. N. Jones, *Can. J. Chem.*, 44, 3031, 1966.
85. B. F. Bacon and J. H. Van der Maas, *Spectrochim. Acta, Part A*, 44, 1243, 1988.
86. P. R. Griffiths, "Chemical Infrared Fourier Transform Spectroscopy," *Chemical Analysis*, Vol. 43, John Wiley and Sons Inc., New York/London/Sydney/Toronto, 1975.
87. P. R. Griffiths and J. A. de Haseth, "Fourier Transform Infrared Spectrometry," *Chemical Analysis*, Vol. 83, John and Wiley and Sons Inc., New York/Chichester/Brisbane/Toronto/Singapore, 1986.
88. A. A. Michelson, *Phil. Mag* (5), 31, 256, 1891.
89. A. A. Michelson, "Light Waves and Their Uses," University of Chicago Press, Chicago, 1902, reissued in the paperback Phoenix Edition, 1961.

90. R. N. Jones and C. Sandorfy, Techniques of Organic Chemistry, Vol. IX, "Chemical Applications of Spectroscopy", p. 271, Ed. A. Weissberger, Interscience Publishers Inc., 1967.
91. R. P. Bauman, "Absorption Spectroscopy", John Wiley and Sons Inc., New York, 1962.
92. W. J. Potts Jr., "Chemical Infrared Spectroscopy", Vol. I, John Wiley and Sons, New York, p. 170, 1963.
93. "Comprehensive Analytical Chemistry", Vol. VI, Ed. G. Svehla, Elsevier Scientific Publishing Co., Amsterdam, 1976.
94. D. A. Ramsay, J. Am. Chem. Soc., 74, 72, 1952.
95. K. S. Sheshadri and R. N. Jones, Spectrochim. Acta, 19, 1013, 1963.
96. Lowell M. Schwartz, Anal. Chem., 43, 1336, 1971.
97. "Digital Computing and Numerical Methods," B. Carnahan and J. O. Wilkes, p. 312, John Wiley and Sons Inc., New York, 1973.
98. J. K. Kauppinen, D. J. Moffatt, D. G. Cameron and H. H. Mantsch, Appl. Opt., 20, 1866, 1981.
99. W. I. Friesen and K.H. Michaelion, Appl. Spectrosc., 39, 484, 1985.
100. S. N. Vinogradov and R. H. Linnell, "Hydrogen Bonding", Van Nostrand Reinhold, New York, 1971.

101. M. D. Joesten, L. J. Schaad, "Hydrogen Bonding",
M. Dekker Inc., New York, 1974.
102. D. Hadzi and S. Bratos, "Vibrational Spectroscopy of The
Hydrogen Bond", Vol. II, Ed. P. Schuster, G. Zundel,
C. Sandorfy, North Holland Publishing Co., Amsterdam,
p. 567, 1976.
103. G.M. Barrow, J. Am. Chem. Soc., 78, 5802, 1956.
104. Ratajczak and Sobczyk, "The Polarity of the Hydrogen
Bond in Acid-Base Complexes", Zh. Strukt. Khim.,
6, 262, 1965.
105. T. H. Apple White and C. Niemann, J. Am. Chem. Soc.,
81, 2208, 1959.
106. F. F. Blicke and P. E. Norris, J. Am. Chem. Soc., 76,
3213, 1954.
107. L. S. Prabhurashi and C. I. Jose, J. Chem. Soc.,
Faraday Trans. 2, 71, 1545, 1975.
108. R. A. Nyquist, Spectrochim. Acta, 19, 509, 1963.
109. P. Ushabai and K. Venkataramiah, Bull. Chem. Soc.,
Japan, 44, 313, 1971.
110. G. Boussard, M. T. Cung, M. Marraud and J. Neel, J.
Chim. Phys., 71, 1159, 1974.
111. G. Boussard, M. Marraud and J. Neel, J. Chim. Phys.,
71, 1087, 1974.

112. D. W. Vidrine, Spectral Lines, 4, 3, 1982.
113. D.A.C. Compton, Spectral Lines, 5, 4, 1983.
114. S. M. Chitale and C. I. Jose, J. Chem. Soc. Faraday Trans. 2, 76, 233, 1980.
115. S. Mizushima, M. Tsuboi, T. Shimanouchi, T. Sugita and T. Yoshimoto, J. Am.Chem.Soc., 76, 2479, 1954.
116. A.W. Burges and H. A. Scheraga, Biopolymers, 12, 2177, 1973.
117. S. Mizushima, T. Shimanouchi, M. Tsuboi and T. Arakawa, J. Am. Chem.Soc., 79, 5357, 1957.
118. L. S. Prabhurashi and C. I. Jose, J. Chem.Soc. Faraday Trans. 2, 74, 225, 1978.
119. V. Madison and K. D. Kopple, J. Am. Chem.Soc., 102, 4855, 1980.
120. M. T. Cung, M. Marraud and J. Neel, "Conformation of Biological Molecules and Polymers", E. D. Bergmann and B. Pullman, Eds. Academic Press, New York, p.69, 1974.
121. J. Smolikova, A. Vitek and K. Blaha, Coll. Czech. Chem. Commun., 36, 2474, 1971.
122. B. Pullman and B. Maignet, "Conformation of Biological Molecules and Polymers", E. D. Bergmann and B. Pullman Eds. Academic Press, New York, p. 13, 1974.

123. V. Renugopalkrishnan, S. Nir and R. Rein, "Environmental Effects on Molecular Structure and Properties," Reidel Dordrecht, p. 109, 1976.
124. D. B. Davies, Md. Abu. Khaled and D. W. Urry, J. Chem. Soc., Perkin II, 1294, 1977.
125. V. N. Solkan and V. F. Bystrov, Bull. Acad. Sci., USSR, 23, 1232, 1974.
126. Yu. D. Gavrilov, V. N. Solkan and V.F. Bystrov, Bull. Acad. Sci., USSR, 24, 2368, 1975.
127. G. N. Ramachandran and Sasisekharan, "Adv. Protein Chem.," 23, 283, 1968.
128. P. N. Lewis, F.A. Momary and H. A. Scheraga, Isr. J. Chem., 11, 121, 1973.
129. B. Pullman and A. Pullman, "Adv. Protein Chem.," 28, 347, 1974.
130. S. S. Zimmerman and H. A. Scheraga, Macromolecules, 9, 408, 1976.
131. S. S. Zimmerman, M. S. Pottle, G. Nemethy and H. A. Scheraga, Macromolecules, 10, p.1-9, 1977.
132. M. Oki and M. Hirota, Bull. Chem. Soc., Japan, 34, 374, 1961.
133. S.C. Johnson and K. A. Rumon, J. Phys. Chem., 69, 74, 1965.
134. D. Hadzi, Pure and Appl. Chem., 11, 435, 1965.
135. K. R. K. Rao, Ph.D. Thesis, Univ. of Poona, 1973.
136. P.J. Krueger, J. Jan and H. Weiser, J. Mol. Struct., 5, 375, 1970.

137. L. Bellamy and D. W. Mayo, J. Phys. Chem., 80,
1217, 1976.
138. D.C. McKean and I.A. Ellis, J. Mol. Struct., 29,
81, 1975.
139. J. Michielsens-Effinger, Ann. Soc. Sci., Bruxelles
Ser.I, 78, 223, 1964.
140. J. M. Bakke, Acta Chem. Scand., 40B, 407, 1986.
141. Martin Karplus, J. Am. Chem. Soc., 85, 2870, 1963.
142. R. M. Hammaker, L. K. Patterson and K. C. Lin, J. Phys.
Chem., 72, 4346, 1968.
143. A. A. Abdurahmanov, R.A. Rahimova and L. M. Imanaov,
Phys. Lett., 32A, 123, 1970.
144. C. P. Rader, J. Am. Chem. Soc., 91, 3248, 1969.
145. R. R. Fraser, M. Kaufman, P. Morand and G. Govil,
Can. J. Chem., 47, 403, 1969.

APPENDIX

IR Spectra and Conformational Behavior of *N*-Acetyl-(Glycine, L-Alanine, L-Leucine)-*N'*-Methylamides in Chloroform*



CHALAKKAL I. JOSE, ANAGHA A. BELHEKAR, and MANGALA
S. AGASHE, *National Chemical Laboratory, Pune 411 008, India*

Synopsis

NH stretching bands of *N*-acetyl-(glycine, L-alanine, L-leucine)-*N'*-methylamides in dilute chloroform solution have shown that these dipeptides are present as a mixture of intramolecularly hydrogen-bonded five-membered ring species and nonhydrogen bonded species. Integrated absorption intensity measurements revealed that the concentration of the intramolecularly hydrogen bonded species decreased from 62% in glycine to 35% in the L-leucine derivatives.

INTRODUCTION

N-acetyl-*N'*-methylamides of amino acids have been studied as model dipeptides for determining polypeptide conformation since 1950. From the ir NH stretching bands observed at 3460–3440, 3420, and 3360–3300 cm^{-1} in dilute carbon tetrachloride ($10^{-4}M$) Mizushima et al.¹ and Efremov et al.² concluded that these exist as a mixture of the intramolecularly hydrogen-bonded seven-membered ring species (Fig. 1, middle) (3360–3300 and 3420 cm^{-1}) and fully extended species (Fig. 1, top) (3460–3440 cm^{-1}).

Portnova et al.,³ who investigated dipeptides of the type $\text{RCON}(\text{R}_1) \cdot \text{CH}(\text{CH}_3)\text{CON}(\text{R}_2) \cdot \text{CH}(\text{CH}_3)\text{COOCH}_3$, where $\text{R} = \text{C}_6\text{H}_5\text{CH}_2\text{O}$, CH_3 , $\text{R}_1 = \text{H}$, CH_3 , $\text{R}_2 = \text{H}$, CH_3 , also came to a similar conclusion regarding the nature of species in solution. Neel⁴ and Ginsburg⁵ who obtained the same spectra for *N*-methyl-*N'*-methylamides of glycine, L-alanine, etc., ascribed the 3420 cm^{-1} to an additional intramolecularly hydrogen-bonded five-membered ring species. These differences in the spectral interpretation led Hraby⁶ to suggest additional work in this area.

Maxfield et al.⁷ and Smolikova et al.⁸ recently found that in very dilute solution of chloroform and carbon tetrachloride the band at 3360–3300 cm^{-1} is absent or very weak. Maxfield et al. further showed that a band in this region could arise from impurities in the solute-solvent systems. In the present study, we have checked the previous results and taking into account the previous assignments arrived at a final picture. In addition, we determined the conformational population using the integrated absorption intensities of the free NH stretching band of *N*-methylacetamide and the intramolecularly hydrogen-bonded five-membered NH ring of *N*-acetyl-glycine-*N'*-dimethylamide, a procedure that has been successfully employed in determin-

*NCL communication No. 4105.

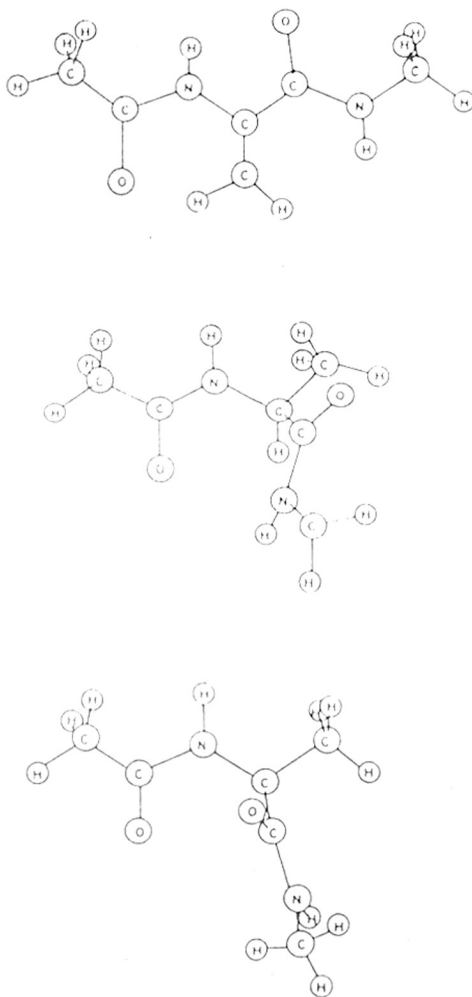


Fig. 1. Conformations of AAMA.

ing conformational equilibria in halo alcohols.⁹ The results are compared with nmr coupling constants^{10,11} obtained under similar conditions and conformational energy calculations.¹²

EXPERIMENTAL

Materials

All starting materials were Fluka Puriss/Purum grade chemicals. In every case, the amino acid ester hydrochloride was first prepared by passing HCl gas through amino acid dissolved in methanol solution at 0°C. Then, using the method of Apple-White and Neiman,¹³ the corresponding *N*-acetyl-*N'*-methyl/dimethyl derivatives were prepared. *N*-acetyl-glycine-*N'*-methylamide (AGMA) and *N*-acetyl-L-alanine-*N'*-methylamide (AAMA) were recrystallized at least five times from an ethanol ethyl acetate (1:9) mixture. *N*-acetyl-L-leucine-*N'*-methylamide (ALMA) was recrystallized similarly from

TABLE I
Melting Point and Microanalysis

	mp (°C)	Observed %			Calculated %		
		C	H	N	C	H	N
1 AGMA	158	45.7	7.63	21.1	46.1	7.7	21.5
2 AAMA	182	50.5	8.37	19.0	50.0	8.3	19.4
3 ALMA	165	58.5	10.0	13.9	58.0	9.65	15.0
4 AGDMA	50	48.5	8.51	17.3	50.0	8.3	19.4
5 ASMA	62	48.5	8.62	17.8	50.0	8.3	19.4

an ethyl acetate hexane (1:1) mixture. *N*-acetyl-glycine-*N'*-dimethylamide (AGDMA) was purified with difficulty due to its high solubility in organic solvents and low melting point. It was crystallized from ethyl acetate hexane mixture seven times. In the case of *N*-acetyl-sarcosine-*N'*-methylamide (ASMA), sarcosine was synthesized using chloroacetic acid and methylamine.¹⁴ The purity as checked by melting point and microanalysis are shown in Table I.

Analytical Fluka grade *N*-methylacetamide was recrystallized from ethanol three times before use. All materials were dried under vacuum before preparing the solutions by direct weighing. Reagent grade Merck chloroform and carbon tetrachloride were washed with water at least five times by vigorous stirring and were dried over calcium chloride (2 days), and twice distilled and stored in dark. An hour before use, activated molecular sieves (Linde 4A) was added for final drying.

Instruments

Infrared spectra were recorded on a Perkin Elmer 221 infrared spectrophotometer using an expanded scale (100 cm⁻¹, 8 cm) and a slit programme (970 × 2). Variable pathlength cells with 4-cm pathlength were employed for all measurements. The integrated absorption intensities were determined by measuring the band areas and applying the necessary corrections¹⁵ as described earlier.¹⁶ The band separation was done either using a graphical method or a computer programme adopted before.⁹

RESULTS AND DISCUSSION

The spectra of *N*-acetyl-glycine(L-alanine, L-leucine)-*N'*-methylamides in dilute chloroform solution ($\sim 5 \times 10^{-4}M$) are shown in Figs. 2-4. While the glycine derivative gave two well-defined bands at 3450 and 3418 cm⁻¹, the L-alanine and L-leucine derivatives showed mainly three bands at ~ 3450 , ~ 3433 , and ~ 3415 cm⁻¹. The exact position of the last band could not be determined as it appeared as a shoulder to the band at 3433 cm⁻¹. There is hardly any absorption below 3400 cm⁻¹. These results are in agreement with those of Maxfield et al.,⁷ who studied these compounds in the same solvent and found no band below 3400 cm⁻¹ at a concentration of 10⁻⁴M. However, they found two bands at 3420 and 3410 for L-alanine, and three at 3425, 3415, and 3405 in leucine in place of the 3415-cm⁻¹ shoulder observed by us.

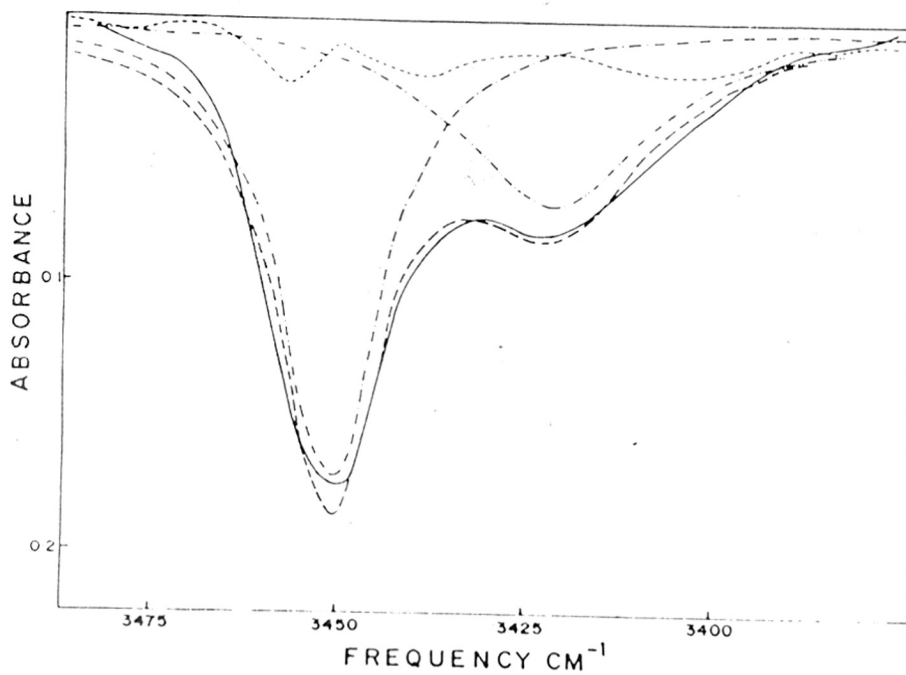


Fig. 2. NH stretching bands of AGMA. (—) Recorded spectrum, (---) band separation, (-----) sum of ---, and (.....) difference.

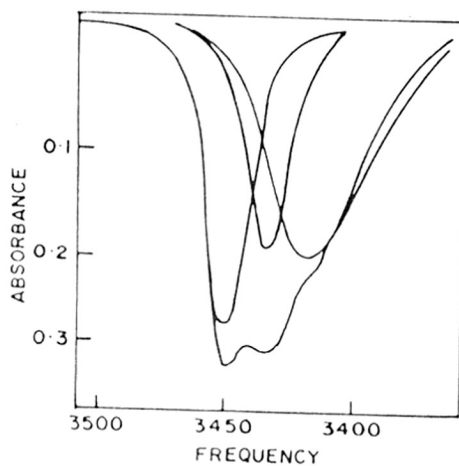


Fig. 3. NH stretching bands of AAMA.

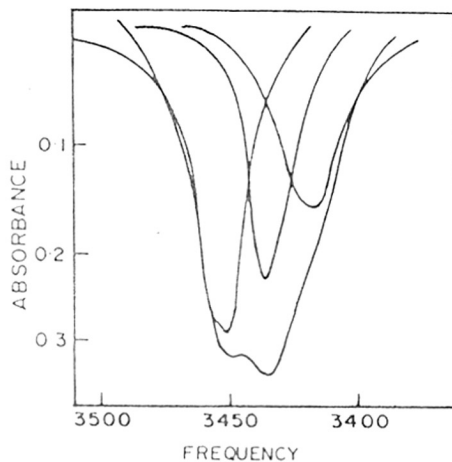


Fig. 4. NH stretching bands of ALMA.

Efremov et al.,² however, reported nearly identical three bands above 3400 cm^{-1} for AAMA in chloroform as found by us. In fact, for most dipeptides only a single band at 3420 cm^{-1} is reported^{1,4,5} in dilute carbon tetrachloride.

Mizushima et al.,¹ Neel,⁴ and Efremov et al.,² however, had observed a band at 3300–3360 cm^{-1} in the same dipeptides in dilute carbon tetrachloride solution ($\sim 10^{-4}M$) in addition to the bands observed above 3400 cm^{-1} . This band was reported weaker in chloroform relative to that in carbon tetrachloride where the seven-membered intramolecularly hydrogen-bonded NH species ascribed to this band were reported⁴ to be as much as 60–75% (glycine, L-alanine, L-leucine). Efremov et al.² calculated the concentration of the seven-membered ring species to be 30–20% in the various *N*-acetyl-(amino acid)-*N'*-methylamides in dilute chloroform solution. Ginzburg⁵ recently reported a band in this region for compounds studied in the present work in dilute carbon tetrachloride ($\sim 10^{-4}M$). An association band was also located in the same region. On the other hand, Smolikova et al.⁸ found hardly any band in this region for *tert*-leucine and L-valine derivatives, although a very weak band was observed for L-alanine and L-leucine derivatives in dilute carbon tetrachloride solution ($\sim 2 \times 10^{-5}M$).

In order to find out whether the band at 3300–3360 cm^{-1} reported for the title compounds was present in $10^{-4}M$ carbon tetrachloride solution, we tried to prepare such a solution of AGMA and found that the maximum solubility was close to $5 \times 10^{-6}M$. Maxfield et al.⁷ have also made a similar observation and, further, had shown how the solubility was enhanced in impure carbon tetrachloride containing contaminants like phosgene, HCl, water, etc. A weak broad band at 3370–3300 cm^{-1} was produced by these impurities as well as by methylamine from unsublimed AGMA. A lower solubility ($< 2 \times 10^{-6}M$) was also found in the case of the L-alanine derivative by us. These results, along with those of Smolikova et al.,⁷ clearly establish that the spectra recorded at $10^{-4}M$ concentration by the various workers are suspect and that the band found in the 3360–3300- cm^{-1} region in both *N*-acetyl-glycine (and L-alanine)-*N'*-methylamides is due to impurities in the solute-solvent systems.

Of the two NH stretching bands in the title compounds, 3460–3440-cm⁻¹ bands are clearly due to free NH groups, as suggested by nearly all the workers. With regard to the band at 3420–10 cm⁻¹, Mizushima et al. and Efremov et al. ascribed it to the free NH group of the seven-membered intramolecularly hydrogen-bonded folded form. This assignment is untenable now since it has been shown above that there is no absorption at 3370–3300 cm⁻¹ ascribed to the seven-membered intramolecularly hydrogen-bonded species in these compounds in chloroform. Neel⁴ have ascribed the 3420–10-cm⁻¹ band to an intramolecularly hydrogen-bonded five-membered NH ring in the title compounds in carbon tetrachloride. Marraud et al.¹⁷ have found two bands at 3460 and 3440 cm⁻¹ in *N*-acetyl amino acid esters in dilute carbon tetrachloride solution that are ascribed to the free and intramolecularly hydrogen-bonded five-membered NH ring species. Further, the absence of the 3420–10 cm⁻¹ in the spectra of *N*-methylated *N*-acetyl-(amino acid)-*N'*-methylamides⁴ strongly supports the above assignment. Thus the present studies establish that there are only two types of species in dilute solution of *N*-acetyl-(amino acid)-*N'*-methylamides, the intramolecularly hydrogen-bonded five-membered ring species (Fig. 1, top) and a form containing only free NH groups (Fig. 1, bottom), also called the nonhydrogen-bonded conformation.

In order to determine the concentrations of the two different species, we separated the free and intramolecularly hydrogen-bonded bands in the spectra and used the integrated absorption intensities (B) of the free and intramolecularly hydrogen-bonded NH groups at 3460 cm⁻¹ in *N*-methylacetamide and at 3405 cm⁻¹ in AGDMA, respectively, for converting the band areas to NH group concentrations. The free NH integrated absorption intensity measured for a number of *N*-alkylacetamides¹⁸ in carbon tetrachloride showed a variation of \bar{B} values ($18\text{--}22 \times 10^{-8}$ cm² mol⁻¹ s⁻¹, $3.6\text{--}4.4 \times 10^3$ dm³ mol⁻¹ cm⁻²) when alkyl was varied from methyl to isobutyl, so that its use as a standard for measuring the free NH group concentration can be justified (within 20%). The mean integrated absorption intensity of the NH group of *N*-methylacetamide measured in dilute chloroform at three concentrations ($1\text{--}5 \times 10^{-3}M$) using procedures reported earlier¹⁶ gave a value of 7.1×10^3 dm³ mol⁻¹ cm⁻². This can only be compared with the values reported^{18,19} in carbon tetrachloride (4.3×10^3 dm³ mol⁻¹ cm⁻², 5.8×10^3 dm³ mol⁻¹ cm⁻², respectively).

The spectrum of AGDMA in chloroform showed a strong band at 3405 cm⁻¹ with a weak shoulder at 3445 cm⁻¹ ascribable to a small amount of free NH species. Maxfield et al.⁷ found only a single band for this compound in chloroform. In carbon tetrachloride, however, two bands each at 3460 and 3412 cm⁻¹ for dimethyl,²⁰ and 3460 and 3415 cm⁻¹, for the diethyl²¹ derivatives have been reported. *N*-acetyl amino acid esters in dilute carbon tetrachloride solution as shown earlier¹⁷ exists as a mixture of the intramolecularly hydrogen-bonded five-membered ring and free species. Due to the weak intramolecular hydrogen bond, the extent of stabilization offered is small and a certain amount of free species would be expected. The concentration of the free NH band in AGDMA was estimated to be 8% from band area measurements and the integrated absorption intensity of the five-membered intramo-

TABLE II
 Calculated Population of Free and Intramolecularly Hydrogen-Bonded Five-Membered Ring Species in
N-Acetyl-(Amino Acid)-*N'*-Methyl-Dimethylamides in Chloroform

	AGDMA	AGMA	AAMA	ALMA	ASSMA
Solution concentration ($10^{-4}M$)	7.6	3.5	5.6	5.6	11.3
Area of 3450 band (cm^{-1})	1.51	13.3	23.5	16.9	21.3
Concentration ($10^{-4}M$) of free NH absorbing at 3450 cm^{-1}	0.61	4.7	8.3	5.9	7.5
Area of 3435 band (cm^{-1})			8.2	11.7	
Concentration ($10^{-4}M$) of free NH absorbing at 3435 cm^{-1}			2.9	4.1	
Total free NH concentration ($10^{-4}M$)	0.61	4.7	8.3	10.0	7.5
Area of 3420 band (cm^{-1})	39.0	12.2	21.3	11.6	11.1
Concentration ($10^{-4}M$) of bonded HN group		2.1	3.8	2.1	2.0
Percentage (mean) of free nonhydrogen-bonded species	8%	38%	47%	65%	65%
Percentage (mean) of five- membered intramolecularly hydrogen-bonded species	92%	62%	53%	35%	35% ^a

^a Refers to seven-membered intramolecularly hydrogen-bonded species.

lecularly hydrogen-bonded NH group was calculated from the band areas to be $14 \times 10^3 \text{ dm}^3 \text{ mol}^{-1} \text{ cm}^{-2}$ (Table II).

Using the two integrated absorption intensities (B) of the free and five-membered intramolecularly hydrogen-bonded NH groups, the concentrations of the free (C_F) and the intramolecularly hydrogen bonded (C_1) NH groups in the title compounds are calculated from band areas (A) using the equation:

$$B = A/Cl$$

where l is the pathlength (4 cm) and C is the concentration in g mole/L. The values thus obtained are given in Table II. Knowing that the free species (A) having two free NH groups would contribute twice the intensity of a free NH group and that the intramolecularly hydrogen-bonded five-membered ring species (B) would contribute to one free NH group intensity, and one bonded NH group intensity, the following equations can be written:

$$C_1 = C_B$$

$$C_A = C_S - C_B$$

where C_S is the solution concentration. The C_F values can be used as a check of the results since

$$C_F = 2C_A + C_B$$

It can be seen that the concentrations of the two species add up to the total NH group concentrations in all cases within $< 10\%$, which shows the validity of the assumptions regarding the use of integrated absorption intensity. The relative proportions of the two species in the title compounds show that the free form increased with increasing bulkiness of the substituent at the C^β . Such a trend has been reported in the case of the series of *N*-acetyl-(amino acid): (glycine, leucine, valine, etc.)-*N'*-dimethylamide by Neel.⁴ This can be understood since such a group could hinder the rotation around the C—N bond and reduce the probability of the C—O and NH groups coming closer for intramolecular hydrogen bonding.

We had seen above that there is hardly any intramolecularly hydrogen-bonded seven-membered ring species formed in the dilute solutions of the present compounds, although such species could be stabilized by their stronger hydrogen-bonding interaction over that in the five-membered ring hydrogen bond. In ASMA, where the formation of the intramolecularly hydrogen-bonded seven-membered ring species is reported,^{1,4} we have determined the concentration of this species using the integrated absorption intensity of the free NH group (Table I). We found that these are present to the extent of 30–35%, the remaining species having the nonhydrogen-bonded conformation. This raises the question as to why the intramolecularly hydrogen-bonded seven-membered ring species are absent in the *N*-acetyl-(amino acid)-*N'*-methylamides in solution. In a somewhat comparable instance, the diethylene glycol-monomethyl-ether²² $[\text{CH}_3(\text{OCH}_2\text{CH}_2)_2\text{OH}]$, which could form both five- and eight-membered intramolecularly hydrogen-bonded species through a single hydroxyl group, the relative proportion of the five- and eight-membered

TABLE III
 Predicted and Observed Proton Coupling Constants for AAMA

	ϕ	3J	ψ	5J	
				I	II
Five-membered conformer					
Pullman and Maigret ²⁵	-180	3.3	180	0.34	0.34
Cung et al. ²³	-160	6.8	170	0.19	0.26
Smolikova et al. ²⁴	-150	8.4	150	0.11	0.11
Nonhydrogen bonded					
Bystrov et al. ²⁶	60	3.3	-60	0.34	0
Renugopalkrishnan et al. ²⁷	-120	10.9	-60	0	0
Maxfield et al. ⁷	-84	7.5	60	0.15	0.34
			150	0.15	0.11
	-150	8.4	70	0.11	0.26
Observed ¹⁰		7.5		0.11	< 0.03

intramolecularly hydrogen-bonded and free species were 62, 31, and 6%, respectively. The frequency shifts for the five- and eight-membered intramolecularly hydrogen-bonded hydroxyl group were 40 and 195 cm^{-1} , respectively. It would appear from the above that the intramolecular hydrogen-bonding interaction in the seven-membered ring of the present compounds ($\Delta\nu = 100 \text{ cm}^{-1}$) is far too small to stabilize such species in the presence of the more facile (entropywise) five-membered intramolecular hydrogen bond.

Comparison with Reported NMR Results

In order to see whether the two conformations found by the ir spectroscopic method are supported by nmr results, we compared the reported 3J HNCH coupling constant¹¹ of 7.5 Hz for *N*-methyl-L-alanine-*N'*-methylamide in dilute chloroform ($7 \times 10^{-4}M$) with those calculated for possible angles suggested by different authors²³⁻²⁷ for the above conformations using the Karplus-Bystrov formula¹⁰ with $A = 9.4$, $B = 1.1$, and $C = 0.4$ (Table III). A perusal of the data revealed that the observed value could arise from a mixture of a five-membered conformer with $\phi = -180^\circ$ (3.3 Hz) and nonhydrogen-bonded conformer with $\phi = -120^\circ$ (10.9 Hz), or a five-membered conformer with $\phi = -155^\circ$ (7.5 Hz) and a nonhydrogen-bonded conformer with $\phi = -84^\circ$ (7.5 Hz). It was found from conformational energy calculations (see later) that $\phi = -180^\circ$ is not allowed with β carbon atom on the side chain, so that the mean value of 7.5 Hz arises from conformers having $\phi = -155$ and -84° .

Davies et al.¹⁰ have shown that five-bond long-range proton-proton coupling existing between the C^αH group of the amino acid in peptide bond, and that the methyl groups (acetyl and *N*-methyl) could be used to predict the torsional angles ϕ and ψ . Although the observed 5J coupling constant for peptide bond 1 (0.1) is close to 0.15 for $\phi = -155^\circ$ (C_5 conformation) and 0.15 for $\phi = -84^\circ$ (nonhydrogen-bonded conformation), the observed 5J coupling constant for peptide bond 2 (< 0.03) is very different from the calculated values ~ 0.2 (for C_5 conformation) and 0.11-0.34 (for nonhydrogen-bonded conformation).

TABLE IV
Calculated and Observed $^{13}\text{C}\dots^1\text{H}$ Vicinal Coupling Constant for AAMA

	$^1\text{HNC}^{\alpha 13}\text{C}'$	$^1\text{HNC}^{\alpha 13}\text{C}^{\beta}$	$^1\text{HC}^{\alpha}\text{N}^{13}\text{C}'$
Calculated ²⁸ for ϕ			
-160	2.6	0.5	1.0
-80	0.8	2.8	0.6
+40	7.0	< 0	4.0
+90	0	4.0	4.0
Observed ²⁹	< 1	1.9	2.5

Solkan and Bystrov²⁸ have theoretically calculated the vicinal spin-spin interaction constants between ^1H and ^{13}C nuclei in a peptide fragment for various ϕ angles and have shown how these, together with the $^3J_{\text{HNC}^{\alpha}\text{H}}$ coupling constant, permit a determination of the torsional angle unambiguously. Gavrilov, Solkan, and Bystrov²⁹ have subsequently measured the vicinal coupling constants $^1\text{HNC}^{\alpha 13}\text{C}'$, $^1\text{HNC}^{\alpha 13}\text{C}^{\beta}$, and $^1\text{H}^{\alpha}\text{CN}^{13}\text{C}'$ of AAMA in methanol (concentration = 1M). Using the observed $^3J_{\text{HNCH}}$ coupling constant of 7.5 Hz in dilute chloroform, we have read out from their graphs²⁸ the three coupling constants for the four ϕ angles (Table IV) and compared them with their experimental results.²⁹ The agreement between the observed values and those calculated for the ϕ angles -160 and -80° are better than those for $+40$ and $+90$, although much better agreement should be expected. This is definitely due to the higher concentration and the relatively polar solvent used for the ^{13}C studies.

Comparison with Conformational Energy Calculations

Zimmerman et al.¹² have concluded from their conformational energy calculations that there are several low energy conformations for *N*-acetyl-(amino acid)-*N'*-methylamide. The C_7 equatorial conformation ($\phi, \psi: -84^\circ, 79^\circ$) was calculated to have the lowest energy. The intramolecularly hydrogen-bonded C_7 conformation, however, has been shown to be absent in the present compounds, but conformations with $\phi = -84^\circ$ but ψ angle different from 79° such that an intramolecular hydrogen bond is not formed are possible. A look at the conformational energy map¹² shows that variations in the ψ angle within 60° - 150° would bring about only marginal change from the lowest energy (1 kcal). Thus a distorted C_7 conformation without any intramolecular hydrogen bond estimated to be $\sim 50\%$ in the L-alanine derivative is satisfactorily explained by the energy calculations. For the other significant conformer ($\phi, \psi: -150^\circ, 70^\circ$) the 3J coupling constant calculated as before gave a value of 8.4 Hz, which is higher but with a value of $\phi = -155^\circ$, an agreement with the reported value is possible. Thus both the above nonhydrogen-bonded conformers could represent 50% of the total conformational species in chloroform solution.

The other probable conformer based on conformational energy calculation is the hydrogen-bonded C_5 species ($\phi, \psi: -180^\circ, 180^\circ$). However, for β carbon on the side chain this conformation is not allowed. Cung et al.²³ and Smolikova et al.²⁴ have suggested C_5 conformation with $(-160^\circ, 170^\circ)$ and with $(-150^\circ,$

150°) for ϕ and ψ , which would give calculated 3J HNCH coupling constants of 6.8 and 8.4 Hz, respectively. These are much closer to the expected value of 7.5 Hz, so that contribution from this species to the extent of 50% as obtained in the present studies would meet the conformational energy calculations.

References

1. Tsuboi, M., Shimanouchi, T. & Mizushima S. (1959) *J. Am. Chem. Soc.* **81**, 1406-1411.
2. Efremov, E. S., Sanyavina, L. B., Zheltova, V. N., Ivanova, A. G., Kostetskii, P. V., Ivanov, V. T., Popov, E. M. & Ovchinnikov, Yu. A. (1973) *Chem. Nat. Compounds* **9**, 308-319.
3. Portnova, S. L., Bystrov, V. F., Tsetlin, V. I., Ivanov, V. T. & Ovchinnikov, Yu. A. (1968) *J. Gen. Chem.* **38**, 424-433.
4. Neel, J. (1972) *Pure Appl. Chem.* **31**, 201-225.
5. Ginzburg, I. M. (1982) *J. Gen. Chem.* **52**, 1445-1451.
6. Hruby, V. J. (1974) in *Chemistry and Biochemistry of Amino Acids, Peptides and Proteins*, Vol. 3, Weinstein, B., Ed., Marcel Dekker, New York, pp. 1-188.
7. Maxfield, F. R., Leach, S. J., Stimson, E. R., Powers, S. P. & Scheraga, H. A. (1979) *Biopolymers*, **18**, 2507-2521.
8. Smolikova, J., Pospisek, J. & Blaha, K. (1981) *Coll. Czech. Chem. Commun.* **46**, 772-780.
9. Chitale, S. M. & Jose, C. I. (1986) *J. Chem. Soc. Faraday I* **82**, 663-680.
10. Davis, B. D. & Khaled, Md. Abu. & Urry, D. W. (1977) *J. Chem. Soc. Perkin II*, 1294-1301.
11. Madison, V. & Kopple, K. D. (1980) *J. Am. Chem. Soc.* **102**, 4855-4863.
12. Zimmerman, S. S., Pottle, M. S., Nemethy, G. & Scheraga, H. A. (1977) *Macromolecules*, **10**, 1-9.
13. Apple-White, T. H. & Niemann, C. (1959) *J. Am. Chem. Soc.* **81**, 2208-2213.
14. Blicke, F. F. & Norris, P. E. (1954) *J. Am. Chem. Soc.* **76**, 3213-3214.
15. Ramsay, D. A. (1952) *J. Am. Chem. Soc.* **74**, 72-80.
16. Prabhumirashi, L. S. & Jose, C. I. (1975) *J. Chem. Soc. Faraday II* **71**, 1545-1553.
17. Boussard, G., Marraud, M. & Neel, J. (1974) *J. Chim. Phys.* **71**, 1081-1091.
18. Nyquist, R. A. (1963) *Spectrochim. Acta* **19**, 509-519.
19. Ushabai, P. & Venkataramiah, K. (1971) *Bull. Chem. Soc. Jpn.* **44**, 313-315.
20. Boussard, G., Cung, M. T., Marraud, M. & Neel, J. (1974) *J. Chim. Phys.* **71**, 1159-1166.
21. Marraud, M., Neel, J. & Avignon, M. (1970) *J. Chem. Phys.* **67**, 959-964.
22. Prabhumirashi, L. S. & Jose, C. I. (1978) *J. Chem. Soc. Faraday II* **74**, 255-262.
23. Cung, M. T., Marraud, M. & Neel, J. (1974) in *Conformation of Biological Molecules and Polymers*, Bergmann, E. D. & Pullman, B., Eds., Academic Press, New York, pp. 69-86.
24. Smolikova, J., Vitek, A. & Blaha, K. (1971) *Coll. Czech. Chem. Commun.* **36**, 2474-2485.
25. Pullman, B. & Maigret, B. (1974) in *Conformation of Biological Molecules and Polymers*, Bergmann, E. D. & Pullman, B., Eds., Academic Press, New York, pp. 13-39.
26. Bystrov, V. F., Portnova, S. L., Tsetlin, V. I., Ivanova, V. T. & Ovchinnikov, Y. A. (1969) *Tetrahedron*, **25**, 493-515.
27. Renugopalkrishnan, V., Nir, S. & Rein, R. (1976) *Environmental Effects on Molecular Structure and Properties*, Reidel Dordrecht, pp. 109-133.
28. Solkan, V. N. & Bystrov, V. F. (1974) *Bull. Acad. Sci. USSR* **23**, 1232-1236.
29. Gavrilov, Y. D., Solkan, V. N. & Bystrov, V. F. (1975) *Bull. Acad. Sci. USSR* **24**, 2368-2373.

Received August 5, 1986

Accepted February 13, 1987

Structural changes of 2-dimethylamino-benzoic acid in solution—a spectral deconvolution study*

CHALAKKAL I. JOSE, ANAGHA A. BELHEKAR and MANGALA S. AGASHE

National Chemical Laboratory, Poona 411 008, India

(Received 11 January 1988; accepted 5 February 1988)

Abstract—Fourier deconvolution has resolved the broad carboxylic bands in 2-dimethylamino-benzoic acid to a number of individual bands which helped to identify the various species in solution. While neutral species with or without an intramolecular hydrogen bond predominate in non-polar solvents, the Zwitterionic species with or without an intramolecular hydrogen bond are the main species in polar solvents. The strong solvating power of water was able to break the strong intramolecular charge transfer hydrogen bond present in 2-dimethylamino-benzoic acid.

INTRODUCTION

Some years ago, one of us [1, 2] showed that dimethylanthranilic acid has an intramolecularly hydrogen bonded Zwitterionic structure in the solid state, later confirmed by X-ray crystallographic analysis [3], while in solutions of cyclohexane, carbon tetrachloride etc, the predominant species were intramolecularly hydrogen bonded neutral species. Because of the broad profile of the absorption at $1750\text{--}1625\text{ cm}^{-1}$, it was not possible to separate the bands and establish the nature of the various other species in solution at that time. Recently, KAUPPINEN *et al.* [4, 5] have reported a deconvolution procedure for band separation which was carried out conveniently in Fourier Space using a computer program. In view of the unusual structural behaviour of dimethylanthranilic acid and the conflicting results [6–8] on the nature of species in solution, we have examined its i.r. spectra in a variety of both polar and non-polar solvents including water (heavy) and using the Fourier deconvolution technique separated the bands and established the various structural species in solution. Proton magnetic resonance spectra were used to support some of the structural features and hydrogen bonding behaviour.

EXPERIMENTAL

2-Dimethylamino-benzoic acid; dimethylanthranilic acid (DMA) was prepared and purified as before [1]. Cyclohexane, carbon tetrachloride, benzene, dioxane, chloroform and acetonitrile were laboratory or analytical reagent grades, while methanol was spectroscopic grade. Reagent grade dimethyl sulphoxide was dried over calcium hydride and vacuum distilled. All solvents were finally dried over zeolites before use. Heavy water (99.9%) was supplied by the Atomic Energy Commission, Trombay, India.

The spectra were recorded on a Nicolet 60 SXB Fourier transform spectrometer at 2 cm^{-1} resolution and co-adding 100 scans to obtain a signal to noise ratio of 1000 to 1. Since the region of interest $1750\text{--}1600\text{ cm}^{-1}$ has strong water vapour absorptions, the instrument was purged for an hour before use. The signal averaged interferograms were apodised

with a Happ Genzel function prior to phase correction and Fourier transformation. Deconvolution was performed with Nicolet programmes [9, 10] IRDCON.FTN and macro CON based on the algorithm of KAUPPINEN *et al.* [4, 5]. The parameters VFO, the width at half height of the line shape function and VFI, a resolution enhancement factor were chosen (VFO = 14–18, VFI = 1.4–2.2) such that the total area under the original spectra and deconvoluted spectra were the same and there were no negative lobes or other artifacts. The solution concentration of 0.06 M was maintained in all solvents except cyclohexane where solubility permitted only 0.01 M. The path length was similarly kept constant at 0.01 cm except in water where it was reduced to 0.0025 cm.

The PMR spectra were taken on a Bruker 90 Mhz FT-NMR Spectrometer using TMS as standard.

RESULTS AND DISCUSSION

Spectra of DMA in various solvents in the region $1800\text{--}1625\text{ cm}^{-1}$ at identical concentration (0.06 M) and path length (0.01 cm) are shown in Fig. 1. It can be seen that the band structure is the simplest in cyclohexane (saturated solution ~0.01 M) with the carbonyl absorption at the highest (1738 cm^{-1}). However, as the solvent was varied to carbontetrachloride

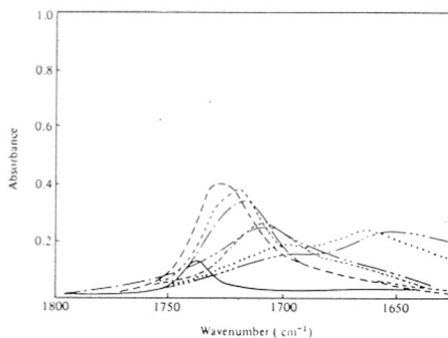


Fig. 1. I.r. spectra of 2-dimethylamino-benzoic acid in: 1, cyclohexane (—); 2, carbon tetrachloride (---); 3, benzene (---); 4, dioxane (· · ·); 5, acetonitrile (---); 6, chloroform (---); 7, dimethyl sulphoxide (· · · ·); 8, methanol (---·---).

*NCL Communication No. 4369.

ide, benzene, dioxane, acetonitrile, chloroform, dimethyl sulphoxide and methanol, peak absorptions continuously decreased with the band profile simultaneously broadening out indicating additional absorptions. As a clear separation of the bands could not be achieved even after taking considerably lower concentrations (0.01 M), a band deconvolution was tried, to obtain the spectra shown in Fig. 2. It is evident

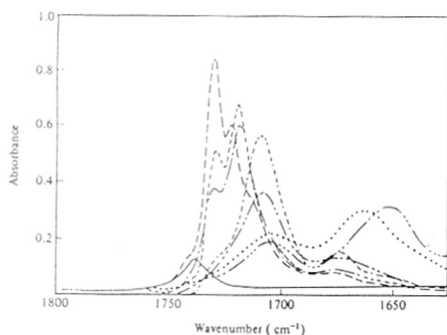


Fig. 2. Fourier deconvoluted i.r. spectra of 2-dimethylamino-benzoic acid in: 1, cyclohexane (—); 2, carbon tetrachloride (---); 3, benzene (- - -); 4, dioxane (- · - ·); 5, acetonitrile (- · - ·); 6, chloroform (- · - ·); 7, dimethyl sulphoxide (- · - ·); 8, methanol (- · - ·).

that the deconvolution has resulted in a fairly good separation of the bands so that their positions could be located (Table 1). It is worth pointing out that no indication of additional bands was observed in the case of cyclohexane on deconvolution. In carbon tetrachloride, benzene and dioxane, there are two sharp bands at 1730 and 1718 with an unresolved band at 1709 and a broad weak band at 1675 cm^{-1} . In acetonitrile, chloroform, dimethyl sulphoxide and methanol on the other hand, there are mainly two broad bands at 1709 and 1670–1650 cm^{-1} with weak unresolved bands at higher frequencies.

From the unusually high value of 1738–1730 cm^{-1} for the carboxylic carbonyl in non-polar solvents like cyclohexane, carbon tetrachloride etc., it is evident that the carboxylic group is in the unfavourable *trans* form stabilised by an intramolecular hydrogen bond between the carboxylic hydroxyl and the lone pair electrons on the nitrogen of the *ortho*-dimethylamino group (Fig. 3, A). The multiple band structure for the hydroxyl stretching vibration at 2540 cm^{-1} etc. reported earlier [1] in carbon tetrachloride supported the involvement of the hydroxyl group in strong intramolecular hydrogen bonding. The chemical shift of 15.23 δ for this hydroxylic proton in the PMR spectrum had confirmed the presence of such species. The band at 1720 cm^{-1} which grows in intensity as the solvent was varied to benzene and dioxane could arise

Table 1. Carboxyl bands of 2-dimethylamino-benzoic acid in solution

Solvents	Frequency in cm^{-1}			
1. Cyclohexane	1738 m			
2. Carbon tetrachloride	1731 s	1722 s	1710 m	1677 mb
3. Benzene	1730 m	1720 s	1708 w	1675 wb
4. Dioxane	1729 m	1719 s	1709 sh	1680 mb
5. Chloroform	1727 m		1709 vs	1672 mb
6. Acetonitrile	1729 w		1708 vs	1675 mb
7. Dimethyl-sulphoxide	1729 w		1703 m	1663 s
8. Methanol	1728 w		1705 m	1685 sb
9. Water (heavy)				1565 m

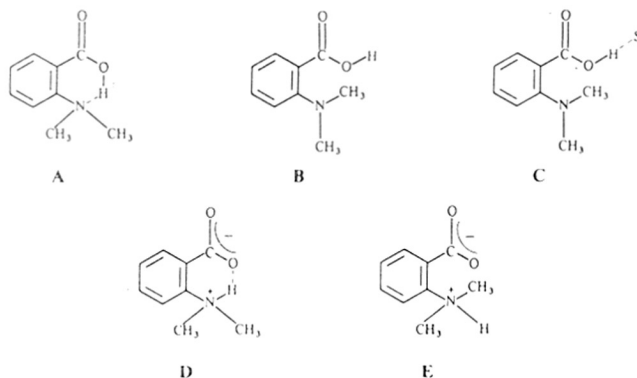


Fig. 3. Dimethylanthranilic acid structures.

from the carbonyl of the stable *cis* carboxylic group (Fig. 3, B) which has a strong tendency to dimerise. As the polarity of the solvent was increased these dimers could break down and form intermolecular complexes with the solvent and the carbonyl of such a carboxylic group (Fig. 3, C) could absorb at 1709 cm^{-1} . These complexes could predominate in solvents like acetonitrile, chloroform etc. In more polar solvents like dimethyl sulphoxide and methanol, charge transfer takes place resulting in Zwitterions, which would form a charge transfer intramolecular hydrogen bond (Fig. 3, D). The asymmetric stretching mode of such a carboxylate group could absorb at 1670 cm^{-1} , close to what has been observed in the Zwitterionic intramolecularly hydrogen bonded solid DMA at 1650 cm^{-1} . In order to confirm the nature of these species, the PMR spectrum of DMA in dimethyl sulphoxide- d_6 was taken which showed a proton with a chemical shift of 17.30δ (with respect to TMS), which is much higher than that found for the hydroxyl group in the neutral hydrogen bond of DMA in carbon tetrachloride. Such a high value could only be ascribed to a charge transfer $\overset{+}{\text{N}}-\text{H}\cdots\overset{-}{\text{O}}$ hydrogen bond. BRZEZINSKI and ZUNDEL [11] have observed similar behaviour in a closely related compound *N,N*-dimethyl 5-*R* anthranilic acid *N*-oxide in similar solvents.

The spectrum of DMA in water (heavy) showed a doublet in the aromatic region (1606 and 1613 cm^{-1}) and medium broad band at 1565 cm^{-1} which is very similar to the spectrum of the sodium salt of dimethylanthranilic acid in the solid state (1605 , 1585 and 1560 cm^{-1}). In organic solvents on the other hand, DMA had shown only a single aromatic band near 1600 cm^{-1} . As the doubling could arise from conjugative effects, the band near 1565 cm^{-1} has been ascribed to the carboxylate group of the Zwitterionic species of DMA which is solvated and not involved in intramolecular hydrogen bonding (Fig. 3, E). It is worth noting that the strong solvating power of water

in relation to dimethyl sulphoxide and methanol was capable of breaking the strong intramolecular charge transfer hydrogen bond between the COO^- and $\text{N}^+(\text{CH}_3)_2\text{H}$ groups. This is largely due to the ability of water to solvate both the above groups while the other two solvents could only solvate one of them.

SUMMARY

The present studies thus establish that dimethylanthranilic acid which as an intramolecularly hydrogen bonded Zwitterionic species in the solid, is capable of taking both free and intramolecularly hydrogen bonded, neutral and Zwitterion structures in solution. The relative proportion of the various structures is dependent on the nature of the solvent, the neutral forms predominating in non-polar solvents and Zwitterionic species in polar solvents. Fourier deconvolution was found very useful in separating overlapping bands with similar half band widths in condensed phase.

REFERENCES

- [1] K. R. K. RAO and C. I. JOSE, *J. molec. Struct.* **18**, 447 (1973).
- [2] K. R. K. RAO and C. I. JOSE, *Spectrochim Acta* **30A**, 859 (1974).
- [3] N. N. DHANESHWAR and L. M. PANT, *Acta Crystallogr.* **29B**, 2980 (1973).
- [4] J. K. KAUPPINEN, D. J. MOFFAT, H. H. MANTSCH and D. G. CAMERON, *Appl. Spectrosc.* **35**, 271 (1981).
- [5] J. K. KAUPPINEN, D. J. MOFFAT, H. H. MANTSCH and D. G. CAMERON, *Anal. Chem.* **53**, 1454 (1981).
- [6] J. T. EDSALL and J. WYMAN, JR., *J. Am. chem. Soc.* **57**, 1965 (1935).
- [7] H. C. BROWN, D. H. MCDANIEL and O. HAFFLINGER, *Dissociation Constants in Determination of Organic Structures by Physical Methods*, Vol. I. Academic Press, New York (1955).
- [8] A. TRAMER, *J. molec. Struct.* **4**, 313 (1969).
- [9] D. W. VIDRINE, *Spectral Lines* **4**, 3 (1982).
- [10] D. A. C. COMPTON, *Spectral Lines* **5**, 4 (1983).
- [11] B. BRZEZINSKI and G. ZUNDEL, *J. phys. Chem.* **87**, 5461 (1983).

Conformational Equilibria in n-Alkanols

Infrared Spectral Deconvolution of the Unsymmetric Hydroxyl Band Profile†

A. A. Belhekar, M. S. Agashe and C. I. Jose
National Chemical Laboratory, Pune 411 008, India

The uncertainty in the separation of the asymmetric profile of the hydroxyl band of normal alcohols has been overcome by the use of a Fourier deconvolution technique which determined component-band parameters to carry out the band separation unambiguously. The nearly similar rotamer population of *trans*:*gauche* of 1.6:1 in the n-alcohols showed that the n-alkyl chain does not hinder the rotation around the C—O bond. The enthalpy change of *gauche*–*trans* conversion in solution (ca. 7 kJ mol⁻¹) was much larger than the torsional barrier in the gaseous state.

The asymmetric profile of the free hydroxyl band of aliphatic alcohols in solution is the subject of much controversy being variously attributed to rotational isomerism,¹⁻⁹ Fermi resonance¹⁰ and intramolecular hydrogen bonding.^{11,12} Systematic studies² of deuterated compounds have ruled out Fermi resonance as a possible explanation. Intramolecular hydrogen bonding between C—H and O, a controversial concept, has not found favour with many.^{5,7} Strong experimental support for rotational isomerism as a possible cause has come from the nearly symmetric profiles of the hydroxyl band of methanol and t-butyl alcohol in which rotamers due to rotation around the C—O bond are identical. Though it is now well established that the complex band profile has its origin in rotational isomers, it is not clear whether rotation around the C—O bond alone is responsible and/or whether rotation around the C—C bonds is also important. Thus, the free hydroxyl-band profile of n-propanol has been resolved into two bands by some workers^{1-7,9,10} and into three by others.^{8,12}

The main problem with this band profile is the strong overlapping which does not permit the number and the position of the component bands and the half-band widths to be determined with any certainty to carry out a separation. Two methods have generally been used for band resolution. In the graphical separation (G)^{1,3,4,6} the band parameters are arbitrarily assumed. In the non-linear least-squares curve analysis (L)^{5,13} the bands are separated assuming Lorentzian band shape and arbitrary band parameters. These methods give widely different component band area ratios ($K = B_H/B_L$, where B_H and B_L are band areas of the high- and low-frequency components, respectively) for ethanol (L: 1.7;⁵ G: 11.0⁴) and n-propanol (L: 1.2¹³ and G: 4.7¹⁰).

Since both these methods assume component band parameters, the results obtained must be termed arbitrary. With the advent of Fourier transform spectrometers and availability of software for handling the spectral data directly band deconvolution methods have found increasing applications in band separation. Though Fourier deconvolution has been used in the separation of a variety of complex bands, we found only Bacon and Van der Maas¹⁴ using a self-enhancement procedure, similar to Fourier deconvolution, to separate the hydroxyl-band profile of allylic alcohols. In the present work, we have carried out Fourier deconvolution of the free hydroxyl band of ethanol, n-propanol, n-butanol, n-pentanol and n-hexanol to determine the correct band positions and half-band widths of the component bands necessary for unambiguous band separation. From the component-band

areas the rotameric populations were calculated to obtain reliable equilibrium constants, and from their measurements, at various temperatures, the thermodynamic quantity, ΔH , of the rotameric change was extracted.

Experimental

Analytical grade Merck/B.D.H. samples dried over molecular sieve, Linde 4 Å, and chromatographically tested were used. Sample purities were: ethanol, 99.7%; n-propanol, 99.7%; n-butanol 99.8%; n-pentanol, 99.0%; and n-hexanol, 97.9%. The analytical grade Glaxo tetrachloromethane was dried over molecular sieve. Dilute solutions ≤ 0.011 mol dm⁻³ were used in variable-pathlength cells (0.8 cm) having a heating device and temperature-monitoring diode connected to a display unit.¹⁵ The temperatures were controlled within $\pm 0.2^\circ\text{C}$ in the range 25–55°C.

100 co-added interferograms were collected at 2 cm⁻¹ resolution on a Nicolet 60 SXB FTIR spectrometer to obtain a signal-to-noise ratio of ca. 1000:1. The signal-averaged interferograms were deconvoluted as detailed before,¹⁶ in the range 3675–3575 cm⁻¹ using half-band widths (VF0) varying between 14 and 18 cm⁻¹ and resolution enhancement factor (VF1) 1.7–2, such that the total band areas after deconvolution remained the same as before (VF0 and VF1 are program variables). Good separation was obtained without any side lobes and other artifacts. After the deconvolution the bands were separated graphically using the band positions, now precisely located, and reflecting one half of each band, which was not overlapped, at the band centres. Care is taken to see that the two separated bands add up to the total band profile. The band areas were measured using the expression $B = 2.303 \log(I_0/I)$ with appropriate limits. The half-band widths were obtained by multiplying the half-band widths in the deconvoluted spectra with VF1. The ratios of the isomers ($K = B_H/B_L$) were calculated at various temperatures assuming the integrated absorption intensities of the two-component bands to be the same at every temperature. These ratios were plotted against 1/T to obtain ΔH from Arrhenius equations using a least-squares fit.

Results and Discussion

A few typical spectra from the large number of hydroxyl stretching-band spectra of ethanol, n-propanol, n-butanol, n-pentanol and n-hexanol taken at three concentrations (in the range 0.006–0.011 mol dm⁻³) in tetrachloromethane at temperatures 303–328 K, are given in fig. 1–3. Thus, the free-hydroxyl band of ethanol (0.0066 mol dm⁻³) and its deconvoluted and separated band spectra are shown in fig. 1. The

† N.C.L. Commn. No. 4784.

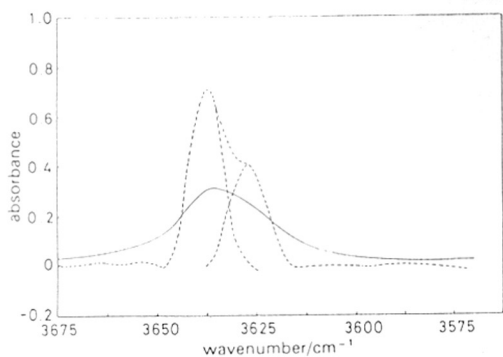


Fig. 1. Ethanol hydroxyl band (—); deconvoluted (---).

hydroxyl band of *n*-propanol ($0.0092 \text{ mol dm}^{-3}$) and the deconvoluted spectra at two temperatures are given in fig. 2; *n*-butanol, *n*-pentanol and *n*-hexanol hydroxyl bands at concentrations of 0.011 , 0.0098 and $0.0082 \text{ mol dm}^{-3}$, respectively, at 303 K and their deconvoluted spectra are presented in fig. 3. It is clear that, except in the case of ethanol, the band positions (ν_{H} and ν_{L}) and to a great extent the half-band widths, are clearly established by the spectral deconvolution for carrying out unambiguous band separation. In the case of ethanol, even with variations in the half-band width parameter between 15 and 20 cm^{-1} and an enhancement factor of 1.5 – 2 , no clear separation could be effected. However, the two

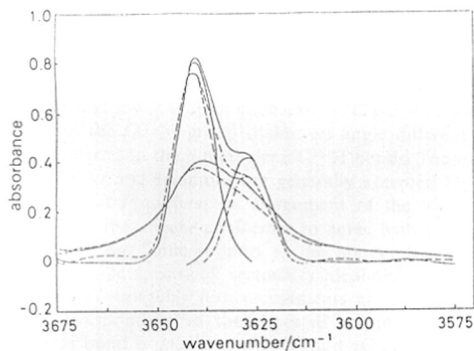


Fig. 2. *n*-Propanol hydroxyl and deconvoluted bands: (—) 303 K ; (---) 328 K .

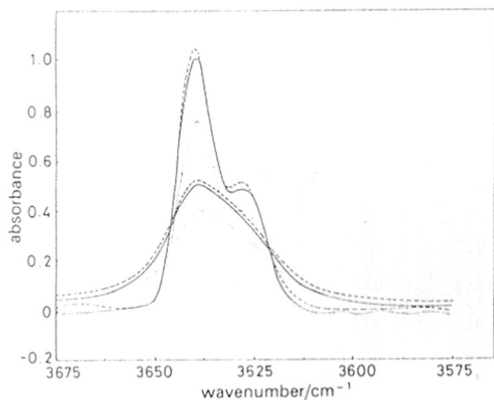


Fig. 3. Hydroxyl and deconvoluted bands: *n*-butanol 303 K (—); *n*-pentanol 303 K (---); *n*-hexanol 300 K (.....).

bands are considerably sharper than the original spectrum to effect a satisfactory separation. It was found during deconvolution that the asymmetric band profile of the above alcohols could be separated into two bands only, for all reasonable values of half-band width and enhancement factors, without developing side lobes and other artifacts. In the case of methanol, Fourier deconvolution with similar parameters did not produce any splitting of the band. Thus the present results clearly establish that the asymmetric band profile of *n*-alcohols consists of two bands ascribable to two rotational isomers resulting from rotation around the $\text{C}-\text{O}$ bond. Many earlier workers have separated the hydroxyl band of primary alcohols into two bands using graphical/non-linear least-squares curve analysis, but owing to the assumption of arbitrary band parameters their results were unreliable. Some workers^{8,12} have separated the band profile into three components and postulated rotation around the $\text{C}_\alpha-\text{C}_\beta$ bond to explain their results. In view of the uncertainties involved in the resolution of the asymmetric profile of the parent spectra, it is difficult to attribute much significance to these separations and the possibility of additional rotamers from rotation around the $\text{C}_\alpha-\text{C}_\beta$ bond.

In table 1, the typical band areas for the two rotamers of ethanol, *n*-propanol, *n*-butanol, *n*-pentanol and *n*-hexanol at various temperatures 303 – 328 K , are given. The positions, half-band widths of the component bands and mean equilibrium constants at 303 K are given in table 2 with reported parameters for comparison. The ΔH values obtained from a plot of $\log K$ vs. T^{-1} (fig. 4) are also given in this table along with reported values. An examination of the various band parameters shows that the high-frequency bands of the *n*-alkanols from *n*-propanol to *n*-hexanol (3639 – 3640 cm^{-1}) are decidedly higher than the 3637 cm^{-1} band of ethanol, though the low-frequency band is nearly the same in all cases (3627 – 3628 cm^{-1}). The low-frequency band has a higher half-band width (22 – 24 cm^{-1}) compared with the high-frequency band (20 cm^{-1}). The present band positions and half-band widths are quite close to those quoted by Oki and Iwamura,¹ but

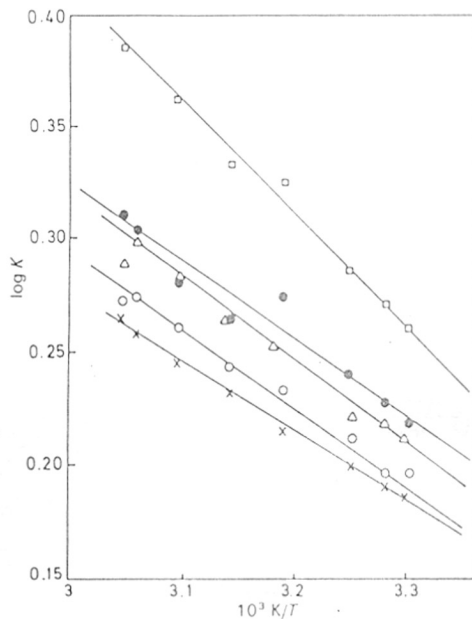


Fig. 4. Plot of $\log K$ vs. $10^3 K/T$ for: (●) ethanol, (□) *n*-propanol, (Δ) *n*-butanol, (×) *n*-pentanol, (○) *n*-hexanol.

Table 1. Temperature dependence of rotamer band areas (cm^{-1}) in n-alcohols

	303 K	308 K	313 K	318 K	323 K	328 K
ethanol ($0.0066 \text{ mol dm}^{-3}$)						
B_{H}	16.8	16.8	16.1	15.2	14.0	14.2
B_{C}	10.2	9.5	8.6	8.2	7.3	6.9
n-propanol ($0.0092 \text{ mol dm}^{-3}$)						
B_{H}	23.8	23.5	22.9	22.6	22.5	22.4
B_{C}	13.4	12.6	10.6	10.4	9.6	9.2
n-butanol ($0.011 \text{ mol dm}^{-3}$)						
B_{H}	25.1	25.0	24.7	24.4	24.2	24.2
B_{C}	15.2	14.0	13.6	13.2	12.8	11.6
n-pentanol ($0.0098 \text{ mol dm}^{-3}$)						
B_{H}	24.4	24.3	23.9	23.8	23.5	23.2
B_{C}	15.9	15.3	14.6	13.9	13.4	12.6
n-hexanol ($0.0082 \text{ mol dm}^{-3}$)						
B_{H}	17.9	17.9	17.1	17.3	17.3	16.9
B_{C}	12.1	10.9	10.4	10.1	9.8	9.2

generally different from those of others. Since these parameters are crucial for the curve resolution, even small changes in them can alter the band-area results. Thus, one of the authors¹³ using non-linear least-squares analysis obtained band positions and half-band widths of 3637, 18 cm^{-1} and 3625, 22 cm^{-1} for n-propanol, which were considerably different from those obtained in the present case. This also resulted in a K value of 1.2 as against 1.76 found from the Fourier deconvolution method.

The assignments of the bands to specific rotamers were based on the early work of Oki and Iwamura,¹ who argued that the hydroxyl frequency in alcohols depended on the disposition of the O—H bond with respect to the $\alpha\text{C—H}$ and $\alpha\text{C—alkyl}$ bonds (fig. 5). Thus, the 3637–3640 cm^{-1} band in the present alcohols was ascribed to the *trans* conformer in which the O—H bond is *gauche* to the two methylene C—H bonds, and the band at 3627 cm^{-1} was ascribed to the two *gauche* conformers in which the O—H bond is *gauche* to the $\alpha\text{C—H}$ and $\alpha\text{C—alkyl}$ bonds. Since the *trans*-conformer frequency is somewhat lower than in methanol (3643 cm^{-1}), it is quite likely that the O—H group makes an angle different from 60° with respect to the α methylene C—H bonds. These assignments of Oki and Iwamura are generally accepted by others though Kolbe⁶ prefers the assignment of the high-frequency band to the *gauche* conformer to agree with their statistical distribution. Some support to the present assignment comes from the spectra of secondary alcohols¹ which have band profiles separable into components at 3627 and 3617 cm^{-1} , corresponding to the expected conformers in which the O—H bond is *gauche* to $\alpha\text{C—H}$ and $\alpha\text{C—alkyl}$ and to two C-alkyl bonds, respectively.

The above assignments are in line with the observations of Krueger *et al.*,¹⁷ who found that the NH/OH stretching frequencies in amines/alcohols were higher when αCH bonds were lying *trans* to the lone-pair electrons. The CH bonds in

turn also showed lower frequencies. McKean and Ellis¹⁸ found support for the lower CH stretching frequencies, when the CH bonds lie *trans* to the oxygen/nitrogen lone pair, in the form of bond lengthening. Bond-length calculations of a few selected nitrogen compounds such as CH_3NH_2 , $(\text{CH}_3)_2\text{NH}$ *etc.*, using dissociation energies had shown lengthening in these bonds. In the context of the present alcohols, methanol would have two CH bonds lying *trans* to the oxygen lone pairs in both its conformers. In the primary alcohols, the *trans* form would have two CH bonds *trans* to the oxygen lone pairs, whereas the *gauche* form would have one CH bond only *trans* to the oxygen lone pair. Thus, the higher frequency of the *trans* form relative to the *gauche* form can be understood.

The temperature studies on the rotamers showed that at room temperature (25°C) the *trans* species in these alcohols predominated to the extent of *ca.* 1.6:1 over the *gauche*, which is nearly the opposite of what is expected statistically

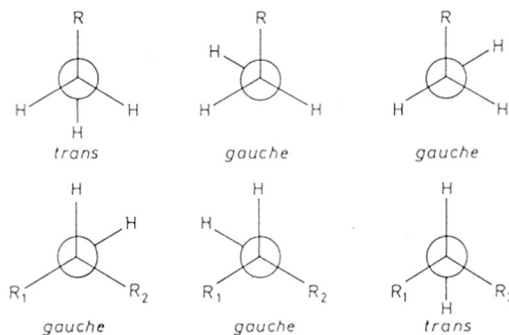


Fig. 5. Rotamers around the C—O band in alcohols. Top, primary; bottom, secondary.

Table 2. Hydroxyl band and thermodynamic parameters of n-alcohol rotamers

alcohol	$\nu_{\text{H}}/\text{cm}^{-1}$	ν/cm^{-1}	$\Delta\nu_{1/2}/\text{cm}^{-1}$		K		$\Delta H/\text{kJ mol}^{-1}$	
			H	L	found	reported	found	reported
ethanol	3637.0	3627.0	21.0	20.0	1.65	1.7, ^a 1.8, ^b 8.0 ^c 7.7, ^e 11.0, ^f 2.7 ^d	6.8	6.3 ^d
n-propanol	3639.5	3627.5	20.0	23.0	1.76	2.6, ^b 4.7, ^e 6.2 ^f 3.5, ^d 1.2, ^g 3.8 ^h	9.8	7.6 ^d
n-butanol	3640.0	3628.0	19.0	22.0	1.59	2.2, ^b 6.9, ^e 5.3 ^f 3.6 ^h	5.9	—
n-pentanol	3639.0	3627.0	17.0	22.0	1.49	5.0, ^e 5.1 ^c	6	—
n-hexanol	3639.5	3627.0	18.0	23.5	1.47	4.0 ^c	6.8	—

^a Ref. (5). ^b Ref. (1). ^c Ref. (3). ^d Ref. (6). ^e Ref. (10). ^f Ref. (4). ^g Ref. (13). ^h Ref. (11).

(1:2). The reversal in the rotameric population can be ascribed to the larger separation between the O—H and α -C-alkyl substituent in the *trans* species than in the *gauche* form where they are much closer and could cause steric repulsion. Further microwave spectra of ethanol¹⁹ showed predominance of the *trans* conformer over the *gauche* conformer.

Bakke²⁰ has recently determined $^3J(\text{HCOH})$ coupling constants from nuclear magnetic resonance studies of a series of alcohols including ethanol in dilute $\text{CCl}_4/\text{CFCl}_3$ solution (0.01 mol dm⁻³) and arrived at a rotameric population. In the case of ethanol, he found the predominant conformer to be *gauche* with 65% population (statistical value), against the infrared results, which showed the *trans* species to predominate at 62%. Bakke, in fact, suggested the reversal of the present infrared assignments of bands at 3637 and 3627 cm⁻¹ to *trans* and *gauche* species, respectively, to agree with the NMR results. He felt that reliable values of rotameric concentrations cannot be obtained from band separation of the asymmetric broad hydroxyl-band profile. He found, however, that the rotameric population calculated from $^3J(\text{HCOH})$ coupling constants in propan-2-ol (*gauche* 75%) was in reasonable agreement with infrared results (*gauche* 63%), based on the assignment of the 3627 cm⁻¹ band to *gauche* species in which the O—H bond lies between the C-alkyl and C—H bonds as in ethanol.

Our results on ethanol and other n-alcohols also arrived at the predominance of the *trans* species (*trans/gauche* \approx 1.6) in solution and the question of unreliability of infrared results no longer exists. To understand this discrepancy in the rotameric populations derived from NMR $^3J(\text{HCOH})$ coupling constants and infrared hydroxyl bands, one would have to look into the assumptions made with regard to the possible conformations of ethanol and other n-alcohols.

It is assumed that the rotation around the C—O bond results in staggering of the O—H bond with respect to the C—H/C—C bond at a dihedral angle of 60° (fig. 5). We feel that in the *gauche* species of ethanol and other n-alcohols, O—H may be making dihedral angles much smaller than 60° and 180° with the methylene C—H bonds, to avoid steric interaction with the CH₃ alkyl group. We had found that assuming dihedral angles of 30° and 150° in the *gauche* species (and using the Karplus equation) the observed $^3J(\text{HCOH})$ coupling constant of 5.1 Hz would yield predominantly *trans* species in agreement with infrared results.

The rotamer equilibrium constants obtained for the various alcohols, as can be seen from table 2, are close to those reported from non-linear least-squares curve analysis using arbitrary band parameters and Lorentzian band shape^{1,5,13} (1.2–2.6) and much smaller than those determined graphically^{3,4,6,10,11} using arbitrary band parameters (2.7–11.0). It is interesting to note that general agreement was obtained with the results of Oki and Iwamura,¹ whose assumed band parameters of ethanol, n-propanol and n-butanol were closer to those determined by the deconvolution method. The rotameric equilibrium constants of the various normal alcohols from ethanol to n-hexanol in the present study varied only marginally from one another (table 2) thus confirming that sterically unhindered straight-chain substituents do not affect the conformational equilibria arising from rotation around the C—O bond to any appreciable extent.

The observed ΔH values can be compared with the results obtained on ethanol and n-propanol by Kolbe,⁶ who

ascribed the higher-frequency band to *gauche* (opposite to our assignment) and obtained values of 6.3 and 7.6 kJ mol⁻¹. Microwave spectral investigations report a difference of 1.3 and 1.2 kJ mol⁻¹ between the *gauche* and *trans* isomers in ethanol¹⁹ and n-propanol,²¹ respectively. We are not aware of any ΔH value reported for other alcohols studied by us. ΔH values of 8.9 kJ mol⁻¹ have been reported²² for n-octanol in tetrachloromethane. While intramolecular hydrogen bonding between C—H and the lone pair of electrons on oxygen has been suggested⁸ for the formation of the *gauche* form, the possible difference in the hydrogen-bonding interaction between the solvent, CCl_4 , and the rotamers ($\text{Cl}\cdots\text{H}-\text{O}$) has also been suggested⁶ for the stability of the *trans* conformer. However, only a detailed ΔH study of rotameric equilibria in other types of alcohol can offer a satisfactory explanation.

The present study has confirmed that the broad hydroxyl-band profiles in primary alcohols are the result of rotational isomerism of the C—O bond. In straight-chain alcohols, the high-frequency *trans* conformer predominates over the *gauche* conformer approximately to the extent of 1.6:1 with an enthalpy difference of 7 kJ mol⁻¹ suggesting little hindrance to rotation around the C—O bond from such a chain.

References

- 1 M. Oki and H. Iwamura, *Bull. Chem. Soc., Jpn.*, 1959, **32**, 950.
- 2 R. Piccolini and S. Winstein, *Tetrahedron Lett.*, 1959, **13**, 4.
- 3 F. Dalton, G. D. Meakins, J. H. Robinson and W. Zaharia, *J. Chem. Soc.*, 1962, 1566.
- 4 J. Fruwert, G. Hanschmann and G. Geiseler, *Z. Phys. Chem.*, 1965, **228**, 277.
- 5 L. Joris, P. von R. Schleyer and E. Osawa, *Tetrahedron*, 1968, **24**, 4759.
- 6 A. Kolbe, *Z. Phys. Chem. (Leipzig)*, 1972, **250**, 183.
- 7 J. H. van der Maas and E. T. G. Lutz, *Spectrochim. Acta, Part A*, 1974, **30**, 2005.
- 8 R. Salzer, J. Fruwert and G. Franz, *Z. Phys. Chem. (Leipzig)*, 1978, **259**, 154.
- 9 J. H. van der Maas and E. T. G. Lutz, *Spectrochim. Acta, Part A*, 1978, **34**, 915.
- 10 T. D. Flynn, R. L. Werner and B. M. Graham, *Aust. J. Chem.*, 1959, **12**, 575.
- 11 E. L. Saier, L. R. Cousins and M. R. Basila, *J. Chem. Phys.*, 1964, **41**, 40.
- 12 P. J. Krueger and H. D. Mettee, *Can. J. Chem.*, 1964, **42**, 347.
- 13 S. M. Chitale and C. I. Jose, *J. Chem. Soc., Faraday Trans. 1*, 1986, **82**, 663.
- 14 B. F. Bacon and J. H. van der Maas, *Spectrochim. Acta, Part A*, 1988, **44**, 1243.
- 15 S. M. Chitale and C. I. Jose, *J. Chem. Soc., Faraday Trans. 2*, 1980, **76**, 233.
- 16 (a) J. K. Kauppinen, D. J. Moffatt, H. H. Mantsch and D. G. Cameron, *Appl. Spectrosc.*, 1981, **35**, 271; (b) C. I. Jose, A. A. Belhekar and M. S. Agashe, *Spectrochim. Acta, Part A*, 1988, **44**, 899.
- 17 P. J. Krueger, J. Jan and H. Weiser, *J. Mol. Struct.*, 1970, **5**, 375.
- 18 D. C. McKean and I. A. Ellis, *J. Mol. Struct.*, 1975, **29**, 81.
- 19 J. Michielsen-Effinger, *Ann. Soc. Scient. Bruxelles Ser. I*, 1964, **78**, 223.
- 20 J. M. Bakke, *Acta Chem. Scand.*, 1986, **40B**, 407.
- 21 A. A. Abdurahmanov, R. A. Rahimova and L. M. Imanov, *Phys. Lett.*, 1970, **32A**, 123.
- 22 J. Fruwert, G. Geiseler, W. Geyer and S. Sieber, *Z. Phys. Chem. (Leipzig)*, 1969, **241**, 74.